Phosphatidylcholines in different aggregational states : a 13C NMR study of the fluidity of model membranes

Please check the document version of this publication:

PHOSPHATIDYLCHOLINES
IN DIFFERENT AGGREGATIONAL STATES

A ^{13}C NMR study of the fluidity of model membranes

PROEFSCHRIFT

ROELAND JACOBUS EDUARD MARIA DE WEERD

GEBOREN TE TILBURG

DIT PROEFSCHRIFT IS GOEDGEKEURD DOOR

DE PROMOTOREN

PROF. DR. H.M. BUCK

EN

PROF. DR. IR. C.A.M.G. CRAMERS

DE CO-PROMOTOR

DR. IR. J.W. DE HAAN

Aan mijn ouders
Aan Marja

"Originality consists not in saying
what no one has ever said before,
but in saying what you think yourself".
                                        -James F. Stephen-

Contents

Chapter I

General introduction

I.1 Molecular aggregation

Amphiphilic molecules such as fatty acid salts and phospholipids consist of a polar (hydrophilic) head group and an apolar (hydrophobic) tail. Depending on the nature of the head group, amphiphiles can be anionic, cationic, zwitter-ionic or non-ionic. When dispersed in water at a concentration above the so-called critical micelle concentration (CMC) they can achieve segregation of their hydrophobic portions from the solvent by self-association. This segregation is frequently referred to as the "Hydrophobic Effect"[1]. Such aggregates are known as micelles (Figure 1.1). Below the CMC insufficient molecules can associate to achieve an effective elimination of the hydrocarbon-water interface. Consequently, only monomers are observed. Around the CMC, a delicate balance between monomers and micelles occurs which is dictated by the "Hydrophobic Effect". Accordingly, the transition between monomers and micelles is not distinct, but has a broad range. Growth of small micellar spheres or disks can develop ultimately into parallel layers of amphiphiles with the polar head groups located on the outside, the so-called bilayer (Figure 1.1)[2]. The self-association of amphiphiles in aqueous solution into aggregates can readily be accounted for by the "Hydrophobic Effect". However, as in many cases relatively small micelles are preferred, an opposing force has to be present as well, which prevents the growth of the aggregates to larger sizes. Even for the largest possible aggregates (*i.e.*, the bilayer sheet) such a repulsive force must also occur to oppose separation into an entirely separate phase. The opposing force comes primarily from the electrostatic
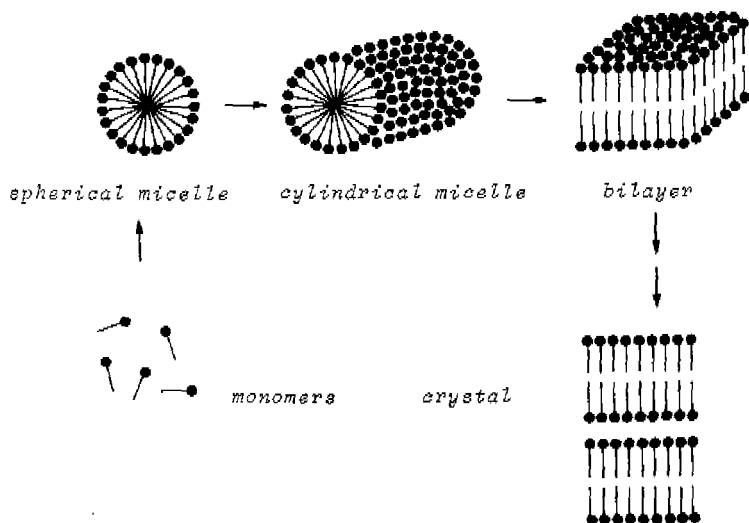
Figure 1.1   Molecular aggregational states.

repulsion between identically charged ionic head groups. In
the case of non-ionic detergents, a preference for hydration
is involved. In this context it can be envisaged that simple
aliphatic alcohols, which form complexes with one another throug
hydrogen bonds, separate from the aqueous medium as a distinct
phase. It should be noted that the "Hydrophobic Effect"
induces a *lower* limit to the micelle size, because a minimal
number of amphiphiles have to associate with each other to
eliminate hydrocarbon-water interactions effectively. Thus
micelle formation is necessarily a cooperative process,
requiring simultaneous participation by many amphiphiles[3].
The *upper* limit of the aggregate dimension can be visualized
by means of pure geometrical considerations. When the
aggregation number increases, the packing between the head
groups also increases. The repulsive force acts against too
close an approach, thereby keeping the dimension limited.
As single stranded amphiphiles form micellar structures under
standard conditions, amphiphiles containing two chains mainly

10

build up bilayer structures[1]. Such a number of chains per
amphiphile results in half as many head groups as there would
be for single stranded surfactants. The average *head group
area* will be twice as large as the area per chain. An optimal
aggregational state will now be reached not in the micelles
but in the bilayers where the head groups become more closely
packed. This offers a description without the use of complicated
theoretical considerations, why single stranded amphiphiles
prefer the micellar state, and phospholipids are mostly found
in the bilayer state.

These descriptions have shown, that the thermodynamic
principles underlying aggregation are conceptually simple:
the "Hydrophobic Effect" provides the driving force for
aggregation (*i.e.*, a positive entropy change), whereas repulsion
between head groups limits the size that a particle can attain.
Both factors must vary, however, with the particle size.
Aggregation is thus shown to be cooperative and non-specific.

I.2 Membranes

Biological activity, particularly the specificity of many
metabolic processes, demands molecular order. Aggregation
(see Section I.1) provides one way of ordering molecules and
it is a reversible process. The transitions monomer-micelle
and micelle-bilayer seem widely accepted as a means of
controlling and regulating membrane properties[4-8]. Phospholipids
are the major class of membrane lipids. Other kinds of membrane
lipids are glycolipids, triglycerides and cholesterol. In
biological membranes, the lipids form a bilayer matrix in
which the proteins are embedded or surface bound. Although
many biological activities are understood at a pharmacological
or biochemical level, the behaviour of the individual membrane
components and especially the phospholipids on a molecular
basis, is often less well known. In contrast, macroscopic
characteristics of the entire membrane have been investigated
thoroughly in the past. It was shown that membranes are sheet-
like structures of relatively small molecules. They form closed
boundaries between compartments of different composition (*i.e.*,
the unit membrane, the nuclear membrane and the membranes of

the mitochondria, Golgi-bodies, ribosomes and the endoplasmic
reticulum of the living cell). Membranes mainly consist of
lipids, proteins and in some cases pigments and carbohydrates.
The phospholipid bilayer part of the membrane is highly
impermeable to ions and most polar molecules. Permeability
of the phospholipid section can only be established at local
disturbances of the bilayer orientation, the so-called local
micelle formation[5] and local inverted micelle formation[6-9]
(*i.e.*, polar discontinuities). In all other cases specific
membrane bound proteins mediate distinct functions of the
membrane. They serve as pumps, gates, receptors, energy-
transducers or enzymes. They can be bound at the surface
of the membrane (extrinsic or peripheric proteins) or within
the hydrophobic core (intrinsic or integral proteins).

I.3 *Membrane fluidity*

Only non-covalent interactions, such as hydrophobic
van der Waals type interactions or electrostatic interactions,
keep the membrane components together. From these considerations
it will be obvious that the membrane lipids and especially the
phospholipids must not be considered as static, but as dynamic
membrane components (*i.e.* the "Fluid Mosaic Model")[18], capable
of regulating metabolic important processes, such as enzym
expression, membrane fusion and transbilayer transport[8,10-17].
This dynamic behaviour can also be made plausible by the
observations that phospholipid bilayers undergo a phase
transition of the hydrophobic core from a relatively viscous
fluid (the gel) to a relatively non-viscous fluid (the liquid
crystalline) phase at a certain temperature, the so-called
phase transition temperature. This temperature is strongly
dependent on the nature of the hydrophobic tails and it readily
decreases upon higher degrees of unsaturation[19-27].
Unsaturations induce a disordering, thus eliminating the
anti-parallel stacking of the phospholipid chains as compared
with the saturated system. Consequently, the transition
between the gel and liquid crystalline phase of the
unsaturated lipid will occur at a lower temperature. Not only
unsaturated phospholipid acyl chains alter the fluidity of

12

the hydrophobic core of the membrane. Incorporated cholesterol also affects membrane fluidity. Under physiological circumstances, cholesterol induces a profound condensing effect when the phospholipids are in the liquid crystalline state. On the other hand, a liquefying effect occurs for the gel state phospholipids[28].

From these points of view, it will be valuable to investigate fluidity as a contributing factor for regulating several membrane functions. A clear definition of the meaning of the term fluidity is hard to offer. Several types of motion (inter- and intramolecular) have to be considered to contribute to membrane fluidity, such as lipid exchange between the bilayer and the surrounding medium. However, this process is very slow (average exchange time of the order of 24 hrs.), and thus hardly contributes. Another slow process is the interchange of lipid molecules between the outside and inside of the bilayer: transverse diffusion or "flip-flop" (Figure 1.2), with an average interchange time of the order of minutes. In contrast to these kinds of motion, the lateral diffusion of lipid molecules in the plane of the bilayer is a fast process (correlation time $\sim 10^{-8}$ s). Besides this latter process, fluidity also depends upon uncorrelated and correlated molecular processes generated by the coherence with neighbouring lipids (the correlated process is frequently referred to as the "Correlated Molecular Ordering")[29]. Examples of the former type are conformational changes between *anti* and *gauche* and rotations about individual bonds. Examples of the latter type are correlated phenomena such as intermolecular packing, kink-diffusion and axial rotation of the entire phospholipid chains[30-34]. It should be realized, however, that these molecular processes might not be entirely independent of each other. For example, diminishing the coherence between neighbouring chains will induce more kinks within and/or less packing between the lipid molecules, which in turn influences rates and types of intramolecular mobilities.

I.4 Mixed micelles and mixed bilayers as model membranes
Just as ordinary micelles, phospholipid membranes are

miscible with various kinds of substrates possessing
hydrophobic groups (see Section I.2)[1]. Non-amphiphilic
substrates such as cholesterol and proteins only penetrate
the phospholipid bilayer, while amphiphiles can also induce
for instance former mentioned polar discontinuities, due to
their nature to adopt micellar structures. As is generally
accepted, mixed micelles/bilayers play an important role in
the process of cell-division, cell-fusion, reconstitution
of biomembranes and they also act as pharmaceutical drug
carriers[8,35-36]. All natural occurring membranes are mixed
aggregates, containing different types of lipids and proteins.
Knowledge of the fluidity of simple mixed aggregates can
offer a relevant contribution to the elucidation of specific
interactions between biomembrane phospholipids and their
substrates. Model studies are most conveniently carried out
on simple well-defined systems.

monomeric exchange

transverse diffusion

lateral diffusion
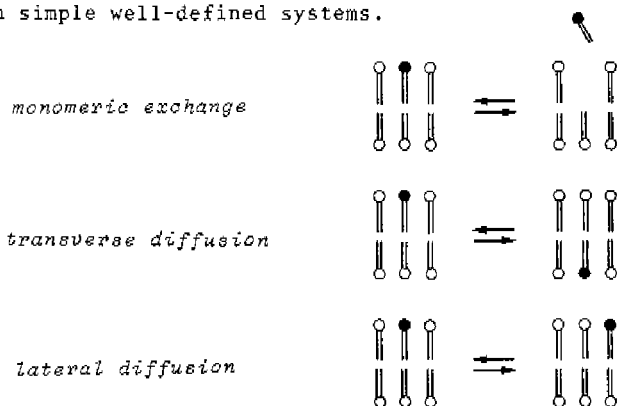
Figure 1.2   Exchange processes within the bilayer.

I.5 Scope of this thesis

In the past decade, many biophysical studies have been
performed on model systems of biomembranes, by means of a
wide variety of analytical methods, such as ESR-, NMR-, IR-,
Raman and Fluorescence spectroscopy, Differential Scanning
Calorimetry, X-ray and Neutron Diffraction[34]. *The subject
of this thesis is to apply ^{13}C NMR spectroscopy in particular
to investigate the fluidity, caused by interactions between*

neighbouring constituents, of mixed micelles and bilayers
of phospholipids and their substrates (for instance fatty
acid derivatives and cholesterol) *on a molecular basis.*
Moreover, the applicability of ^{13}C NMR spectroscopy in this
particular field of research is extended. Attention will be
paid to the extent that incorporation of substrates modulate
the intermolecular packing, the intramolecular conformational
equilibria and mobilities of the components of the mixed
aggregates.

At this point it is essential to notice which motions
can contribute on the ^{13}C NMR time scale. These can be divided
into three classes: motions within the molecules, motions of
the entire molecules and motions of the molecular aggregate.
Only small amplitude, high frequency bond rotations such
as *anti-gauche* rotations and kink diffusion build up the
first class. The second class surrounds molecular motions,
which have already been mentioned (see Section I.3), such as
axial rotation, rigid body motions and lateral diffusion.
Other types of motion such as "flip-flop" and interbilayer
exchange are normally too slow to be detected by means of
^{13}C NMR spectroscopy. The third class represents motions
of the entire aggregate, such as tumbling of bilayer sheets
or bilayer fragments. The extent to which these types
contribute mainly depends on the size of the fragment. On the
^{13}C NMR time scale of observation large fragments tumble too
slow to affect the former defined fluidity (see Section I.3).
From these considerations it is shown unambiguously that ^{13}C
NMR spectroscopy is a most valuable tool to investigate
membrane fluidity. In the subsequent chapters the following
points regarding fluidization of the membrane will be
discussed in detail. Chapter II will deal with a concept
which distinguishes changes in intermolecular packing
from changes in intramolecular conformational
equilibria as contributors to the fluidization of the
hydrophobic interior. Mixed micelles of saturated fatty acid
salts of variable chain lengths will serve as subject of
investigation. In Chapter III this concept is applied to
mixed micelles of short-chain lecithins and saturated
hydrocarbon compounds which differ in *n*-alkyl chain lengths.

As for the hydrophobic region, results were obtained similar
to the mixed micelles of the fatty acid salts. For the
hydrophilic head group region the function of molecular
mobility is introduced. It will be shown that the multiplicity
of the carbon resonances of the methyls of the cationic site
are highly influenced by the rate of motion of the CH_2-$\overset{+}{N}$ site
around the CH_2-CH_2 head group bond. In Chapter IV the
principles of packing, conformations and head group mobility
are extended towards bilayer structures. Mixed-vesicle systems
of long-chain phospholipids and n-alkyl trimethylammonium
bromides of different chain lengths are studied. A dynamic
picture is offered for lysis of the bilayer when raising the
concentration of the lytic n-alkyl compounds to ca. one equiv.
Contrary to the decrease of the particle size upon lysis, in
Chapter V inclusion of cholesterol is studied to monitor the
effects of increasing particle sizes, and concomitant
increasing aggregational densities[1] (*i.e.* packing), on the
fluidity of the hydrophobic and hydrophilic region of the
bilayer structure. For both types of intercalations (*i.e.*
cholesterol and the lytic compounds), it will be shown that
the surrounding phospholipids possess an intrinsic property
which acts against disruption of the bilayer: the lecithins
reduce the degrees of freedom of the disturbing substrates.
Chapter VI surveys the effects optically active n-alkyl
quaternary nitrogen substrates have on the fluidity within
the chiral phospholipid bilayer, and *vice versa*. It is
demonstrated that the chiral substrate is pressed between
the surrounding chiral lecithins. Analogous to the single
stranded lytic compounds, it results in conformational changes
of the chain of the chiral substrate, as monitored by ^{13}C NMR.
Moreover, the chirality of the head groups of the substrate
is affected, as detected by CD spectroscopy. Finally, Chapter
VII describes the fluidity changes in the flat bilayer
orientation of phospholipids upon intercalation of former
mentioned n-alkyl trimethylammonium bromides. Analogous to
the vesicular dispersions, also for the flat bilayer
dispersions the intrinsic property of the lecithins of reducing
the degrees of freedom of the lytic compounds is again

demonstrated by means of relaxation data. These relaxation data are obtained by means of a new NMR technique for anisotropic systems: the ^{13}C-CPMAS experiment.

References and notes

1. C. Tanford, "The Hydrophobic Effect: Formation of Micelles and Biological Membranes", Wiley & Sons, New York, 1980.
2. K.L. Mittal and P. Mukerjee, "Micellization, Solubilization and Microemulsions", Part 1 (K.L. Mittal, Ed.), Plenum Press, New York, 1977,1.
3. B. Lindman and H. Wennerström, "Topics in Current Chemistry" Springer Verlag, New York, 1980, *87*.
4. J.N. Israelachvilli, D.J. Mitchell and B.W. Ninham, J. Chem. Soc., Faraday Trans. 2, 1976, *72*,1525.
5. A.T. Florence, "Micellization, Solubilization and Microemulsions", Part 1 (K.L. Mittal, Ed.), Plenum Press, New York, 1977,55.
6. B. de Kruijff, A.J. Verkley, C.J.A. van Echteld, W.J. Gerritsen, C. Mombers, P.C. Noordam and J. de Gier, Biochim. Biophys. Acta, 1979, *555*,200.
7. B. de Kruijff, P.R. Cullis and A.J. Verkleij, TIBS, 1980, *79*.
8. P.R. Cullis and B. de Kruijff, Biochim. Biophys. Acta, 1979, *559*,399.
9. P.C. Noordam, C.J.A. van Echteld, B. de Kruijff, A.J. Verkleij and J. de Gier, J. Chem. Phys. Lipids, 1980, *27*,222.
10. R. Coleman, Biochim. Biophys. Acta, 1973, *300*,1.
11. B. Fourcans and M.K. Jain, Adv. Lipid Res., 1974, *12*,147.
12. M. Esfahami, B.B. Rudkin, C.J. Cutler and P.E. Waldron, J. Biol. Chem., 1974, *252*,3194.
13. Y.C. Awasthi, T.F. Chung, T.W. Keenan and F.L. Crane, Biochem. Biophys. Res. Comm., 1970, *39*,822.
14. A. Watts, D. Marsh and P.F. Knowles, Biochem. Biophys. Res. Comm., 1978, *81*,403.
15. Y.C. Awasthi, F.J. Ruzicka and F.L. Crane, Biochim. Biophys. Acta, 1970, *203*,233.
16. W.L. Dean and C. Tanford, Biochemistry, 1979, *17*,1683.
17. E.H.B. de Lacey and J. Wolfe, Biochim. Biophys. Acta, 1982, *692*,425.
18. S.J. Singer and G.L. Nicholson, Science, 1972, *175*,720.

19. D. Chapman (Ed.), "Biological Membranes, Physical Fact and Function", Academic Press, London, 1968.

20. G. Govil, "NMR Basic Principles and Progress", Part 20, Springer Verlag, New York, 1982.

21. S.C. Chen and J.M. Sturtevant, Biochemistry, 1981, *20*,713.

22. K.C. Cho, C.L. Choy and K. Young, Biochim. Biophys. Acta, 1981, *663*,14.

23. A. Watts, D. Marsh and P.F. Knowles, Biochemistry, 1978, *17*,1792.

24. H.H. Füldner, Biochemistry, 1981, *20*,5707.

25. B. de Kruijff, P.R. Cullis and G.K. Radda, Biochim. Biophys. Acta, 1975, *406*,6.

26. J.R. Silvius and R.N. McElhaney, Chem. Phys. Lipids, 1979, *24*,287.

27. C.B. Berde, H.C. Andersen and B.S. Hudson, Biochemistry, 1980, *19*,4279.

28. G.A. Thompson, "The Regulation of Membrane Lipid Metabolism", CRC Press Inc., Boca Raton, 1980.

29. P. Tancrède, D. Patterson and P. Bothorel, J. Chem. Soc., Faraday Trans. 2, 1977, *73*,29;
    P. Tancrède, P. Bothorel, P. de St. Romain and D. Patterson, J. Chem. Soc., Faraday Trans. 2, 1977, *73*,17;
    F.M. Fowkes, J. Phys. Chem., 1980, *84*,510;
    B. Lemaire and P. Bothorel, Macromolecules, 1980, *13*,311.

30. N.O. Petersen and S.I. Chan, Biochemistry, 1977, *16*,2657.

31. R.J. Pace and S.I. Chan, J. Chem. Phys., 1982, *76*,4217.

32. R.J. Pace and S.I. Chan, J. Chem. Phys., 1982, *76*,4228.

33. R.J. Pace and S.I. Chan, J. Chem. Phys., 1982, *76*,4241.

34. S.I. Chan, D.F. Bocian and N.O. Petersen, "Molecular Biology, Biochemistry and Biophysics", Part 31, Springer Verlag, New York, 1981 and references therein.

35. S. Razin, Biochim. Biophys. Acta, 1972, *265*,241.

36. D.A. Wienstein, Pure and Appl. Chem., 1981, *53*,2241.

CHAPTER II

A ^{13}C NMR study of mixed micelles.
Variation of interchain distances
and conformational equilibria

II.1 *Introduction*

Short-chain lecithins exist as large micellar aggregates
in water above a given critical micelle concentration (CMC).
The CMC depends on the fatty acyl chain length[1]. Lipid micelles
and mixed micelles of lipids and fatty acid derivatives are of
biological interest. They introduce the so-called polar dis-
continuities within the phospholipid bilayer, thereby altering
the permeability of the cell membrane for vital compounds[2,3].
They also play an essential role in the process of cell
division[2,4]. Furthermore, the large rate of hydrolysis of
lecithins by phospholipases occurs also in the micellar state[5,6].
It is generally presumed, that conformational changes in the
head groups and/or the lipid chains as well as their relative
orientations and order, are of importance for the physical
chemistry of the lecithins[3,7].

Recently, much work has been done explaining the acyl
chain conformation of long-chain lecithins in different
aggregational states[8,9](see Figure 2.1). The *sn*-1 chain is
orientated perpendicular to the bilayer surface and the *sn*-2
chain is bent at the C-2 carbon atom and runs from thereon
parallel with the *sn*-1 chain[8,9]. In order to gain more insight
into the conformational behaviour of phospholipids, *Roberts et
al.*[10] applied ^{1}H NMR techniques to several lecithins in different
mixed micelles. The observed magnetic nonequivalences of the
four α-protons of the *sn*-1 and *sn*-2 chain were explained in
terms of different conformational equilibria for the two chains[8].
Because of the difference in effective lengths of the *sn*-1 and
sn-2 chains, lecithin micelles as such qualify as *mixed micelles*
to a certain extent[11].
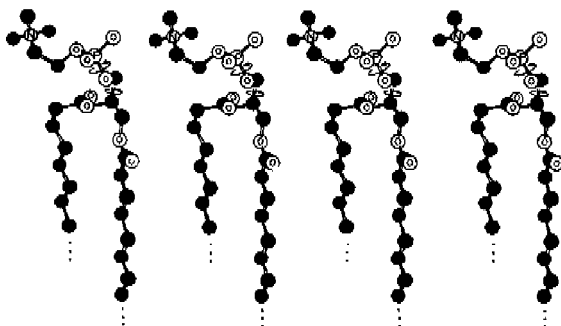
Figure 2.1 Average orientation of lecithin head groups and the conformational nonequivalence of lecithin acyl chains in lipid aggregates[8-10].

On the other hand, single micelles of simple detergents are studied frequently by means of a wide variety of physical methods[12]. A number of discrepancies, notably about the CMC, still exists between the different analytical methods[13,14]. More details regarding dynamics and conformational equilibria of the acyl chains have been reported by *Lindman et al.*[13,15,16]. Topics as solubilization and aggregation numbers were also included using ^{13}C NMR[17]. Specific statements regarding mixed micelles of C_{14}TAB and C_{16}TAB[18] were reported[17]. The difference in chain lengths of the partners in these mixed micelles is of the same order of magnitude as that which might prevail in phospholipid micelles (with *nominally* equal *sn*-1 and *sn*-2 chain lengths)[19]. The different chemical shifts of the terminal methyls of the C_{14}TAB and the C_{16}TAB constituents were explained in terms of increased chain folding of the longer chain near the apolar end. A similar explanation had been offered previously for the solubilization of *n*-decanol in sodium octanoate micelles[17].

In our opinion, alternative descriptions involving the occurrence of chain separation and, consequently, changes in *van der Waals* solvent effects on the chain should be considered as well. A recent publication by *Roberts et al.*[20] concerning

^{13}C NMR of simple phospholipid micelles did not take into account either solvent effects or the model descriptions of *Lindman et al.*[17] regarding mixed micelles. In the following Sections it will be discussed that conformational changes as well as changes in packing contribute to the ^{13}C NMR chemical shifts of the hydrocarbon region of mixed micelles of salts of fatty acids with different chain lengths.

II.2 *Results*

^{13}C NMR chemical shifts of the micelles have been assigned by combining literature data[16,17] and relative relaxation data, assuming that T_1-values increase towards the apolar end[21,22,23]. Results are presented in Table II.1. When mixed micelles are formed, the ^{13}C NMR chemical shifts of the constituent chains change with respect to the single micelles (see Table II.2). When the potassium dodecanoate solution was diluted from 1.5 M to 0.15 M, no changes in chemical shift were observed. It indicates, that no changes in aggregation numbers occur in this concentration range[13].

II.3 *Single micelles as reference solutions for the mixed-micellar solutions*

For the hexanoate NMR measurements indicate the formation of aggregates of ca. five molecules of amphiphile in water[13]. Other experimental methods really indicate the formation of micelles with larger aggregational numbers[14]. The octanoate forms micelles with an average aggregation number of ca. seventeen[13,24], while the dodecanoate forms much larger micelles. Previous reports[12,25] revealed no appreciable interaction of water with the hydrophobic core of closely packed surfactant micelles such as sodium dodecanoate[26,27]. Contradictory results have been shown to be due to deficiencies in the analytical procedures[28,29].

The ^{13}C NMR chemical shifts (see Table II.1) of the ω-methyl groups fall roughly into three groups: 14.00 ppm for the hexanoate, 14.18 ppm (±0.01) for the heptanoate and the octanoate, and 14.25 ppm for the nonanoate, the decanoate and the dodecanoate micelles. Similar observations, albeit with

larger discrepancies (due to non-negligible through bond δ-effects of the polar head group in the hexanoate chain) can be made for the ω-1 methylene chemical shifts.

Table II.1 ^{13}C *NMR chemical shifts of the single-micelle solutions (1.5 M), relative to Me_4Si^{α}*

atom	$n\text{-}C_{12}$	$n\text{-}C_{10}$	$n\text{-}C_9$	$n\text{-}C_8$	$n\text{-}C_7$	$n\text{-}C_6$
2	38.40	38.48	38.45	38.39	38.34	38.22
3	26.90	26.89	26.83	26.73	26.59	26.15
4	30.47	30.23	30.13	29.89	29.40	31.68
5	30.33	30.23	29.90	29.39	31.78	22.40
6	30.47	30.06	29.81	32.13	22.76	14.00
7	30.20	29.93	32.33	22.90	14.17	
8	30.47	32.46	23.06	14.19		
9	30.04	23.09	14.25			
10	32.52	14.25				
11	23.12					
12	14.25					

$^{\alpha}C_6D_6$ at 128 ppm downfield from Me_4Si.

Corresponding shift differences are observed for carboxylic acids in chloroform. However, these compounds may form inverse micelles in this solvent. A comparative study was also carried out for solutions of n-alkyl TABs[11] in chloroform and water (below the CMC for the latter solvent). The results indicate clearly that the variation within a homologous series of the ^{13}C NMR shifts of inverse micelles and of monomers do not differ significantly. Solutions of n-alkanes do not show a comparable behaviour[30]. Therefore, it is suggested that the observed shift differences for the methyl carbons of the alkanoate micelles indicate the formation of three different micellar solutions. The reason for the differences between n-alkanes and substituted derivatives over such long distances must be due to the propagation of conformational perturbations caused by the substituents. Through bond substituent effects

Table II.2 (De-)shieldings upon mixed-micelle formation as compared with the corresponding single-micelle solutions

affective concentration	mixing ratios [a]	dodecanoate carbons [b]							shorter amphiphile carbons								
		2	3	7	9	10	11	12	2	3	4	5	6	7	8	9	10
1.00:0.50	2:1	+0.05	+0.01	−0.02	−0.05	−0.04	−0.03	−0.02	+0.02	+0.06	+0.15	+0.12	+0.06				
0.75:0.75	1:1		−0.01	−0.12	−0.19	−0.16	−0.13	−0.09	+0.02	+0.04	+0.11	+0.06	+0.03				
0.50:1.00	1:2	+0.09	−0.01	−0.11	−0.21	−0.17	−0.13	−0.08	+0.03	+0.04	+0.09	+0.05	+0.03				
0.38:1.12	1:3	+0.06	−0.01	−0.08	−0.18	−0.15	−0.10	−0.09	+0.01	−0.04	+0.06	+0.03	+0.04				
0.30:1.20	1:4	+0.09	−0.01	−0.12	−0.22	−0.16	−0.11	−0.04	+0.01	−0.04	+0.06	+0.06	+0.04				
0.17:1.33	1:8	+0.09		−0.13	−0.24	−0.20	−0.12	−0.02	+0.01	−0.03	+0.04	+0.05	+0.04				
1.00:0.50	2:1	+0.10	+0.03	−0.04	−0.08	−0.06	−0.06	−0.03	+0.01	−0.03	+0.06	+0.09	−0.07	−0.30			
0.15:0.15	1:1	+0.11	+0.03	−0.03	−0.11	−0.09	−0.06	−0.03	+0.02	−0.04	−0.08	+0.10	+0.09	−0.11			
0.50:1.00	1:2	+0.10	+0.01	−0.10	−0.22	−0.15	−0.13	−0.07	+0.01	+0.02	−0.05	+0.05	+0.04	−0.05			
0.38:1.12	1:3	+0.07	+0.01	−0.10	−0.23	−0.19	−0.16	−0.05	+0.00	−0.02	−0.05	+0.05	+0.05	−0.05			
0.30:1.20	1:4	+0.09	−0.01	−0.09	−0.26	−0.22	−0.16	−0.05	−0.00	+0.01	−0.04	+0.04	+0.03	+0.03			
0.17:1.33	1:8	+0.08	−0.15	−0.00	−0.51	−0.55	−0.17	−0.05	−0.02	−0.01	+0.03	+0.04	+0.03	+0.03			
0.75:0.75	1:1	+0.12	+0.05		−0.03	−0.05	−0.04	−0.02	−0.01	−0.03	−0.08	+0.09	−0.06	+0.12	+0.16		
0.50:1.00	1:2	+0.11	+0.04		−0.12	−0.14	−0.14	−0.09	+0.03	+0.02	+0.06	+0.05	+0.06	+0.06	+0.10		
0.75:0.75	1:1	+0.23	+0.08		−0.02	−0.02	−0.02	−0.06	−0.01	−0.01				+0.05	+0.05	+0.14	
0.50:1.00	1:2	+0.16	+0.06		−0.03	−0.05	−0.03	−0.09	−0.00	−0.01				+0.03	+0.08	+0.11	
0.75:0.75	1:1	+0.13	+0.07			−0.01	−0.00	−0.06	−0.01	−0.02					+0.01	+0.03	+0.10
0.50:1.00	1:2	+0.14	+0.03			−0.06	−0.09	−0.08	−0.01	−0.01					+0.00	+0.02	+0.07

[a] Mixing ratios (m/m) are defined as the quotient of the concentrations of the dodecanoate and the shorter amphiphile.

[b] Spectral assignments of the C-4, C-5, C-6 and C-8 atoms of the C_{11} chain were impossible because of overlapping signals, just as the carbons corresponding to the vacancies in the table. About the C-2 and C-3 effects of the C_{11} surfactant in its mixed micelles, one can only speculate. Small deviations in the basicity may bring about these divergences on the chemical shift differences.

are measurable only over small distances (maximally *five* C-C bonds) and thus can hardly contribute. The fact that comparable shift differences are found in the inverse micelles and in the monomers of the fatty acid salts indicates that conformational freedom is not significantly impaired in the latter.

II.4 Theoretical considerations and model description for the mixed-micellar solutions

In Figure 2.2a, the conventional picture of a micelle is presented, according to the classical *Hartley-model*[31]. However, the rodlike shape of the surfactant chains is *not* meant to represent *all-extended* conformations. It is only presented in this way to demonstrate that, on a time averaged basis, all monomers forming the micelle will be equivalent. This also pertains to the number and positions of *gauche* conformers[30].

Recently, theoretical descriptions of micelles have been put forward by *Dill* and *Flory*[32] and *Pratt*[33]. These descriptions are based on a space lattice model combined with *Monte Carlo* type simulations. In the former case, a cubic lattice is used without weighing different chain conformations according to their different energies. In the latter model a diamond lattice is combined with weighing based on a number of interaction energies between head groups and chains, both intra- and intermolecular. In these two respects, the *Pratt model* seems more realistic than the model of *Flory*. Both descriptions share the disadvantage of not being able to accommodate chain conformations of the crank shaft type as proposed many times for lipid bilayers[34] and polymer chains[35]. Even in other simulations these "kinks" are also taken into account[36]. Further arguments against the theory of *Dill* and *Flory* are found in the data of *Zemb* and *Chachaty*[37]. The latter showed that the experimental data of *Cabane*[38], to which *Dill* refers in a more recent paper[39], were unreliable. *Zemb* and *Chachaty* indicated that the paramagnetic relaxation data of *Cabane* did not depend on the absolute rate of internal motions of the micellar particle.
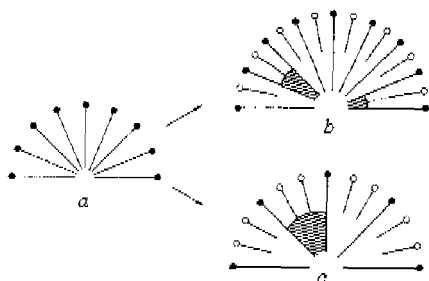
*Figure 2.2   Model for mixed-micelle formation: a) the C_{11}
single micelle; b) the mixed micelle for the 1:1 mixing ratio;
c) the mixed micelle for the 1:2 mixing ratio; the methyls
of the long and short surfactants are denoted as ω_1 and ω_s,
respectively. At constant conformational equilibria of the
C_{11} chains upon mixing, intramicellar cavities (shaded areas)
decrease in dimension upon elongation of the acyl chain length
of the short surfactant (see Figure 2.2b) and increase upon
lowering the mixing ratio (see Figure 2.2c). Open circles
represent the head groups of the short soaps and full circles
represent the head groups of the long (C_{11}) amphiphiles; the
dimensions are not correct. Only a schematic representation
is offered. Rod-like shapes of the acyl chains do not represent
all-extended conformations. The actual conformational behaviour
can be viewed for instance as follows:*
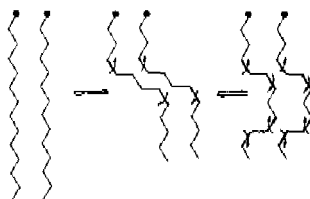
*or any other conformation in which kinks are confined to certain
non-neighbour layers. In reality, the assembled kinks will move
in time about the longitudinal directions of the chains. Kinks
in the shorter amphiphiles in mixed-micellar systems also have
the above-mentioned requirements. The motional freedom in the
ω_s-ω_1 part of the longer chains may be larger.*

26

With regard to the single micelles (see Section II.3), consideration of lattice models instead of conventional micelles would not influence the discussion of our NMR results. However, the lattice model representation is rather convenient to visualize the model of *mixed* micelles of fatty acid soaps of different acyl chain lengths (see Figure 2.3a). A number of facts can be deduced.
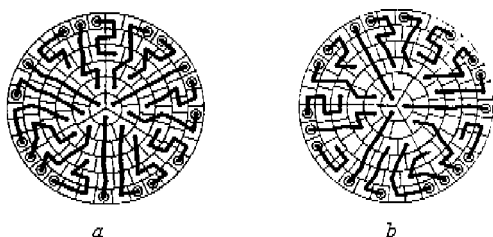
Figure 2.3   Lattice model representation after Dill and Flory[32]; a) twodimensional representation of the cross section of a cylindrical micelle. Lattice sites, each containing ca. 3.6 methylene groups[32], are indicated. Head groups are situated in the outer layer. The figure is not meant to reproduce a time-averaged basis, but rather a momentaneous view; b) two-dimensional representation of the cross section of a cylindrical mixed micelle, analogous to a).

First, with complete filling of all outer lattice sites by chain segments (it is more appropriate to consider methylene groups rather than chain segments[32], as this is more realistic from a practical point of view), the long amphiphile chains would have to assume lateral displacements (*gauche* conformations in reality) at or very close to the ω_s carbon atom, which should lead to open lattice sites in the center of the micelle. Under the assumption of complete filling, however, this results in smaller micelle diameters[32]. This conforms to the strategy taken by, e.g., *Lindman et al.*[17]. Secondly, without complete filling[32], open lattice sites are created between two adjacent long chains (between the ω_{s+1} carbons). These vacancies or cavities "move" in time over a complete layer parallel to the

27

aqueous interface occupied by the polar head groups[32], thus creating larger *average* distances between the long chains. The same occurs for layers farther inside the micellar core, *but to a lesser extent* (see Figure 2.3b). Thirdly, the number of lattice sites within a given layer could be adapted for mixed micelles compared with the single micelles. So complete filling over all lattice sites is maintained. These sites, however, have to possess larger dimensions. This would lead to essentially the same consequences and conclusions as in the second case (*vide supra*).

We are thus left with two basically different possibilities: increased "folding" (with respect to their single micelles) of the long chains in the mixed micelles (*vide supra:* the first consequence) or rather constant conformational equilibria of the long chains (with respect to their single micelles) leading to larger average interchain distances (*vide supra:* the second and third consequence). Both processes would lead to increased shielding for the $\omega_s - \omega_l$ parts of the long-chain surfactant molecules but with *different relative magnitudes*. A detailed interpretation in terms of ^{13}C NMR chemical shifts can therefore be offered. The shieldings, concomitant with *gauche conformations* in the acyl chains, are given in Table II.3a. These values are derived from literature data[30,40-43]. Shieldings arising from *increased interchain distances* should reflect the relative sensitivities or site factors of the methyl and the various methylene groups[44,45]. In practice, this means that relatively large effects are observed for the methyl signals[30]: ca. three times larger as compared with methylene carbon signals (for different methylenes, the variance of the extra interchain distances along the direction of the chains would have to be considered as well, in theory).

The consequences of the model presented here in terms of ^{13}C NMR chemical shift differences can be summarized as follows (see also Figure 2.2b and Figure 2.2c). Shielding effects are to be expected for the ω_1 through the ω_{s+1} carbon atoms of the $n\text{-}C_{11}$ chains, caused by decreasing *van der Waals* interactions and increasing contributions of *gauche* conformations. These effects will be enhanced upon

solubilization of more short chain amphiphile (Figure 2.2b and 2.2c). If only decreasing *van der Waals* interactions participate upon mixed-micelle formation without conformational changes, it is possible to offer the contributions to the chemical shift changes purely from geometrical considerations. The methyl carbons of the short soap molecules will approach the ω_{s+1} carbons of the longer $n\text{-}C_{11}$ chain. Consequently, a maximal shielding will appear at or near the ω_{s+2} carbon of the $n\text{-}C_{11}$. Furthermore, there will be a gradient of shielding, decreasing towards the terminal methyl carbon of the long surfactant. When the concentration of the short chain amphiphile is raised, the changes for the $\omega_s\text{-}\omega_1$ part of the dodecanoate molecules will be larger, but it is expected that the maximum effects remain on the same carbons of the long chains. This is borne out by our results. In addition, the possibility of a maximum solubility of the shorter soap molecules into the longer soap micelles always has to be taken into account. For the short-chain soap molecules, deshieldings with respect to its single micelle are to be expected because of three reasons. First, the chain is transferred from a medium consisting of short acyl chains (plus water in the case of monomeric solutions) to longer dodecanoate chains[44-46]. Secondly, the packing in the mixed micelle presumably will be tighter than in the short-chain single micelle, causing smaller interchain distances and larger *van der Waals* interactions. If only these solvent effects participate, the deshieldings should reproduce the respective site factors, thus leading to maximal differences for the methyl carbons[30,44-46]. Thirdly, also conformational changes towards extension may contribute. Then, contrary to the effects packing induces, relative deshieldings as indicated by *opposite* values of Table II.3a should occur.

II.5 *Discussion*

The observed ^{13}C NMR chemical shifts of the dodecanoate single micellar solution upon dilution over the concentration range of 1.5 M to 0.15 M indicate that no changes in aggregation numbers and concomitant changes in chain

	C-12	C-11	C-10	C-9	C-8	C-7	C-6
I				-4	-2	-2	-4
II			-4	-2	-2	-4	
III		-4	-2	-2	-4		
IV	-5	-2	-2	-4			

I: *gauche* C-7/C-8; II: *gauche* C-8/C-9; III: *gauche* C-9/C-10; IV: *gauche* C-10/C-11. [a]From references[36-40].

Table II.3b   Simulations of the experimental data in terms of conformational changes only (in ppm)[b]

	C-12	C-11	C-10	C-9	C-8	C-7	C-6
C_{11}/C_7[a] (1:2)	-0.07	-0.13	-0.20	-0.17	-0.10	-0.13	
C_{11}/C_6[a] (1:2)	-0.10	-0.11	-0.15	-0.22	-0.15	-0.11	-0.08

[b]Only decimals best resembling the experimental values (see Table II.2) are mentioned. Conformational ratios were 1.4% IV; 2.5% III and 3.2% II for the C_{11}/C_7 mixed micelle and 2.0% IV; 1.8% III; 1.8% II and 2.0% I for the C_{11}/C_6 mixed micelle.
[a]Mixing ratios: see footnote Table II.2.

conformations occur (*vide supra*)[13]. Therefore, the shift differences for the dodecanoate chains which occur upon formation of mixed micelles are to be ascribed exclusively to the inclusion of shorter chains or the replacement of *n*-C_{11} chains by shorter ones. NMR-measurements would probably not distinguish between these phenomena. The latter model,

however, was postulated by *Brady*[47]. Although the conditions
for the latter experiments and those described in this
Section differ significantly, a certain analogy between the
two situations cannot be denied. The basic idea of the model
presented here is not impaired by the uncertainty regarding
inclusion versus replacement.

The enclosure of hexanoate molecules in dodecanoate
micelles causes a clear gradient of shielding along the long
chains from the ω_1 methyl towards the ω_s (i.e. C-6) methylene
group. It indicates that changes in *van der Waals*
interactions prevail over conformational changes. A measurable
contribution of the latter effect can, however, not be ruled
out. This stands in contrast with mixed micelles of
dodecanoate and heptanoate or longer soaps than the latter.
Consider, e.g., the dodecanoate/heptanoate mixed micelle
at a mixing ratio of 1:2. The following shieldings were
observed for the dodecanoate chain with respect to its single
micelle (see Table II.2):

C-12	C-11	C-10	C-9	C-8	C-7	C-6
-0.07	-0.13	-0.18	-0.22	-	-0.10	-

In order to explain these changes as far as possible in terms
of conformational changes, one would have to assume the
following percentages of *extra gauche* conformers (see
Table II.3b): 1.4% of IV, 2.5% of III and 3.2% of II. This
optimal conformational rearrangement is closest to the
experimental values (see Table II.2). It is still impossible
to take large contributions of *gauche* conformers into account
due to the discrepancy between the observed and calculated
relative shift differences. Other simulated conformational
rearrangements resulted in even larger discrepancies with
the observed chemical shift differences. It is useful to
mention, that the interchain distances between the
dodecanoate chains may be only 10-30% larger than in the
single micelles (sum of *van der Waals* radii) to cause
sizeable shielding[50].

From these simulations, it can be observed that a definite conclusion, regarding the distinction between changes in packing or in conformation of the $n\text{-}C_{11}/n\text{-}C_6$ mixed micelles, could not be reached due to the inability to resolve the relevant C-8 resonance of the dodecanoate chain properly. However, it seems very unrealistic to explain a shielding gradient, comparable to the one observed, completely in terms of conformational changes, because there should be a large contribution of kinks around the $\omega_{1-4}\text{-}\omega_{1-3}$ bond, which seems very unlikely from a steric point of view. Furthermore, kinking around the $\omega_{1-1}\text{-}\omega_{1-2}$ linkage would result in a large shielding at the ω_1 methyl group which has not been observed. Thus, as already stated, decreasing *van der Waals* interactions (i.e. packing) are the factors mainly governing the results described here. This occurrence of chain separation between the dodecanoate chains in their mixed micelles is contrary to previously reported results on $C_{16}TAB/C_{14}TAB$ mixed micelles and solubilization of 1-decanol in octanoate micelles[17].

The values of the $n\text{-}C_{11}/n\text{-}C_5$ mixed micelles (see Table II.2) show increased shielding for the dodecanoate chain protruding from the solubilized short soap molecules, for the 2:1 through the 1:1 mixing ratio. At smaller ratios the shieldings remain fairly constant. This implies a maximal solubilization of ca. one equiv. of hexanoate. At higher concentrations of the $n\text{-}C_5$ surfactant, mixed micelles coexist with monomers of the hexanoate anion. In the following scheme the observations are summarized:

$$C_{11} \quad + \quad aC_5 \quad \longrightarrow \quad C_{11}/C_5 \quad + \quad (a\text{-}1)C_5$$

single micelle   monomers   1:1 mixed micelle   monomers

For the $n\text{-}C_{11}/n\text{-}C_6$ mixed micelles comparable observations were made. As already mentioned (*vide supra*) comparison of calculated (Table II.3) with observed (Table II.2) *shieldings* indicated pronounced contributions of *van der Waals* solvent effects rather than conformational changes. Consequently,

it was made plausible that chain separation mainly caused
the observed shieldings. Moreover, the solubilization of
heptanoate increases to ca. two equiv., as can be deduced
from Table II.2. *Monte Carlo* calculations[48] reveal that
the conformational free energy minimum of closely packed
alkyl chains is proportional to the alkyl chain length.
Under the assumption that head group/solvent and head
group/head group interactions in single micelles of
dodecanoate are comparable to their mixed micelles, only
alkyl interchain interactions are important in the process
of mixed-micelle formation. This explains an enhanced
solubilization when increasing the acyl chain length from
six to seven carbons. Dodecanoate shielding effects increase
from the 1:2 mixing ratio and reach a constant value at
lower ratios. The chemical shift changes of the heptanoate
component upon increasing its percentage proceed
analogously to those observed for the hexanoate detergents
in their mixed micelles. Thus, for lower mixing ratios, it
is obvious that 1:2 mixed micelles coexist with heptanoate
monomers up to the 1:8 mixing ratio. At this ratio, the
remaining heptanoate detergent molecules would form a
solution with a concentration exceeding their CMC-value[49].
Consequently, heptanoate micelles would be formed. The
heptanoate soaps would equilibrate between the mixed and
the single micelles. As random mixing is preferred, a new
situation for the dodecanoate soap molecules might occur,
involving a statistical distribution over the available
micelles. In this way, heptanoate micelles would be formed
with one to two dodecanoate molecules included. We like to
speculate, that for the latter chains the C-9 and C-10
carbons would presumably be located in the center of the
heptanoate micelle. In this region, the average distance
of both carbon atoms to other ones will be relatively large,
causing smaller *van der Waals* interactions. The ω_1 methyl
effects are almost independent of the n-alkyl chain length
of the solubilized partner as can be seen from the chemical
shift differences of the mixed soaps. The intermolecular
distances between the ω_1 methyls apparently depend only on

the concentration of solubilized short-chain component. So
at comparable mixing ratios elongation of the chain of the
short amphiphile decreases the volume of the cavities
between the $n-C_{11}$ chains, as can be deduced from the
decreasing shielding effects of the $n-C_{11}$ methylenes from
ω_s to ω_1 (see also Figure 2.2). From the deshieldings of
the short-chain soap molecules in the mixed micelles ($n-C_5$
up to $n-C_9$), it is clear that both the decanoate and the
nonanoate are in good agreement with previously observed
solvent effects[30,46]. The octanoate and the heptanoate are
borderline cases, while the hexanoate matches with the
deshielding effects of solubilized pentanol in octanoate
micelles[17]. These deshieldings are attributable to the
extension of the hexanoate molecules as compared with their
single-micellar reference solution[17]. This can be seen
by using the *opposite* values of Table II.3a. In the next
chapter of this thesis, this extension and its simulation
will be discussed in more detail by means of mixed micelles
of a short-chain lecithin and hydrocarbon compounds of
different chain lengths. Finally, the ^{13}C NMR data of the
$C_{16}TAB/C_{14}TAB$ mixed micelles, studied by *Lindman et al.*[17],
correspond nicely with those of the 1:1 mixed micelle of
the $n-C_{11}$ and $n-C_9$ soaps of this study. In retrospect, the
$C_{16}TAB/C_{14}TAB$ mixed micelles form a special case of the more
general situation as presented in detail in this chapter.

II.6 Summary/Conclusions
   Observed ^{13}C NMR chemical shift changes with respect
to their single micelles upon mixed-micelle formation of
potassium dodecanoate and short-chain potassium carboxylates
(hexanoate up to and including decanoate) were ascribed in
all but one case to increasing distances between the apolar
ends of the long amphiphile chains as compared with its
single micelle. Only at an effective chain length difference
of ca. *six* carbon atoms as for the dodecanoate/hexanoate
micellar systems can a different conformational equilibrium
of the dodecanoate chain not be excluded.
   Furthermore, recently observed solvent effects upon

mixing of *n*-alkanes of different chain lengths[30,40] are compared with both the decanoate and nonanoate chemical shift changes upon mixing with the dodecanoate amphiphiles. This leads to the conclusion that the former detergents are mainly subject to increased intermolecular chain packing. Observed effects for the octanoate and heptanoate are not as pronounced, and these soaps should be considered as borderline cases, while the hexanoate undergoes conformational changes towards more extension.

Finally, it is observed that maximally ca. one equiv. of hexanoate or ca. two equiv. of heptanoate can be incorporated into micelles of potassium dodecanoate. At higher percentages of short-chain soaps, these maximally incorporated mixed micelles coexist with short-chain soap monomers up to the concentration where the short-chain soaps reach their CMC-value and form micelles. Then a statistical distribution of dodecanoate molecules in short-chain micelles is attained.

II.7 Experimental

Potassium alkanoates were prepared by neutralizing the corresponding carboxylic acids (Fluka AG) with potassium hydroxide (Merck AG) and purified by recrystallization from methanol. Stock solutions of 1.5 M were prepared with deionized water and stabilized with 0.1 M of potassium hydroxide. Mixed-micelle solutions were obtained from the stock solutions by adding the appropriate amounts. The resultant solutions were sonicated for 15 min. at 25°C and then allowed to stand for 5 days before measurement.

All ^{13}C NMR spectra were run at 62.93 MHz on a Bruker WM 250 spectrometer under proton noise decoupling. The deuterium signal from C_6D_6 was employed as external lock signal. All chemical shifts are related to Me_4Si (C_6D_6 at 128 ppm downfield from Me_4Si). Eight transients corresponding to a spectral width of 2 KHz were accumulated in 32K data points limiting the resolution to 0.005 ppm. Pulse width was set to a 90° flip angle.

1. R.J.M. Tausk, J. Karmiggelt, C. Oudshoorn and J.Th.G. Overbeek, Biophys. Chem., 1974, *1*,175;
   R.J.M. Tausk, J. van Esch, J. Karmiggelt, J. Voordouw and J.Th.G. Overbeek, Biophys. Chem., 1974, *1*,184;
   R.J.M. Tausk, C. Oudshoorn and J.Th.G. Overbeek, Biophys. Chem., 1974, *2*,53.

2. A.T. Florence, "Micellization, Solubilization and Microemulsions", Part 1 (K.L. Mittal, Ed.), Plenum Press, New York, 1977, 55.

3. B. de Kruijff, A.J. Verkleij, C.J.A. van Echteld, W.J. Gerritsen, C. Mambers, P.C. Noordam and J. de Gier, Biochim. Biophys. Acta,1979, *555*,200.

4. a) P.R. Cullis and B. de Kruijff, Biochim. Biophys. Acta, 1979, *559*,399.
   b) D.A.N. Morris, R. McNeil, F.J. Castellino and J.K. Thomas, Biochim. Biophys. Acta, 1980, *599*, 380.
   c) K. Elamrani and A. Blume, Biochemistry, 1982, *21*,521 and references therein.
   d) S.E. Schullery, T.A. Seder, D.A. Wienstein and D.A. Bryant, Biochemistry, 1981, *20*,6818.

5. R. Verger and G.H. de Haas, Annu. Rev. Biophy. Bioeng., 1976, *5*,77.

6. G.H. de Haas, A.J. Slotboom and H.M. Verheij, "Cholesterol Metabolism and Lypolytic Enzymes", (J. Polonovski, Ed.) Masson, New York, 1977, 191.

7. T.T. Algyer and M.A. Wells, Biochemistry, 1979, *18*,4354.

8. J. Seelig and A. Seelig, Biochim. Biophys. Acta, 1975, *406*,1.

9. J. Seelig, Biochem. Soc. Trans., 1978, *6*,40 and references therein.

10. M.F. Roberts, A.A. Bothner-By and E.A.Dennis, Biochemistry, 1978, *17*,935.

11. Chapter III of this thesis.

12. B. Lindman and H. Wennerström, Top. Curr. Chem., 1980, *87*,1.

13. B. Persson, T. Drakenberg and B. Lindman, J. Phys. Chem.,

1979, *83*,3011.

14. J. Umemura, D.G. Cameron and H.H. Mantsch, J. Phys. Chem., 1980, *84*,2272.

15. B. Persson, T. Drakenberg and B. Lindman, J. Phys. Chem., 1976, *80*,2124.

16. T. Drakenberg and B. Lindman, J. Colloid Int. Sci., 1973, *44*,184.

17. a) J.B. Rosenholm, T. Drakenberg and B. Lindman, J. Colloid Int. Sci., 1978, *63*,538.
    b) J. Ulmius, B. Lindman, G. Lindblom and T. Drakenberg, J. Colloid Int. Sci., 1978, *65*,88.

18. Abbreviations used: $C_{16}TAB$, hexadecyl trimethylammonium bromide; $C_{14}TAB$, tetradecyl trimethylammonium bromide; $n-C_{11}$, potassium dodecanoate; $n-C_9$, potassium decanoate; $n-C_8$, potassium nonanoate; $n-C_7$, potassium octanoate; $n-C_6$, potassium heptanoate; $n-C_5$, potassium hexanoate; CMC, critical micelle concentration.

19. S.C. Chen and J.M. Sturtevant, Biochemistry, 1981, *20*,713, and references therein.

20. R.A. Burns and M.F. Roberts, Biochemistry, 1980, *19*,3100.

21. a) D. Canet, J. Brondeau, H. Nery and J.P. Marchal, Chem. Phys. Lett., 1980, *72*,184 and references therein.
    b) E. Williams, B. Sears, A. Allerhand and E.H. Cordes, J. Amer. Chem. Soc., 1973, *95*,4871.

22. H. Wennerström, B. Lindman, O. Söderman, T. Drakenberg and J.B. Rosenholm, J. Amer. Chem. Soc., 1979, *101*,6860.

23. M. van Bockstaele, J. Gelan, H. Martens, J. Put, F. de Schrijver and J.C. Dederen, Chem Phys. Lett., 1980, *70*, 605.

24. R. Friman, K. Petterson and P. Stenius, J. Colloid Int. Sci., 1975, *53*,90.

25. B. Lindman, H. Wennerström, H. Gustavsson, N. Kamenka and B. Brun, Pure Appl. Chem., 1980, *52*,1307.

26. T.S. Brun, H. Høiland and E. Vikingstad, J. Colloid Int. Sci., 1978, *63*,89.

27. E. Vikingstad and H. Høiland, J. Colloid Int. Sci., 1978, *64*,510.

28. D. Stigter, J. Phys. Chem., 1974, *78*,2480.

29. P. Mukerjee and K.J. Mysels, ACS Symp. Ser., 1975, *9*, 239.

30. J.W. de Haan, L.J.M. van de Ven and L. Bučinská, J. Phys. Chem., 1982, *86*,2517.

31. G.S. Hartley, "Aqueous solutions of paraffin chain salts", Herman and Cie, Paris, 1936.

32. a) K.A. Dill and P.J. Flory, Proc. Natl. Acad. Sci. U.S.A., 1980, *77*,3135.
    b) K.A. Dill and P.J. Flory, Proc. Natl. Acad. Sci. U.S.A., 1981, *78*,676.

33. S.W. Haan and L.R. Pratt, Chem Phys. Lett., 1981, *79*, 436.

34. A. Seelig and J. Seelig, Biochemistry, 1974, *13*,4839 and references therein.

35. C. Blomberg, Chem. Phys., 1979, *37*,219 and references therein.

36. J. Skolnick and E. Helfand, J. Chem. Phys., 1980, *72*, 5489.

37. T. Zemb and C. Chachaty, Chem. Phys. Lett., 1982, *88*, 68.

38. B. Cabane, J. Physique, 1981, *42*,847.

39. K. Dill, J. Phys. Chem., 1982, *86*,1498.

40. J.W. de Haan, L.J.M. van de Ven, A.R.N. Wilson, A.E. van den Hout-Lodder, C. Altona and D.H. Faber, Org. Magn. Res., 1976, *8*,477.

41. H.N. Cheng and F.A. Bovey, Org. Magn. Res., 1978, *11*, 457.

42. H.J. Schneider and W. Freitag, J.Amer. Chem. Soc., 1976, *98*,478.

43. G. Mann, E. Kleinpeter and H. Werner, Org. Magn. Res., 1978, *11*,561.

44. D. Cans, B. Tiffon and J.E. Dubois, Tetrahedron Lett., 1976, *34*,2075.

45. B. Tiffon and J.P. Doucet, Can. J. Chem., 1976, *54*,2045.

46. A.R.N. Wilson, L.J.M. van de Ven and J.W. de Haan, Org. Magn. Res., 1974, *6*,601.

47. G.W. Brady, Acc. Chem. Res., 1974, *7*,174.

48. B. Lemaire and P. Bothorel, Macromolecules, 1980, *13*,311.

49. P. Mukerjee and K.J. Mysels, Natl. Stand. Ref. Data
    Ser. (U.S., Natl. Bur. Stand.), NSRSDS-NBS, 1971, *36* .
50. a) W.L. Earland and D.L. Vanderhart, Macromolecules,
    1979, *12*,762.
    b) C.A. Fyfe, J.R. Lyerla, W. Volksen and C.S. Yannoni,
    Macromolecules, 1979, *12*,757.

CHAPTER III

Mixed micelles of dioctanoyl-L-α-lecithin and hydrocarbon amphiphiles. Aspects of fluidization

III.1 Introduction

The importance of micelle-forming phospholipids in biomembranes has often been stated, for example, as carriers for membrane-bound enzymes[1,2] or transmembrane transport-enhancing constituents within a bilayer membrane or particles stimulating cell division[2]. Conformational and motional behaviour of head groups and acyl tails and perhaps also intermolecularly correlated molecular ordering[3] may well be of great interest for these regulations. Efforts have been made in the elucidation of the conformational structures of micelles of short-chain lecithins by means of different spectroscopic methods. By ^{1}H NMR the intrinsic nonequivalence of the *sn*-1 and *sn*-2 acyl chains of dioctanoylphosphatidylcholine and dipalmitoylphosphatidylcholine is visible[4]. In total, four separate α protons were observed; the remaining proton signals either overlapped or were not assigned. The explanation was given in terms of different conformational behaviours of both chains, as suggested earlier by *Seelig et al.*[6], who studied the gel phase and liquid crystalline phase of dipalmitoylphosphatidylcholine and dipalmitoylphosphatidylethanolamine. In this picture, the *sn*-1 and *sn*-2 chains run parallel to each other except for bending of the *sn*-2 chain near the C-2 carbon atom. This results in different effective chain lengths[6]. Recently, also ^{13}C NMR spectra were published for dibutyryl-, dihexanoyl-, diheptanoyl- and dioctanoylphosphatidylcholine[5]. Again, the intrinsic nonequivalent chains resulted in partially resolved spectra. In the present study ^{13}C NMR spectra with considerably better resolution will be presented. For all

40

but two carbons separate signals were observed and assigned to the *sn*-1 and *sn*-2 chains. It will be shown that micelles of DOPC[7] resemble mixed micelles of *n*-alkyl detergents bearing chains of nonequivalent lengths. Increasing the effective chain length difference upon elongation of the *sn*-1 chain causes fluidization near the apolar middle region of the bilayer. *Keough et al.*[8] described this fluidization in terms of intermolecular ordering. *Stümpel et al.*[9] supposed intramolecular contributions like disordering conformational changes. However, *van der Waals* attractive interactions either were ignored[9] or were presumed to be constant[8]. In our opinion, the latter have to contribute (see Chapter II). More explicitly, the extent to which (intermolecular) *van der Waals* attractions on the one hand and (intramolecular) conformational changes on the other hand cause fluidization should be a function of the effective chain length difference. Recently, a method has been developed for interpreting ^{13}C NMR spectra of mixed micelles of different alkanoates[10]. This was performed in terms of conformational equilibria changes with respect to the single micelles on the one hand and decreasing chain packing on the other hand (see Chapter II). It was possible to distinguish these two factors to a certain extent. Also the possible influence of solvent effects on the spectra were mentioned. The model of Chapter II will now be applied to mixed micelles of DOPC and several TABs. It describes the connection between packing, conformations and the effective chain length difference (*vide supra*) with respect to the process of fluidization.

III.2 *Results*

^{13}C NMR chemical shifts of the micelles have been assigned by combining literature data and relative relaxation time values, assuming that T_1 values increase towards the apolar ends[5,12]. Such a pattern was first suggested by *Allerhand et al.*[12a] and subsequently by others[12b-e]. It is primarily based on increased segmental motions or rotational diffusions near the free ends of the chains.

Such a pattern is quite general. Results are presented in Table III.1. Tables III.2-6 show the chemical shift changes of the mixed micelles with respect to the micelle solutions of the pure detergents. Assignments of the different carbon pairs to the *sn*-1 and *sn*-2 chains have been performed by assuming that the spin-lattice relaxation times of the carbons of the *sn*-1 chain are larger compared to those of the *sn*-2 chain[5]. Figure 3.3 shows the effects of TABs on the head group mobility of the DOPC in the mixed micelles. Table III.7 indicates the effects of TABs on the chemical shifts and line widths of individual lipidic head group nuclei.

III.3 Reference solutions for the mixed micellar solutions: the single micelles

The present measurements yield a better resolution for the DOPC micelles (see Table III.1) with respect to recently published data[5]. The visibility of the nonequivalent behaviour is *not* restricted to carbon atoms close to the carbonyl function[5] but extends over almost the complete chains. The ω-methyl resonances of the lecithin show shielding compared with *micellar* solutions of the quaternary ammonium detergents. Since water penetration can be ruled out[5], it will be shown that a decreased chain packing within the lecithin micelles may be possible. From geometrical considerations[13], the micellar shape of the lecithin aggregates has an average area per lipid head group comparable with that of the TABs, because lipid head group repulsions should not be affected significantly by the presence of one or two alkyl chains attached to each head group. If the lecithin aggregates were spherical, the average head group area would be twice as large as the area per emerging chain with respect to spherical TAB micelles. The increase in the lipid particle size results in a decrease of the average surface area[13], which in turn results in a tighter packing of the head groups, in order to optimize head group interactions, and consequently in a looser packing of the ω-methyls. Indeed, the lecithin micellar

42

shape was found to be rather rod-like[14].

The ^{13}C NMR chemical shifts of the DOPC micelles were insensitive to concentrating the solution from 5 mM to 50 mM. It indicates that no changes in molecular packing and conformational changes occur[15]. As the micellar size of the lecithin aggregates is larger than spherical, this growth of the DOPC micelles apparently does not influence the ^{13}C NMR spectra significantly, since the line widths are also constant over the entire concentration range.

Furthermore, the results indicate a similarity between the behaviour of mixed n-alkanoates of different chain lengths[10] and synthetic short-chain lecithins in an aqueous medium. Both systems represent a magnetic nonequivalence between the different alkyl chains for comparable carbon atoms.

In Table III.1 the chemical shift values of the TABs are mentioned, which will serve as the reference systems for the TABs in their mixed micellar systems with DOPC.

III.4 Mixed micelles of DOPC and several n-alkyltrimethylammonium bromides

III.4.1 Hydrophobic region: analytical considerations

Several aspects have to be considered upon interpreting ^{13}C NMR chemical shifts of DOPC micelles mixed with amphiphiles of different effective chain lengths. Analogous situations in simple mixed micelles of alkanoates have been discussed in detail in the preceding Chapter (see Section II.4). It was shown that mainly two factors will influence ^{13}C NMR chemical shifts of alkane moieties, *vis.* different conformational equilibria and/or different environments[10,18]. Sometimes, these two factors are interconnected[17]. Different environments per se (solvents, packing) will cause different medium effects on the chemical shifts. The relative magnitudes at different positions in a solute are governed by site factors[18,20]. For convenience, *relative* site factors (in ppm) within an alkane fragment are presented in Figure 3.1e. So that *van der Waals* solvent effects on the one

43

hand and conformational changes on the other hand could be distinguished, a schematic representation of the chemical shift changes is also offered (Figure 3.1). In terms of ^{13}C NMR chemical shift changes Figure 3.1a reproduces schematically the influence of contributions of *gauche* conformers for the alkyl fragments investigated here. Literature data from *Mann*, *Bovey*, *Schneider*, *de Haan* and coworkers[17,21] were combined in order to arrive at the absolute values of the chemical shift changes upon the formation of a single *gauche* from an *anti* conformer. With respect to an *anti* conformer, carbons at a relative 1,4 *gauche* position are shifted upfield by about 4 ppm (except ω-methyls which are shifted upfield by about 5 ppm). Intermediate carbons change by about half this magnitude. Taking into account all possible *gauche* conformers in different ratios results in the shielding patterns presented in Figure 3.1b-c. Figure 3.1d shows the opposite effects due to generating possible *anti* conformers from *gauche* conformers. Quite obviously, no clear-cut distinction between the two aspects is possible in all cases. However, combining the literature data of Figure 3.1 and the experimental data of Tables III.2-6, it is possible to indicate approximately to what extent conformational changes on the one hand and medium effects on the other hand will contribute to the observed chemical shift changes.

III.4.2 Hydrophobic region: geometrical considerations

A few consequences of the combined influences of conformational changes and alterations in environment will now be discussed, in close analogy with mixed fatty acid soap micelles[10].

First, shielding is expected for carbon atoms of those parts of the TAB chains which protrude from the DOPC acyl chains (Figure 3.2). The average distances between those alkyl chain fragments are then larger than in their single micellar solutions. This is the case for the $C_{12}TAB$ up to the $C_{18}TAB$ detergent. Larger interchain distances cause a diminution of *van der Waals* solvent effects. In addition,

a

-5 CH3   -4 CH2   -4 CH2   -4 CH2
CH2 — CH2   CH2 — CH2
-2   -2   -2   -2

b

I   II

ratio I:II = 1:9

	C-16	C-15	C-14	C-13	C-12
Calc.	-0.32	-0.16	-0.14	-0.27	-0.03
Exp.	-0.30	-0.16	-0.16	-0.17	-0.12

c

I   III
II   IV

ratio I:II:III:IV = 0:2:2:6

	C-18	C-17	C-16	C-15	C-14	C-13	C-12
Calc.	-0.29	-0.19	-0.23	-0.30	-0.12	-0.08	0.00
Exp.	-0.29	-0.20	-0.23	-0.29	-0.22	-	-

d

	C-8	C-7	C-6	C-5	C-4	C-3	C-2	C-1
Calc.	+0.10	+0.12	+0.21	+0.26	+0.26	+0.21	+0.12	+0.08
Exp.	+0.10	+0.13	+0.21	+0.26	+0.26	+0.19	+0.16	-

e

-5 -3 -1 -2 -2 -2
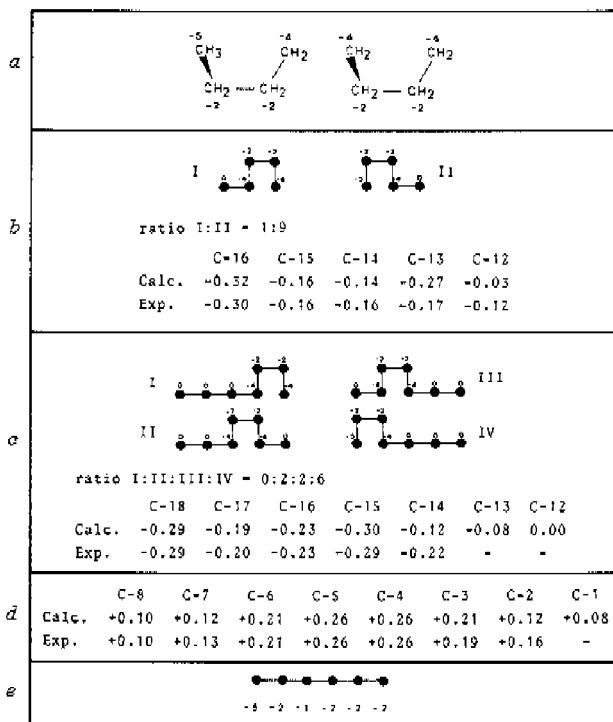
Figure 3.1   The influence (in ppm) of single gauche conformers on the ^{13}C NMR chemical shifts of all-extended hydrocarbon chain fragments (a).(b) Possible gauche conformers of that part of the C_{16}TAB chain protruding from the DOPC molecules in their mixed micelles. Full circles at the left side of the chain fragments represent the methyls. The calculated shielding pattern which resembles closest the experimental data of the C-12/C-16 segment is given. It was obtained by weighing the gauche conformers in the ratio indicated. (c) Similar to b, for C_{18}TAB in mixed micelles with DOPC. Again only values which are closest to the experiments are mentioned. (d) Deshielding pattern of C_8TAB in DOPC micelles obtained with opposite values of a, assuming almost equal contributions of anti conformers around all bonds. (e) Relative site factors within an alkane chain fragment due to decreasing van der Waals interactions[18].

Table III.1 References for the mixed-micellar systems.
^{13}C NMR chemical shifts of the single-micelle solutions
(50 mM) relative to Me_4Si[a]

atom	DOPC sn-1	sn-2	C_8TAB	C_{12}TAB	C_{14}TAB	C_{16}TAB	C_{18}TAB
2	34.43	34.52	22.40	23.08	23.26	23.32	23.38
3	25.18	25.31	25.93	26.38	26.59	26.66	26.72
4	29.45	29.51	28.55	29.20	29.52	29.62	29.72
5	29.35[b]	29.41[b]	28.55	29.57			
6	32.12	32.12	31.41	29.71[b]			
7	22.89	22.94	22.71	29.84[b]			
8	14.08	14.13	13.87	29.84[b]			
9				29.51			
10				32.11	30.14		
11				22.84	29.79	30.38	
12				14.17	32.32	30.22	
13					22.99	29.87	
14					14.25	32.38	30.25
15						23.03	29.96
16						14.26	32.44
17							23.08
18							14.29

^{a}C_6D_6 at 128 ppm downfield from Me_4Si.
^{b}Resonances could not be assigned properly because of little
or no differences in T_1-values.

Figure 3.2 Average orientation of monomers within a part of
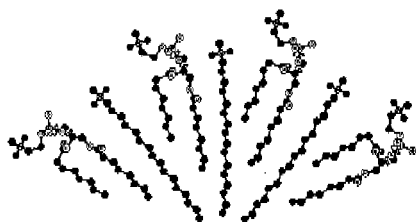a cross-section of a 1:1 mixed micelle of DOPC and C_{16}TAB.
For convenience all-extended conformations are drawn.

increased differences in effective chain lengths possibly
lead to conformational changes towards more kinking. This
is consistent with the conclusions of *Petersen* and *Chan*[16],
and *de Haan* and *van de Ven*[17], who describe intramolecular
alterations as a consequence of correlated intermolecular
van der Waals attractive interactions going from a relatively
ordered (single micellar) state to a relatively disordered
(mixed micellar) state, rather than the reverse. A decrease
in intermolecular interactions (*i.e.* by "chain unpacking")
will lead to shielding, as mentioned for neat and diluted
alkanes[18]. Similar conclusions were reached from ^{13}C NMR
studies of polyethylene in different packing states[19].
Furthermore, it will be obvious that effects are most distinct
in mixed micelles containing an excess of lecithin (*i.e.*,the
4:1 m/m mixing ratio), in which TAB undergoes the largest
perturbation from the surrounding lecithin molecules.

   *Secondly, for the carbons in the part of the TAB chains
which are situated directly in the DOPC acyl chain region
of the mixed micelle, deshieldings are anticipated.* These
are caused by increased *van der Waals* interactions and/or
by an increase in the ratio of *anti* to *gauche* isomers. These
effects are expected also to increase upon raising the
concentration of the zwitterionic detergent (*vide supra*).
Consequently, for the lecithin acyl chains incorporated
in micelles of longer *n*-alkyl chain amphipiles, also
deshieldings are expected due to increasing solvent effects
along with conformational changes towards more extended
forms. If only solvent effects participate, deshieldings
should correspond to the respective site factors, thus
leading to maximal differences for the methyl carbons[20].
These differences increase upon lowering the lipid
concentration.

   *Finally, for the TABs possessing effectively shorter
alkyl chains as compared with DOPC, only deshieldings
are anticipated (vide supra).* Thus, shieldings will occur
for the carbons for those parts of the lecithin acyl chains
which protrude from the *n*-alkyl TAB chains. Recapitulating,
combining literature data of Figure 3.1 and the experimental

data of Table III.2-6 we are now able to indicate approximately to which extent conformational changes on the one hand and solvent effects on the other hand will contribute to the observed chemical shift changes.

carbon no.	mixing ratios				
	4:1	2:1	1:1	1:2	1:4
	C$_8$TAB				
C$_2$	+0.16	+0.11	+0.08	+0.06	+0.03
C$_3$	+0.19	+0.14	+0.10	+0.07	+0.04
C$_4$	+0.26	+0.17	+0.13	+0.08	+0.04
C$_5$	+0.26	+0.17	+0.13	+0.08	+0.04
C$_6$	+0.21	+0.14	+0.10	+0.07	+0.04
C$_7$	+0.13	+0.11	+0.05	+0.04	+0.02
C$_8$	+0.10	+0.07	+0.05	+0.04	+0.02
	DOPC				
C$_2$ (sn-1)	+0.00	+0.00	+0.00	+0.00	+0.00
(sn-2)	+0.00	+0.00	+0.00	+0.00	+0.00
C$_3$ (sn-1)	+0.02	+0.01	+0.01	+0.01	+0.00
(sn-2)	+0.02	+0.00	+0.00	+0.00	-0.01
C$_4$ (sn-1)	+0.00	-0.02	-0.03	-0.04	-0.05
(sn-2)	+0.05	+0.03	+0.02	+0.01	+0.00
C$_5$	+0.04	+0.03	+0.02	+0.01	-0.01
	+0.04	+0.03	+0.02	+0.01	-0.01
C$_6$ (sn-1)	+0.03	+0.01	+0.00	+0.00	-0.02
(sn-2)	+0.03	+0.01	+0.00	+0.00	-0.02
C$_7$ (sn-1)	+0.02	+0.00	+0.00	-0.01	-0.02
(sn-2)	+0.02	+0.00	-0.01	-0.01	-0.03
C$_8$ (sn-1)	+0.00	0.03	-0.03	-0.03	-0.04
(sn-2)	+0.00	-0.02	-0.02	-0.02	-0.03

Table III.2 (De-)shieldings upon mixed-micelle formation of C$_8$TAB and DOPC[a]

[a]The total amphiphile concentration is 50 mM. Mixing ratios are defined as the quotient of the concentrations of the DOPC and the TAB.

carbon no.	mixing ratios				
	4:1	2:1	1:1	1:2	1:4
	C$_{12}$TAB				
C$_2$	+0.21	+0.15	+0.09	+0.04	+0.01
C$_3$	+0.37	+0.28	+0.17	+0.10	+0.04
C$_4$	+0.55	+0.41	+0.29	+0.16	+0.07
C$_5$	+0.59	+0.44	+0.29	+0.17	+0.08
C$_6$[b]	+0.51	+0.43	+0.28	+0.16	+0.08
C$_7$[b]	+0.41	+0.39	+0.26	+0.15	+0.07
C$_8$[b]	+0.49	+0.30	+0.19	+0.10	+0.03
C$_9$	+0.31	+0.26	+0.17	+0.10	+0.04
C$_{10}$	+0.20	+0.16	+0.11	+0.05	+0.02
C$_{11}$	+0.13	+0.06	+0.05	+0.01	+0.00
C$_{12}$	-0.12	0.11	0.10	-0.09	-0.07
	DOPC				
C$_1$ (sn-1)	+0.02	+0.03	+0.06	+0.06	+0.09
(sn-2)	+0.01	+0.03	+0.05	+0.06	+0.09
C$_3$ (sn-1)	+0.03	+0.04	+0.04	+0.04	+0.04
(sn-2)	+0.02	+0.01	+0.01	+0.00	+0.00
C$_5$ (sn-1)	+0.01	-0.01	-0.04		
(sn-2)	+0.05	+0.04	+0.03	-0.01	
C$_3$	+0.06	+0.04	+0.02	+0.01	
	+0.05	+0.04	+0.02	+0.01	
C$_6$ (sn-1)	+0.04	+0.04	+0.02	+0.01	+0.01
(sn-2)	+0.04	+0.04	+0.02	+0.01	+0.01
C$_7$ (sn-1)	+0.04	+0.03	+0.03	+0.03	+0.02
(sn-2)	+0.03	+0.02	+0.02	+0.00	+0.00
C$_8$ (sn-1)	+0.03	+0.05	+0.06	+0.08	+0.09
(sn-2)	+0.03	+0.05	+0.07	+0.08	+0.09

Table III.3 (De-)shieldings upon mixed-micelle formation of C$_{12}$TAB and DOPC[a]

[a]The total amphiphile concentration is 50 mM.
[b]The signals of the carbons could not be assigned properly.

carbon no.	mixing ratios				
	4:1	2:1	1:1	1:2	1:4
	$C_{14}TAB$				
C_2	+0.10	+0.06	+0.03	+0.02	+0.01
C_3	+0.27	+0.20	+0.14	+0.08	+0.05
C_4	+0.38	+0.30	+0.21	+0.13	+0.07
C_{10}			+0.08	+0.08	+0.04
C_{11}	-0.01	+0.03	+0.03	+0.04	+0.03
C_{12}	-0.06	-0.03	-0.01	-0.00	-0.00
C_{13}	-0.11	-0.09	-0.07	-0.03	-0.01
C_{14}	-0.32	-0.30	-0.24	-0.15	-0.08
	DOPC				
C_1 (sn-1)	+0.01	+0.03	+0.05	+0.08	+0.09
(sn-2)	+0.00	+0.02	+0.04	+0.07	+0.09
C_2 (sn-1)	+0.03	+0.03	+0.03	+0.04	+0.04
(sn-2)	+0.01	-0.01	-0.01	-0.01	+0.00
C_4 (sn-1)	+0.00	0.04	-0.07	-0.07	-0.07
(sn-2)	+0.05	+0.03	+0.00	+0.00	-0.01
C_5	+0.04	+0.02	+0.00	+0.01	+0.01
	+0.04	+0.02	+0.00	+0.01	+0.01
C_6 (sn-1)	+0.04	+0.01	+0.00	+0.00	+0.00
(sn-2)	+0.04	+0.03	+0.02	+0.02	+0.01
C_7 (sn-1)	+0.04	+0.04	+0.04	+0.06	+0.06
(sn-2)	+0.03	+0.02	+0.02	+0.04	+0.04
C_8 (sn-1)	+0.03	+0.08	+0.13	+0.18	+0.21
(sn-2)	+0.03	+0.09	+0.13	+0.17	+0.20

Table III.4   (De-)shieldings upon mixed-micelle formation of $C_{14}TAB$ and DOPC[a]

[a] The total amphiphile concentration is 50 mM.

carbon no.	mixing ratios				
	4:1	2:1	1:1	1:2	1:4
	$C_{16}TAB$				
C_2	+0.05	+0.02	+0.02	+0.01	-0.01
C_3	+0.22	+0.16	+0.09	+0.05	+0.03
C_4	+0.48	+0.24	+0.16	+0.08	+0.04
C_{11}	+0.16	+0.14	+0.04	+0.03	+0.04
C_{12}	-0.12	-0.07	-0.02	-0.01	-0.00
C_{13}	-0.17	-0.12	-0.07	-0.04	-0.02
C_{14}	-0.16	-0.12	-0.08	-0.04	-0.02
C_{15}	-0.16	-0.13	-0.07	-0.06	-0.03
C_{16}	-0.30	-0.26	-0.19	-0.12	-0.07
	DOPC				
C_1 (sn-1)	+0.03	+0.04	+0.05	+0.08	+0.09
(sn-2)	+0.01	+0.03	+0.06	+0.08	+0.10
C_3 (sn-1)	+0.04	+0.04	+0.04	+0.04	+0.05
(sn-2)	+0.01	+0.00	-0.01	-0.01	+0.00
C_4 (sn-1)	-0.01	-0.03	-0.05	-0.06	-0.09
(sn-2)	+0.05	+0.03	+0.01	+0.00	+0.00
C_5	+0.04	+0.01	+0.02	+0.02	+0.04
	+0.04	+0.01	+0.02	+0.02	+0.04
C_6 (sn-1)	+0.05	+0.04	+0.03	+0.02	+0.02
(sn-2)	+0.05	+0.04	+0.03	+0.02	+0.02
C_7 (sn-1)	+0.05	+0.06	+0.07		
(sn-2)	+0.03	+0.04	+0.05		
C_8 (sn-1)	+0.11	+0.15	+0.20	+0.25	+0.28
(sn-2)	+0.10	+0.14	+0.18	+0.22	+0.24

Table III.5   (De-)shieldings upon mixed-micelle formation of $C_{16}TAB$ and DOPC[a]

[a] The total amphiphile concentration is 50 mM.

carbon no.	mixing ratios

carbon no.	4:1	2:1	1:1	1:2	1:4
C_{18}TAB					
C_2	−0.01	−0.03	−0.03	0.03	−0.03
C_3	+0.17	+0.11	+0.09	+0.05	+0.02
C_4	+0.24	+0.16	+0.13	+0.07	+0.02
C_{14}	0.22	−0.14	−0.10	−0.02	−0.00
C_{15}	0.29	0.20	−0.17	−0.10	0.07
C_{16}	−0.23	−0.17	−0.14	−0.08	−0.06
C_{17}	−0.20	0.15	−0.13	−0.07	−0.06
C_{18}	−0.29	0.23	−0.20	−0.12	−0.08
DOPC					
C_2 (sn-1)	+0.03	+0.05	+0.06	+0.08	+0.09
(sn-2)	+0.01	+0.03	+0.05	+0.07	+0.09
C_3 (sn-1)	+0.04	+0.05	+0.05	+0.06	+0.06
(sn-2)	+0.01	+0.01	+0.01	+0.02	+0.02
C_4 (sn-1)	+0.00	+0.00	+0.00	+0.00	−0.02
(sn-2)	+0.05	+0.05	+0.05	+0.04	+0.03
C_5	+0.05	+0.05	+0.05	+0.06	+0.05
	+0.05	+0.05	+0.05	+0.06	+0.05
C_6 (sn-1)	+0.06	+0.07	+0.06	+0.07	+0.06
(sn-2)	+0.06	+0.07	+0.06	+0.07	+0.06
C_7 (sn-1)	+0.03	+0.09	+0.10		
(sn-2)	+0.02	+0.06	+0.08		
C_8 (sn-1)	+0.15	+0.21	+0.24	+0.29	+0.31
(sn-2)	+0.14	+0.19	+0.21	+0.26	+0.27

Table III.8 (De-)shieldings upon mixed-micelle formation of C_{18}TAB and DOPC[a]

[a] The total amphiphile concentration is 50 mM.

III.4.3 Hydrophobic region: discussion

Combination of the data of Figure 3.1 and the observed deshieldings upon intercalation of C_8TAB in DOPC micelles leads to the following conclusion. C_8TAB becomes more extended with respect to its monomeric solution[23] over the entire concentration range (Table III.2, the 1:4 up to and including the 4:1 mixing ratio). This is in accordance with recently published observations of *Lindman* and coworkers[22]. Effects are most distinct in mixed micelles containing an excess of lecithin (*i.e.*, the 4:1 mixing ratio), where the C_8TAB undergoes the largest disturbing effect from the lecithin molecules.

Regarding the DOPC/C_{12}TAB mixed micelles, deshieldings are observed for the C-2/C-11 fragment indicating effects comparable with the DOPC/C_8TAB mixed micelles. However, pronounced shielding is obtained for the C-12 carbon. Since no *extra* contributions of *gauche* conformers are feasible (Figure 3.1 vs. Table III.3), only decreasing *van der Waals*

solvent effects are responsible. The reason is that the C_{12}TAB surfactant possesses a greater effective length than the DOPC molecules in the mixed micelles[10], and thus protrudes from the lipid acyl chain region.

Incorporating C_{14}TAB in DOPC micelles leads to an increase of the effective chain length of the TAB amphiphile. This is reflected by the observed shieldings for the C-11/ C-14 segment of the C_{14}TAB with respect to its single micelle. It is clear that conformational changes are possible in this case in principle. For folding around the C-12/C-13 bond one would expect shielding at C-11 (see Figure 3.1a). This is not observed, however (see Table III.4). A decrease in molecular packing is able to cause the experimental chemical shift differences (the chemical shift difference of the C-14 carbon is about three times larger than the corresponding value of C-13, and it is about twice as large as the chemical shift difference of C-12 for the 4:1 mixing ratio). Thus alkyl chain separation as compared with the single micelles is accomplished. Furthermore, the pattern of the observed chemical shift differences of the first eleven carbons resembles that of the C_{12}TAB molecules in their mixed micelles.

For the DOPC/C_{16}TAB mixed micelles shieldings are observed for the C-11/C-16 part of the C_{16}TAB amphiphiles, thus showing once more an increase of the effective chain length. It is still impossible to take large contributions of *gauche* isomers into account (see Figure 3.1 and Table III.5), due to the discrepancy between the observed and calculated chemical shift differences (for all *anti/gauche* ratios). However, comparing observed with calculated chemical shift differences for the C-14/C-18 fragment of the C_{18}TAB surfactant in its mixed micellar systems with DOPC indeed indicates pronounced contributions of *gauche* conformers around the C-16/C-17 carbon bond, apart from unpacking effects (*cf.* the experimental shielding of the C-14 methylene carbon with its calculated value based on conformational changes). In retrospect, the situation described here is similar to that of the mixed micelles

of potassium dodecanoate and potassium hexanoate described in the preceding Chapter (see Section II.5). In this latter case, it was not possible to rule out conformational changes of the dodecanoate chains with respect to their single micelles. A definite conclusion could not be reached due to the inability to resolve the C-8 resonance of the dodecanoate properly.

For the phospholipid in its mixed micelles the chemical shift differences of both chains are retained almost independently of chain length and concentration of the *n*-alkyl TAB. Consequently, this implies a rather unaltered average conformational behaviour of the *sn*-1 and *sn*-2 chains in the mixed micelles. Only *van der Waals* solvent effects change upon mixed-micelle formation with the TABs. This is clearly demonstrated by maximum differences in chemical shift for the methyls[18] reflecting the respective site factors[20]. Logically, induced differences are most pronounced for mixed micelles containing less lecithin (*i.e.*, the 1:4 mixing ratio) and decrease towards the 4:1 ratio. At the lowest ratio the lecithin undergoes the largest disturbing effect from the surrounding TABs. This perturbation fades as the lipid concentration is raised to ratios where the *n*-alkyl amphiphilic TABs become the perturbed moieties in mixed micelles containing lipid molecules (*i.e.*, the 4:1 mixing ratio). So, the possibility has been demonstrated to determine, at least approximately, to what extent TABs incorporated in DOPC micelles undergo additional chain bendings as compared with the single micellar solutions.

III.4.4 Hydrophilic region: analytical and geometrical considerations

Prior to the following discussion (see Section III.4.5) a general principle of lecithin aggregates regarding the dynamical behaviour of the CH_2-$\overset{+}{N}$ linkage of the lipid head group will be discussed[24]. In the preceding Sections, two aspects involving fluidization of the *hydrophobic* core were treated, namely packing and *anti-gauche* isomerizations. In this Section fluidization of the *hydrophilic* region will be

discussed. Recently, it became clear that the conformation
of the lecithin head group is similar in the monomeric, the
micellar and the bilayer state[5,25-28]. Even additives such
as fatty acid derivatives, amphiphiles and cholesterol do
not affect the lecithin head group conformational
equilibria[29-32]. The data of Table III.7 indicate that TABs
also are unable to influence either lecithin head group
conformations or head group motions notably.

Table III.7 ^{31}P *and* ^{13}C *NMR chemical shifts (in ppm), line
widths (in Hz) and* $^{31}P-^{13}C$ *coupling constants (in Hz) for the
mixed micellar solutions of DOPC and* $C_{18}TAB^{a,b}$

DOPC/C_{18}TAB mixing ratios (m/m)

		100:0	50:1	4:1	2:1	1:1	1:2	1:4
^{31}P		0.01	0.01	-0.01	-0.03	-0.07	-0.10	-0.12
^{13}C	CHO[a]	71.14	71.14	71.18	71.20	71.22	71.23	71.24
	CH_2OP[a]	64.17	64.17	64.16	64.18	64.20	64.24	64.27
	CH_2O[a]	63.49	63.49	63.51	63.54	63.58	63.62	63.65
	CH_2OP[d]	66.62	66.62	66.61	66.61	66.62	66.60	66.62
	$CH_2\overset{+}{N}$[d]	59.94	59.94	59.93	59.94	59.95	59.96	59.98
	$\overset{+}{N}(CH_3)_3$[d]	54.60	54.60	54.60	54.60	54.62	54.64	54.65
J_{C-P}	CHO[a]	7.6	7.6	7.6	7.7	7.6	7.3	7.6
	CH_2OP[a]	4.6	4.6	5.0	5.0	5.2	4.8	5.9
	CH_2OP[d]	4.6	4.6	5.0	5.0	4.9	5.0	5.1
$\Delta\nu_{\frac{1}{2}}$	^{13}C	2-4 for all backbone and head group resonances						
	^{31}P	12	7	4	4	4	4	4

[a] ^{31}P chemical shifts relative to 85% H_3PO_4.
[b] Similar results were obtained for the other TABs. Total
amphiphile concentration was 50 mM.
[c] Lipid backbone resonances.
[d] Lipid head group resonances.

No changes in chemical shift and line widths were detected. Thus, conformational and motional changes within this part of the lecithin hardly contribute to the fluidization of the hydrophilic region. However, one type of motion has not been discussed yet, *i.e.* motion of the CH_2-$\overset{+}{N}$ vector around the CH_2-CH_2 head group linkage (see Figure 3.2). This motion is monitored by the resolution of the multiplicity of the carbon resonances of the -$\overset{+}{N}Me_3$ group[24]. As the carbon atoms involved are linked to nitrogen as well as to hydrogen, two interactions can contribute to the observed line shape, *viz.* quadrupolar and dipolar interactions.

This type of motion increases when the head group packing becomes looser (*i.e.*, a larger surface area per lipid head group). It results in smaller quadrupolar and dipolar interactions, leading to the appearance of the multiplicity of the ^{13}C resonances of the lecithin -$\overset{+}{N}Me_3$ group. In the Chapters IV and V a more detailed description of the backgrounds of this type of motion will be presented.

III.4.5 Hydrophilic region: discussion
Low aggregational densities, such as for monomeric TABs, result in triplet structures for the -$\overset{+}{N}Me_3$ resonances. On the contrary, high aggregational densities, as for micellar TABs, result in unresolved multiplicities for the -$\overset{+}{N}Me_3$ resonances[33]. It will now be demonstrated that differences in intermolecular head group distances as large as those occurring between aggregated and non-aggregated states are not strictly necessary to obtain enhanced CH_2-$\overset{+}{N}$ site mobilities. In fact lateral expansion (*i.e.*, a small decrease of the aggregational density) may be sufficient.

The intermolecular head group distances of mixed micelles of DOPC and $C_{18}TAB$ were monitored by means of the multiplicities of the lecithin -$\overset{+}{N}Me_3$ carbon resonances as a function of the TAB concentration (Figure 3.3). Intercalation of only 2% detergent at 323K already causes sufficient inter-head-group space and thus better defined splittings. At lower temperature (318K) no increase in mobility can be observed at this point (2% detergent). In this case, the
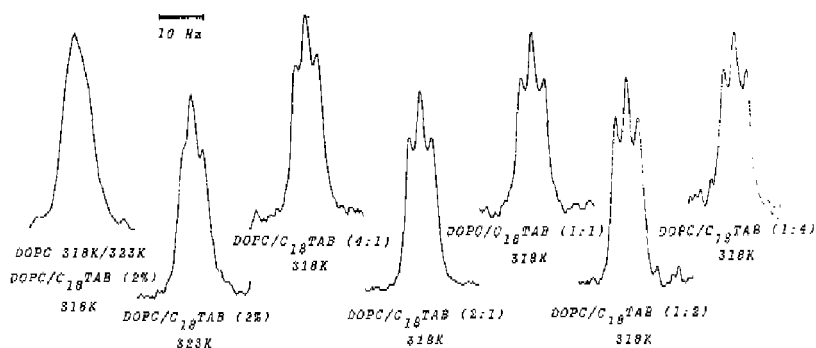
Figure 3.3 Line shapes of the lecithin -ṄMe$_3$ resonances of DOPC observed by means of a decoupling power of 1 Watt. Mixed-micelle ratios are indicated.

splitting only becomes visible at higher concentrations of TAB and it remains approximately the same over the entire concentration range investigated up to and including the 1:4 (m/m) lipid TAB mixing ratio. As a result, these experiments indicate, that only a slight increase in intermolecular lipid head group distance causes an increased surface area per lipid molecule and consequently considerable motional freedom for the CH$_2$-Ṅ vector.

III.5 Summary/Conclusions

^{13}C NMR measurements of DOPC micelles detect an almost complete visibility of the intrinsic magnetic nonequivalency of the two lipid acyl chains. The chemical shift data are interpreted in terms of effectively different lengths of the *sn*-1 and *sn*-2 acyl chains due to a bending near the C-2 carbon atom of the *sn*-2 chain. Mixed micellar systems of DOPC and several TABs show a difference in effective chain lengths of the constituent types of amphiphiles. ^{13}C NMR *shieldings* are observed for the TAB fragments which are longer than both acyl chains of the lipids. At an effective chain length difference of *seven* carbon atoms a sizeable contribution of *extra gauche* conformers, with respect

55

to their single micelles, occur for these TABs. At smaller differences a *decrease* of *van der Waals* interactions (*i.e.*, decreasing molecular packing) participates almost exclusively leading to chain separation. The *deshieldings* observed for the TAB segments situated directly between neighbouring lecithin chains indicate conformational changes towards more extended forms, as compared with their single micellar solutions, rather than an *increase* of *van der Waals* interactions. The DOPC molecules do not undergo measurable conformational changes upon mixed-micelle formation but are only subject to increased molecular packing. This may indicate that lipid conformational changes are of minor importance for solubilizing micelle bound hydrocarbon-like compounds.

Regarding the fluidity of the head group region, incorporation of TABs increases the surface area per lipid head group and consequently increases the mobility of the $CH_2-\overset{+}{N}$ site around the lipid CH_2-CH_2 head group linkage.

III.6 Experimental

The *n*-alkyl TABs were prepared by the reaction of trimethylamine with the *n*-alkyl bromides in alcoholic solution according to literature data[11]. DOPC was purchased from Supelco, Inc. A lipid stock solution was prepared by removal of the organic storage solvent under a stream of nitrogen and by dissolving in $CHCl_3$. This stock solution was stored at $-20^{\circ}C$. Mixed-micelle solutions were obtained by adding the appropriate amounts of deionized water to the solid TABs and dried samples of the lipid stock solutions. The resultant solutions were sonicated for 1 min. at $25^{\circ}C$.

All ^{13}C NMR spectra were run at 62.93 MHz on a Bruker WM 250 spectrometer under proton noise decoupling at $45^{\circ}C$, unless otherwise indicated. The deuterium signal from C_6D_6 was employed as an external lock signal. All chemical shifts are related to Me_4Si (C_6D_6 at 128 ppm downfield from Me_4Si). 2000-9000 transients were accumulated of spectral width 2 KHz in 32K data points limiting the resolution to 0.005 ppm. The pulse width was set to a 90° flip angle.

References and notes

1. C. Baron and T.E. Thompson, Biochim. Biophys. Acta, 1975, *382*,276.
2. B. de Kruijff, A.J. Verkley, C.J.A. van Echteld, W.J. Gerritsen, C. Mambers, P.C. Noordam and J. de Gier, Biochim. Biophys. Acta, 1979, *555*,200.
3. M. Barbe and D. Patterson, J. Phys. Chem., 1978, *82*,40; P. Lemaire and P. Bothorel, Macromolecules, 1980, *13*, 311 and references therein.
4. M.F. Roberts, A.A. Bothner-By and E.A. Dennis, Biochemistry, 1978, *17*,935.
5. R.A. Burns and M.F. Roberts, Biochemistry, 1980, *19*,3100.
6. J. Seelig, Biochem. Soc. Trans., 1978, *6*,40 and references therein; J. Seelig and A. Seelig, Biochim. Biophys. Acta, 1975, *406*,1; G. Büldt and J. Seelig, Biochemistry, 1980, *19*,6170.
7. The following abbreviations have been used: C_8TAB, n-octyltrimethylammonium bromide; C_{12}TAB, n-dodecyltrimethylammonium bromide; C_{14}TAB, n-tetradecyltrimethylammonium bromide; C_{16}TAB, n-hexadecyltrimethylammonium bromide; C_{18}TAB, n-octadecyltrimethylammonium bromide; DOPC, dioctanoyl-L-α-lecithin.
8. K.M.W. Keough and P.J. Davis, Biochemistry, 1979, *18*,1453.
9. J. Stümpel, A. Niksch and H. Eibl, Biochemistry, 1981, *20*,662.
10. R.J.E.M. de Weerd, J.W. de Haan , L.J.M. van de Ven, M. Achten and H.M. Buck, J. Phys. Chem., 1982, *86*,2523 (see also Chapter II of this thesis).
11. A.B. Scott and H.V. Tartar, J. Amer. Chem. Soc., 1943, *65*,692.
12. a) E. Williams, B. Sears, A. Allerhand and E.H. Cordes, J. Amer. Chem. Soc., 1973, *95*,4871; b) D. Canet, J. Brondeau, H. Nery and J.P. Marchal, Chem Phys. Lett., 1980, *72*,184; c) H. Wennerström, B. Lindman, O. Söderman, T. Drakenberg and J.B. Rosenholm, J. Amer. Chem. Soc., 1979, *101*,6860;

d) M. van Bockstaele, J. Gelan, H. Martens, J. Put, F. de Schrijver and J.C. Dederen, Chem Phys. Lett., 1980, *70*,605;

e) R.M. Levy, M. Karplus and P.G. Wolynes, J. Amer. Chem. Soc., 1981, *103*,5998 and references therein.

13. C. Tanford, "The Hydrophobic Effect, Formation of Micelles and Biological Membranes, Wiley & Sons, New York, 1980.

14. R.J.M. Tausk, J. Karmiggelt, C. Oudshoorn and J.Th.G. Overbeek, Biophys. Chem., 1974, *1*,175;
R.J.M. Tausk, J. van Esch, J. Karmiggelt, G. Voordouw and J.Th.G. Overbeek, Biophys. Chem., 1974, *1*,184;
R.J.M. Tausk, C. Oudshoorn and J.Th.G. Overbeek, Biophys. Chem., 1974, *2*,53.

15. B. Persson, T. Drakenberg and B. Lindman, J. Phys. Chem., 1976, *80*,2124.

16. N.O. Petersen and S.I. Chan, Biochemistry, 1977, *16*,2657.

17. J.W. de Haan, L.J.M. van de Ven, A.R.N. Wilson, A.E. van den Hout-Lodder, C. Altona and D.H. Faber, Org. Magn. Res., 1976, *8*,477.

18. J.W. de Haan, L.J.M. van de Ven and A. Bučinská, J. Phys. Chem., 1982, *86*,2517.

19. W.L. Earland and D.L. Vanderhart, Macromolecules, 1979, *12*,762;
C.A. Fyfe, J.R. Lyerla, W. Volksen and C.S. Yannoni, Macromolecules, 1979, *12*,757.

20. D. Cans, B. Tiffon and J.E. Dubois, Tetrahedron Lett., 1976, *24*,2075;
B. Tiffon and J.P. Doucet, Can.J. Chem., 1976, *54*,2045;
A.R.N. Wilson, L.J.M. van de Ven and J.W. de Haan, Org. Magn. Res., 1974, *6*,601.

21. H.N. Cheng and F.A. Bovey, Org. Magn. Res., 1978, *11*,457;
G. Mann, E. Kleinpeter and H. Werner, Org. Magn. Res., 1978, *11*,561;
H.J. Schneider and W. Freitag, J. Amer. Chem. Soc.,1976, *98*,478.

22. J.B. Rosenholm, T. Drakenberg and B. Lindman, J. Coll. Interface Sci., 1978, *63*,538.

23. P. Mukerjee and K.J. Mysels, Natl. Stand. Ref. Data Ser.,

Natl. Bur. Stand., 1971, *36*.

24. Chapter IV of this thesis.

25. R.A. Burns, M.F. Roberts, R. Dluhy and R. Mendelsohn,
    J. Amer. Chem. Soc., 1982, *104*,430.

26. H.Hauser, W. Guyer, I. Pasher, P. Skrabal and S. Sundell,
    Biochemistry, 1980, *19*,366.

27. H. Akutsu, Biochemistry, 1980, *20*,7359.

28. P.L. Yeagle, Acc. Chem. Res., 1978, *11*,321.

29. M.F. Brown and J. Seelig, Biochemistry, 1978, *17*,381.

30. R.A. Burns and M.F. Roberts, J. Biol. Chem., 1981, *256*,
    2716.

31. R.A. Burns and M.F. Roberts, Biochemistry, 1981, *20*,7102.

32. A. Plückthun and E.A. Dennis, J. Phys. Chem., 1981, *85*,
    678 and references therein.

33. E. Williams, B. Sears, A. Allerhand and E.H. Cordes,
    J. Amer. Chem. Soc., 1973, *95*,4871;
    R. Murari and W.J. Baumann, J. Amer. Chem. Soc., 1981,
    103,1238;
    The Appendix of chapter IV of this thesis.

CHAPTER IV

Effects of lytic compounds on the fluidity of lecithin sonicated bilayers

A measure of lipid resistance against disruption of the bilayer orientation

IV.1 Introduction

It has been recognized that single stranded *n*-alkyl amphiphiles within a biological membrane have severe implications for the stability of the cell-interface membrane. An increase in content of these surfactants forms conditions for cell-fusion and an excess of exogenously added surfactant causes lysis[1-4].

Until now, no definite descriptions regarding interactions between lytic compounds and lipids during lysis of the bilayer membrane have been presented. In order to further investigate the aspects of lysis, *n*-alkyl TABs incorporated in sonicated bilayers of dimyristoyl-L-α-phosphatidylcholine (DMPC) and dipalmitoyl-L-α-phosphatidylcholine (DPPC) have been studied in connection with recently published data concerning the fluidity (*i.e.* packing, mobility and conformational phenomena) of phosphatidylcholines and *n*-alkyl amphiphiles in different aggregational states[5,6]. It will be shown that at concentrations of single stranded amphiphiles where no lysis occurs (*i.e.* in the bilayer state), these single stranded compounds are "squeezed" between the lipid molecules. This is due to increased aggregational densities. It results in motional restrictions within both the head group region and the alkyl chain region of the lytic compounds without affecting the lecithin mobilities. Because additives with large internal volumes, such as cholesterol, (see subsequent Chapter) are also reduced in their mobilities, an analogous picture may be obtained for integral proteins, with even larger internal volumes. It has been stated that in these cases proteins adapt the active channel conformation

only at small surface areas per molecule, *i.e.* a large aggregational density[7,8]. From the description given in this Chapter, it can be made plausible that the surrounding lipids induce the desired protein packing.

Lysis of the bilayer occurs when the concentration of the TAB is raised to ca. one equiv. At this point the aggregational density decreases and consequently TAB mobilities increase and TAB chain extension decreases. Also the acyl chain mobilities and acyl chain kinking of the lipids increase. The toxic properties of germicidal *n*-alkyl TABs against bacteriological organisms may be explained in terms of lysis of this particular biomembrane system when such germicides are incorporated[1].

IV.2 Results and discussion

IV.2.1 Head groups

General remarks. In view of the following discussion, a few aspects regarding the dynamic behaviour of the CH_2-$\overset{+}{N}$ linkage of the head groups of the lipids and the TABs are discussed in more detail, as are the consequences for the spectral appearances in ^{13}C NMR.

Quadrupolar relaxation of nitrogen-14 influences the line shapes of the resonances of the carbons directly bonded to nitrogen[10]. Moreover, dipolar ^{13}C-^{1}H interactions modulate the resonances of hydrogen substituted carbons. In the case of examination of the -$\overset{+}{N}Me_3$ moiety of lecithins and TABs, a combination of these phenomena is expected. Consider the case where one aspect is eliminated, *e.g.* dipolar broadening is sufficiently suppressed[11]. Triplet structures, due to scalar coupling to ^{14}N (spin 1), are produced for the carbon resonances when quadrupolar relaxation is slow (*i.e.* ^{14}N quadrupolar relaxation times exceed 0.086 sec[6]). When quadrupolar relaxation becomes faster (*i.e.* ^{14}N quadrupolar relaxation times shorter than 0.086 sec[6]), a collapse of the triplet structure is expected. In the extreme case, a narrow singlet remains[12]. Recently, *London et al.*[11] showed that simple methyl rotation or internal motion about the CH_2-$\overset{+}{N}$

bond will *not* influence the quadrupolar relaxation, because of the molecular symmetry around the nitrogen nucleus. Therefore, *slow and fast quadrupolar relaxation will be correlated with respectively fast and slow mobilities about the CH_2-CH_2 head group bond, affecting the orientation of the $CH_2-\overset{+}{N}$ linkage.*

On the other hand, $^{13}C-^{1}H$ dipolar interactions have to be considered. From a steric point of view, dipolar interactions within the cationic site of trimethylammonium amphiphiles will be averaged (and thus their effects will be decreased) most effectively by motions which take the $-\overset{+}{N}Me_3$ group over the largest number of possible directions in space, namely motions around the CH_2-CH_2 head group bond. Local motions such as internal rotation about the $CH_2-\overset{+}{N}$ bond and methyl rotation are thus of minor importance, apart from the fact that these rotations usually are too fast to be influenced by the environment of the head groups. The rate of motion of the $-\overset{+}{N}Me_3$ site around the CH_2-CH_2 bond is limited by a large aggregational density. Motions around this CH_2-CH_2 bond are decreased when the aggregational density is increased (*i.e.* the "squeezing" of the head groups). This can be envisaged by a study of lipids and lytic compounds in different states (monomers and aggregates). Unfortunately, it is impossible to observe DMPC and DPPC $-\overset{+}{N}Me_3$ line shapes in the *monomeric* phase by ^{13}C NMR without labelling (very low CMC-values[13,14]). Still, in order to shed light on the influence of packing on $-\overset{+}{N}Me_3$ line shapes, the $-\overset{+}{N}Me_3$ resonances of the lytic TABs in non-aggregated and aggregated states were monitored (for a description see Section IV.5). It was shown that increased packing densities lead to a collapse of the triplets. Similar spectra are obtained for pure lecithin *aggregates* (Figure 4.1). Analogously to the lytic TABs, DMPC vesicles produce a broadened resonance at *e.g.* 1 Watt decoupling power. Thus one is tempted to conclude that head group mobilities are slow. However, when sufficient decoupling power (ca. 8 Watts) is applied, triplets are observed. It implies that the mobilities of the nitrogen moiety around the CH_2-CH_2 bond are much faster than one would

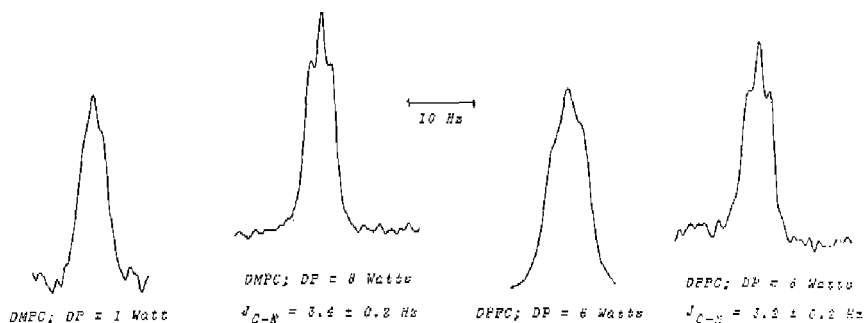expect from the experiments at low level decoupling power alone.

10 Hz

DMFC; DP = 1 Watt

DMPC; DP = 8 Watts
$J_{C-N} = 3.4 \pm 0.2$ Hz

DPPC; DP = 6 Watts

DPPC; DP = 6 Watts
$J_{C-N} = 3.2 \pm 0.2$ Hz

Figure 4.1 $-\overset{+}{N}Me_3$ line shapes of DMPC and DPPC sonicated bilayers (50 mM in water) at 323K and variable magnitudes of proton noise decoupling in 62.9 MHz ^{13}C NMR spectra (DP = decoupling power).

Incorporation of lytic compounds and lysis of the bilayer. At mixing ratios where the bilayer orientation is not (yet) subject to lysis (*i.e.* the 4:1 up to the 1:1 mixing ratio), a triplet structure for the lipid is maintained, indicating relatively large head group mobilities (Figure 4.2a-c). This is also the case for mixing ratios where mixed micelles are formed (*i.e.* the 1:2 and 1:4 mixing ratio). However, for the head group mobility of the penetrating TAB molecules some remarkable changes are perceptible. In the DMPC/C_8TAB dispersions the solubilized n-octyl TAB molecules are in very rapid exchange with their extravesicular monomers, because the effective concentration is far beneath the CMC-value[13]. Thus, an average state is monitored with relatively large intermolecular separations and so a triplet structure for the $-\overset{+}{N}Me_3$ site of the C_8TAB appears. The C_{12}TAB reveals a different behaviour. Up to the 1:1 lipid/detergent mixing ratio a broad resonance is detected, due to enhanced dipolar interactions. Fast quadrupolar relaxation does not contribute to the $-\overset{+}{N}Me_3$ line shape. This was confirmed by

the observation of $-\overset{+}{N}Me_3$ triplets at elevated noise decoupling (*i.e.* 13 Watts) at various temperatures (303K-323K)[15]. An enhanced mobility for the TAB head group is achieved at lower mixing ratios. This is deduced from the appearance of triplets for the TAB. It substantiates literature data[2,4] that bilayer ordering is maintained up to the mixing ratios around 1:1, and lysis of the bilayer towards micelle ordering - and concomitant smaller aggregational densities - is established at lower ratios. Thus, *in the bilayer state, the surrounding lecithin molecules force incorporated lytic compounds to reduced head group mobilities with respect to the pure lytic micelles* (see Section IV.5), *without decreasing notably the time scale of motion of the lipid $CH_2-\overset{+}{N}$ site with respect to the pure lipid vesicle.* This packing situation may be envisaged by the difference in relative orientations of the two types of head groups (Figure 4.3). The lipid head groups are located almost perpendicular to the bilayer normal, while on the average the head groups of the lytic constituents are situated along this bilayer normal and are squeezed between neighbouring lipid molecules. In the Section IV.2.2 it will be shown that this squeezing-picture is consistent with the observations made for the hydrophobic region of the TABs.

For the C_{14}TAB mixed dispersions (Figure 4.2c) a similar change in the dynamic behaviour of the $CH_2-\overset{+}{N}$ site is observed during the transition mixed bilayer into mixed micelle[3]. However, lysis of the bilayer does not provide resolved methyl resonances.
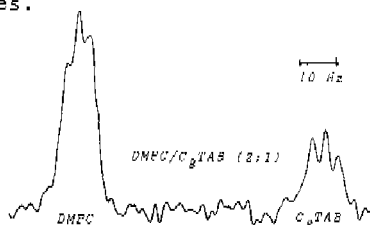

Figure 4.2a $-\overset{+}{N}Me_3$ line shapes for mixed dispersions of C_8TAB and DMPC at 323K and DP = 8 Watts. Similar patterns were observed for other mixing ratios.
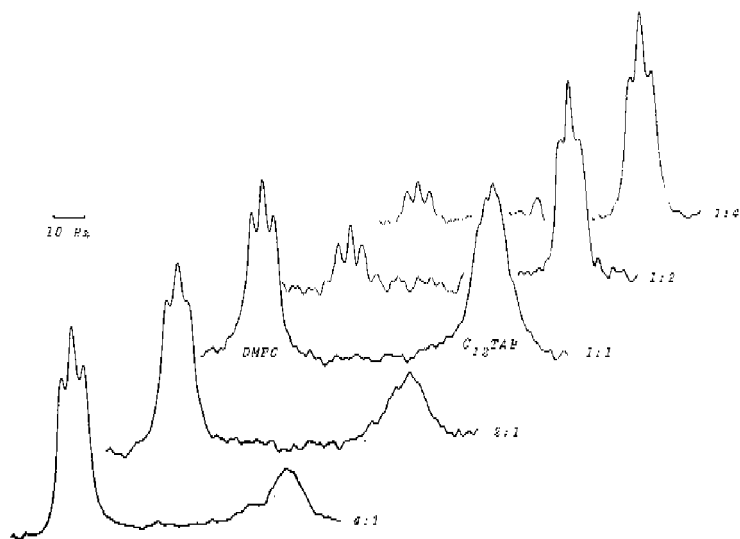
Figure 4.2b $-\overset{+}{N}Me_3$ line shapes for mixed dispersions of $C_{12}TAB$ and DMPC at 323K and DP = 8 Watts. Lipid/detergent mixing ratios are indicated. J_{C-N} couplings were, when visible, 3.0 - 3.6 Hz.
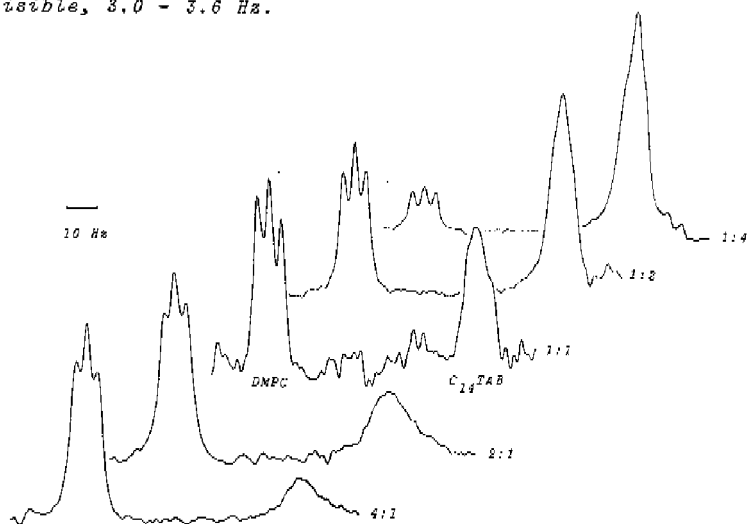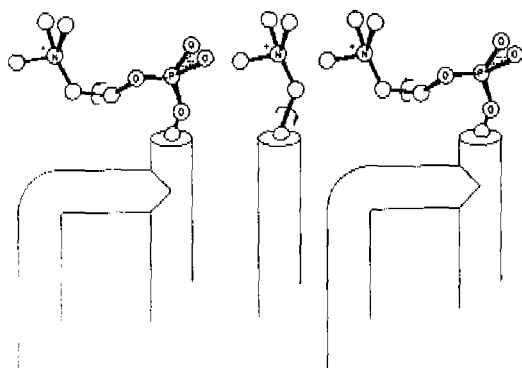

Figure 4.2c $-\overset{+}{N}Me_3$ line shapes for mixed dispersions of $C_{14}TAB$ and DMPC at 323K and DP = 8 Watts. Lipid/detergent mixing ratios are indicated. J_{C-N} couplings were, when visible, 3.0 - 3.6 Hz.

65

Figure 4.3 Relative average orientations of the lecithin and the TAB in their mixed dispersions. The hydrophobic interior is indicated by tubes.

The increase in line width at high mixing ratios has to be ascribed to enhanced dipolar interactions, similar to the C_{12}TAB mixed bilayers. Fast quadrupolar relaxation could not be excluded, however, because at elevated noise decoupling (*i.e.* ca. 13 Watts) a "singlet" structure was still detected[15] (due to thermal degeneration of the constituents of the aggregates, it was impossible to apply proton noise decoupling exceeding 13 Watts). Yet a difference exists between the single and the 1:4 mixed micellar solution of this TAB detergent (compare the data of Figure 4.7 with Figure 4.2c). Obviously, the presence of only small amounts of lecithin molecules already decreases the head group mobility of this particular TAB. Similar patterns were obtained when intercalating these lytic compounds in vesicle structures of DPPC.

IV.2.2 Hydrophobic tails

The ^{13}C NMR spectra of the pure vesicles of DMPC and DPPC - which will serve as reference samples for the mixed lipid systems - are presented in Figure 4.4. As indicated, the line widths are very much smaller than previously reported[16].
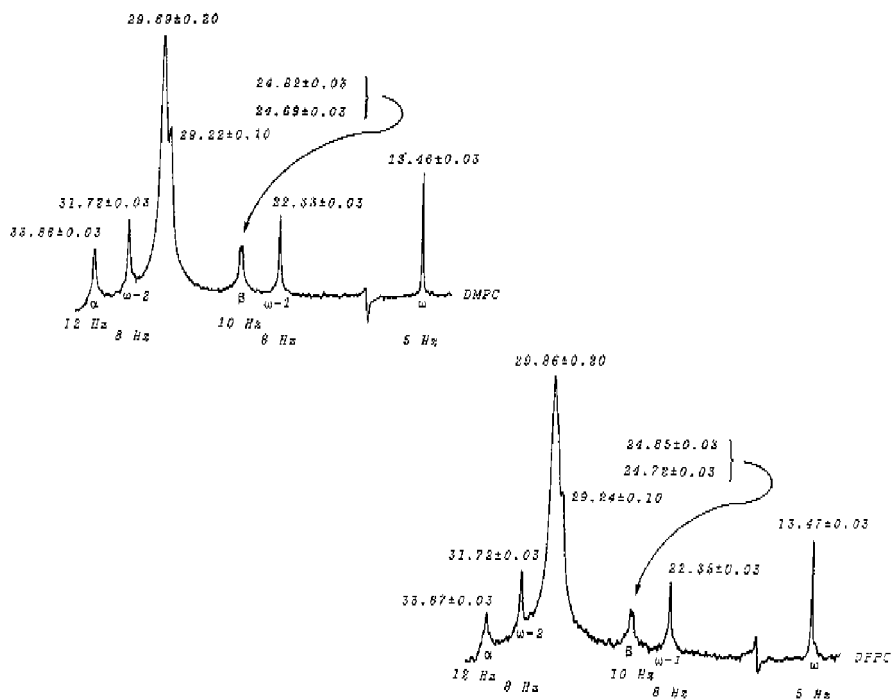
Figure 4.4 ^{13}C NMR spectra of the acyl chain region of DMPC and DPPC sonicated bilayers at 323K and DP = 8 Watts. Line widths and chemical shifts are indicated. Dilution of the samples from 50 mM to 20 mM did not affect the line widths or chemical shifts.

The latter line widths were at least three times larger than those presented in Figure 4.4. It became clear that the main part of this line narrowing was a consequence of eliminated dipolar coupling. This was indicated by spectra recorded at lower levels of proton noise decoupling. A comparison of the spectra of sonicated bilayers of DMPC and DPPC shows no significant differences: line widths and chemical shifts are nearly identical. From this point of view, in combination with the results of the head groups (Figure 4.1), it is stated that on the ^{13}C NMR time scale

the vesicular dispersions of DMPC and DPPC are motionally
and conformationally equivalent. This stands in contrast to
earlier reports based on vibrational spectroscopy[17].

Recently, a description of the phenomena involving
fluidization of the hydrophobic core of mixed micellar systems
of lipids and lytic TABs has been offered[5]. It was shown that
those hydrophobic parts of the TAB located between the lipid
molecules altered their conformational equilibria towards
more extension, and were subject to increased chain packing.
The lipid molecules, however, were not shown to change their
conformations upon solubilization of these TABs. Furthermore,
it was discussed that the hydrophobic part of the the TAB
protruding from the lipid hydrophobic region was subject to
conformational changes towards more kinking and/or decreased
packing with respect to its single micelles. In similar terms,
the lysis of the (curved) bilayer upon incorporation of
TABs is now discussed. ^{13}C NMR line widths and chemical shifts
were investigated. Incorporation of C_{14}TAB in DMPC sonicated
bilayers resulted in *undetectable* signals for the tail of the
single stranded amphiphile from the 4:1 to the 3:2 lipid/
detergent mixing ratio. Also, *no* line width and chemical shift
changes occurred for the lecithin chains within this
concentration interval. The latter indicates that no significant
changes occur within the bilayer ordering and dynamics. The
undetectability of the TAB resonances must be due to
immobilization and subsequent dipolar broadening. Up to now,
only the ^{13}C-resonances of intercalated substrates with a
large internal volume such as cholesterol[16] and proteins[18]
were shown to broaden extremely. It is now demonstrated that
relatively small lytics act in a similar way. (It is suggested
that free axial rotation of the entire tail of the TAB is
limited. Thus, TAB mobilities are diminished by the lipid, withou
affecting partial rotation or kink diffusion in the lecithins
about their long axis. Model studies show that in the bilayer
ordering intermolecular distances between the hydrophobic
chains of C_{14}TAB and DMPC are on the average smaller than
between the lipid *sn-1* and *sn-2* chain, resulting in smaller
mobilities of the TAB chains and concomitant intensities

of the corresponding ^{13}C NMR resonances with respect to those of the lipid molecules in the bilayer). *Obviously, when the membrane contains only small quantities of TABs, these TAB molecules are pressed between neighbouring lipid molecules, the consequence being that head group* (see Section IV.2.1) *as well as tail mobilities of the TABs are reduced.* At higher quantities of the $C_{14}TAB$ (*i.e.* at mixing ratios lower than 3:2), the resonances of the $C_{14}TAB$ become visible, because the bilayer undergoes lysis and mixed micelles, with lower aggregational densities and concomitant enhanced mobilities are formed[2-4,19]. In addition, the decrease of the DMPC acyl chain line widths is another indication for this disruption of the bilayer: line widths are typically 2 - 3 Hz for mixed micelles (Figure 4.6). Then one is able to notice (Figure 4.5a) that the $C_{14}TAB$ shows deshieldings compared with its single micelle solution.
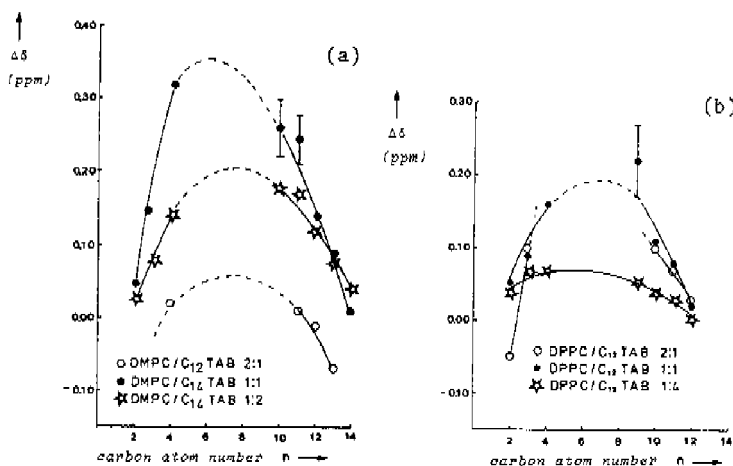

Figure 4.5   Deshieldings (ppm) of $C_{14}TAB$ and $C_{12}TAB$ upon incorporation in DMPC sonicated dispersions at 323K and DP = 8 Watts (a). Deshieldings (ppm) of $C_{12}TAB$ upon incorporation in DPPC sonicated dispersions at 323K and DP = 8 Watts (b). Molar lipid/detergent mixing ratios are indicated. Total amphiphile concentration equals 50 mM (see the experimental Section IV.4).

The pattern of deshieldings indicates that the lipid molecules force the C_{14}TAB towards more extension upon incorporation, analogously to the detailed description regarding mixed aggregates of short-chain lecithins and several TABs[5]. Also the lipid resonances change position when lysis of the bilayer takes place. The observed shieldings for the C-12/C-14 lipid fragment (see Table IV.1) suggest that increased chain folding and/or decreased chain packing[5] are the result of the bilayer disruption. Moreover, the line widths of the ^{13}C NMR resonances of the acyl tails (Figure 4.6) decrease.
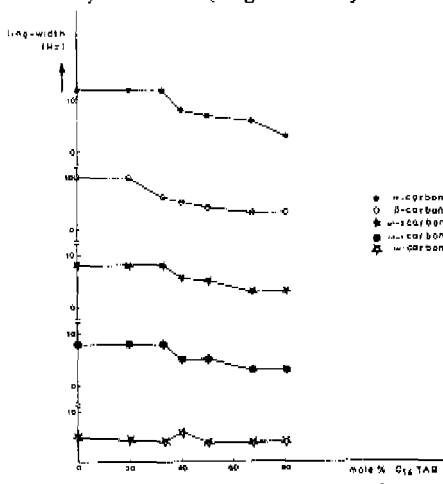

Figure 4.6   Line widths (Hz) of the acyl region of DMPC vs. the concentration of incorporated C_{14}TAB at 323K and DP = 8 Watts (the decrease in line width is not due to a decrease of the magnetic non-equivalence between similar carbons of the sn-1 and sn-2 acyl chains. The magnetic non-equivalence remains ca. 0.1 ppm for the micellar as well as for the bilayer state).

Compared with the DMPC/C_{14}TAB mixed bilayers, an enhanced detectability for the single stranded TAB occurs in the DMPC/C_{12}TAB and especially in the DMPC/C_8TAB mixed bilayer systems. This is a result of the relatively enhanced exchangeability between intravesicular aggregated and

Table IV.1 Chemical shift changes of the acyl region of
DMPC and DPPC upon mixing with C_{14}TAB in different ratios
at 323K and DP = 8 Watts. Resolved resonances, obtained
by means of resolution enhancement, are mentioned separately

	DMPC mixing ratios:						DPPC mixing ratios:		
atom[a]	2:1	3:2	1:1	1:2	1:4	atom[a]	2:1	1:1	1:4
α	+0.00	+0.06	+0.10	+0.13	+0.15	α	+0.07	+0.08	+0.14
α			+0.04	+0.08	+0.08	α	+0.01		+0.08
β	-0.05	-0.00	-0.01	-0.01	-0.04	β		-0.03	-0.08
β		-0.00	-0.01	-0.01	-0.04	β		-0.03	-0.08
ω-2	-0.06	-0.02	-0.05	-0.07	-0.15	ω-2	-0.00	-0.05	-0.19
ω-1	-0.07	-0.05	-0.06	-0.07	-0.13	ω-1	-0.06	-0.06	-0.17
ω	-0.07	-0.03	-0.10	-0.11	-0.16	ω	-0.00	-0.10	-0.15
ω				-0.14	-0.20				

[a]The resolved resonances correspond to the sn-1 and the sn-2
chains of the DMPC.

extravesicular monomeric C_8TAB and C_{12}TAB compared with the
C_{14}TAB. As a consequence, chemical shift changes of the
former surfactants are less pronounced than for the C_{14}TAB,
but point out a comparable behaviour (a typical example is
given in Figure 4.5a). Mixed bilayer systems of DPPC and TABs
revealed quite the same pattern: for example, C_{12}TAB is
forced by the surrounding lecithin molecules towards more
extended forms as compared with its single micelle
(Figure 4.5b), as can be observed from the deshielding pattern.
When disrupting the bilayer structure, also the lipid
molecules are subject to increased kinking and/or decreased
chain packing (Table IV.1), analogous to the DMPC mixed
systems.

IV.3 Summary/conclusions

Intercalation of low percentages (<50% m/m) of several
n-alkyl TABs in lecithin vesicles preserves the lipid bilayer
orientation. In these mixed vesicles, the TAB molecules are

forced towards *restricted motions* of the $-\overset{+}{N}Me_3$ site and the
alkyl chains due to an increased density for the TABs.
Moreover, the TABs are compelled towards *more chain extension*
as compared to their single micelles. However, neither a
decrease of the lecithin $-\overset{+}{N}Me_3$ site mobility around the
CH_2-CH_2 head group linkage, nor a decrease in acyl chain
mobility, nor a change in acyl chain kinking is detected.
In other words, the lecithin bilayer reacts upon disruption
by squeezing "intruding" compounds towards less mobility.

The disruption of the bilayer is achieved when the
TAB concentration is raised to ca. one equiv.: lysis of the
bilayer occurs and mixed micelles are formed. It results in
a decrease of the aggregational density. Consequently, the
TAB mobilities increase and their chain extension decreases.
At this point, also an increase of the lecithin acyl chain
mobility and acyl chain kinking are detected. Thus, the
driving force for lysis of the bilayer has to be ascribed
solely to the potency of the TABs to form micellar structures.

IV.4 Experimental

The *n*-alkyl TABs were prepared by the reaction of
trimethylamine and the *n*-alkyl bromides in alcoholic solution
according to literature data[9]. DMPC and DPPC were purchased
from Supelco, Inc. and Sigma. To obtain mixed micelle and/or
bilayer solutions of DMPC and DPPC, dry samples of the lecithin
and the TABs were added to the appropriate amount of deionized
water. Solutions were sonicated in NMR-tubes within a Branson
Model 50-D ultrasonic water bath between $0^{o}C$ and $20^{o}C$.
Typically, solutions were clear after a period of ten miutes.
During this interval no thermal degeneration or hydrolysis
occurred, as monitored by thin layer chromatography with
$CHCl_3$: MeOH: H_2O = 65: 25: 4 (w/w) as eluens. Multibilayer
suspensions of DMPC and DPPC were prepared by adding the
appropriate amounts of deionized water to dry lecithin and
vortexing vigourously above the main phase transition
temperature. Pure DMPC and DPPC vesicles were prepared by
means of sonication in the above mentioned water bath between
$0^{o}C$ and $20^{o}C$; operation time : typically one hour. Solutions

were blueish transparant and no hydrolysis or thermal degeneration occurred according to thin layer chromatography. Laser beat spectroscopy showed that these samples were not monodispers: particle sizes varied between 250 Å and 1000 Å. The distribution function showed a large fraction of small particles (around 250 Å) and a small fraction of large particles (exceeding 1000 Å). The total amphiphile concentration was 50 mM for all pure and mixed lipid samples.

All ^{13}C NMR spectra were run at 62.93 MHz on a Bruker WM 250 spectrometer under proton noise decoupling at 323K, unless indicated otherwise. The deuterium signal from C_6D_6 was employed as an external lock signal. All chemical shifts are related to Me_4Si (C_6D_6 at 128 ppm downfield from Me_4Si). 10,000-100,000 transients were accumulated in 4K data points zerofilled to 32K points before Fourier Transformation. Spectral width was 2 KHz. No relaxation delay was employed. Pulse width was set to a 90° flip angle. The decoupling circuit was carefully tuned prior to the various experiments in order to operate at levels exceeding 2 Watts.

IV.5 Appendix

To demonstrate the influence of molecular packing on the line shape of $-\overset{+}{N}Me_3$ resonances, several TABs were studied in the monomeric and micellar state. The results are also useful for the study of the line shapes of lecithin $-\overset{+}{N}Me_3$ resonances. It should, however, be stressed that, whereas in lecithin vesicles the $CH_2-\overset{+}{N}$ vector will be approximately parallel to the bilayer plane, corresponding vectors in the TABs will be perpendicular to the aggregate surface (Figure 4.3).

The *n*-octyl TAB is not capable of forming aggregates at the concentration investigated[13], and shows well resolved triplets for the $-\overset{+}{N}Me_3$ moiety (Figure 4.7). The large C_{18}TAB micelles show "singlet" structures under these conditions. It is consistent with the picture of a highly mobile $CH_2-\overset{+}{N}$ vector when the aggregational density is low, as for monomeric C_8TAB; at high aggregational densities a "singlet" resonance is observed, as for micellar C_{18}TAB. Thus, when the molecular
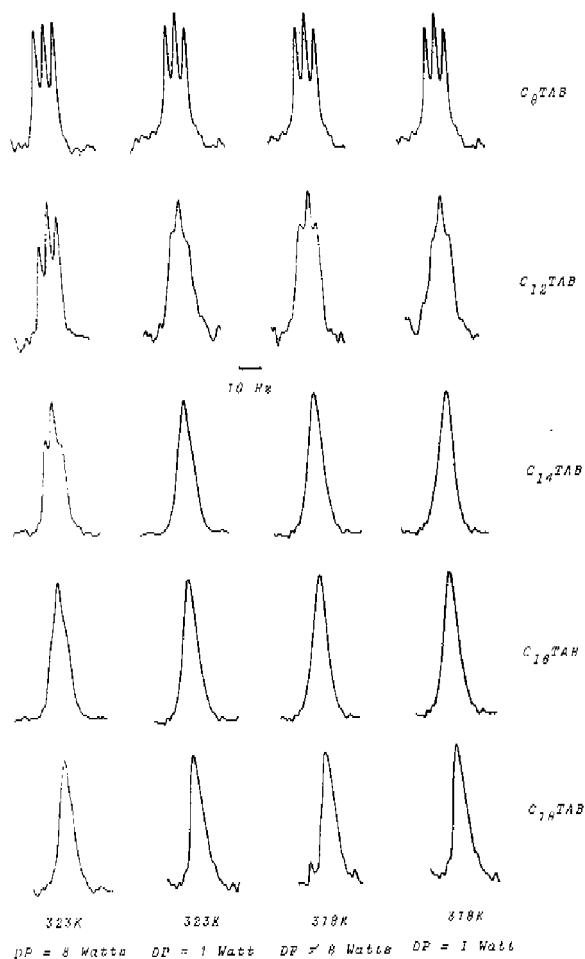
73

Figure 4.7 -ṄMe₃ line shapes of several TABs at different temperatures and decoupling power.

packing increases, head group mobilities around the CH_2-CH_2 bond decrease. However, for the TABs possessing intermediate chain lengths, interesting developments occur. For these detergents, the appearance of triplet structures is strongly related to the applied decoupling power and operating

temperature. At 323K and 8 Watts decoupling one can clearly recognize a pattern of head group mobility around the CH_2-CH_2 head group bond. Two reasons may be offered to explain this pattern in terms of aggregational densities. First, the CMC is lowered from C_8TAB to $C_{18}TAB$. Consequently, monomeric concentrations are decreased to almost zero in this series, due to a shift of the equilibrium monomer=aggregate to the right. On the NMR time scale essentially *this* shift is monitored, and it is expressed in the increased contributions of molecular aggregation to the $-\overset{+}{N}Me_3$ line shapes from C_8TAB to $C_{18}TAB$. Secondly, from geometrical considerations[7], also increasing aggregate sizes from C_8TAB up to $C_{18}TAB$ lead to the observed change in mobility due to stronger head group interactions (larger radii of curvature) and consequently larger aggregational densities.

1. C.A. Lawrence, "Surface-active Quaternary Ammonium Germicides", Academic Press, New York, 1959;
   F. Winternitz, M. Mousseron and M. Canet, Bull. Soc. Chim. Biol., 1951, *33*,369.

2. D.A.N. Morris, R. McNeil, F.J. Castellino and J.K. Thomas, Biochim. Biophys. Acta, 1980, *599*,380 and references therein;
   K. Elamrani and A. Blume, Biochemistry, 1982, *21*,521 and references therein.

3. S.E. Schullery, T.A. Seder, D.A. Wienstein and D.A. Bryant, Biochemistry, 1981, *20*,6818 and references therein.

4. L. Rydhag, P. Stenius, and L. Ödberg, J. Colloid Int. Sci., 1982, *86*,274 and references therein.

5. R.J.E.M. de Weerd, J.W. de Haan, L.J.M. van de Ven and H.M. Buck, J. Phys. Chem., 1982, *86*,2523 and references therein;
   R.J.E.M. de Weerd, J.W. de Haan, L.J.M. van de Ven, M. Achten and H.M. Buck, J. Phys. Chem., 1982, *86*,2528 and references therein;
   Chapter II and III of this thesis.

6. R. Murari and W.J. Baumann, J. Amer. Chem. Soc., 1981, *103*,1238.

7. C. Tanford, "The Hydrophobic Effect", Wiley, New York, 1980.

8. E.H.B. de Lacey and J. Wolfe, Biochim. Biophys. Acta, 1982, *692*,425.

9. A.B. Scott and H.V. Tartar, J. Amer. Chem. Soc., 1943, *65*,692.

10. J. Marsh,Chem. Rev., 1981, *81*,205;
    J.E. Wertz, Chem. Rev., 1955, *55*,829;
    F.A. Bovey, "Nuclear Magn. Res. Spectr.", Academic Press, New York, 1969;
    A. Abragam, "The Principles of Nuclear Magnetism", Oxford Univ. Press, 1961.

11. R.E. Walker, T.E. London, D.M. Wilson and N.A. Watwiyoff, Chem.Phys. Lipids,1979, *25*,7.

12. A. Carrington and A.D. McLachlan, "Introduction to Magnetic

Resonance", Harper & Row, New York, 1967, 210.

13. P. Mukerjee and K. Mysels, Natl. Stand. Ref. Data Ser. (U.S., Natl. Bur. Stand) 36, NSRDS-NBS, 1971.

14. A. Watts, D. Marsh and P.F. Knowles, Biochemistry, 1978, *17*,1792.

15. R.J.E.M. de Weerd, J.W. de Haan, L.J.M. van de Ven and H.M. Buck, unpublished results.

16. J.R. Brainard and E.H. Cordes, Biochemistry, 1981, *20*,4607.

17. B.P. Gaber and W.L. Peticolas, Biochim. Biophys. Acta, 1977, *465*,260.

18. R.L. Ong and J.H. Prestegard, Biochim. Biophys. Acta, 1982, *692*,252.

19. T. Zemb and C. Chachaty, Chem. Phys. Lett., 1982, *88*,68.

CHAPTER V

Effects of cholesterol on the fluidity
of lecithin sonicated bilayers

V.1 Introduction

Various analytical methods have been applied to shed
light on the complex behaviour of cholesterol solubilized
in a membrane. These studies showed for instance that
cholesterol broadens, lowers or disrupts the phospholipid
phase transitions; alters membrane permeability; influences
phospholipid chain conformations and/or chain packing;
condenses the bilayer fluidity at temperatures above the
main phase transition and liquefies the bilayer at
temperatures below the main phase transition[1-16]. In this
Chapter it will be described that, upon rigidification of
the bilayer by the solubilization of cholesterol, one type
of motion which has not been discussed earlier is affected,
namely the motion of the phospholipid $CH_2-\overset{+}{N}$ head group site
around the CH_2-CH_2 head group bond.

V.2 Results and discussion

Membrane fluidity is strongly related to inter- and
intramolecular mobilities, conformational changes and
alterations in packing of the phospholipids and membrane
bound substrates, the constituents of the bilayer[18]. Several
details regarding the dynamic behaviour of the $CH_2-\overset{+}{N}$ site
of the phospholipid head group have been offered in the
preceding Chapter. Also, for the lipid acyl chain region
data have been presented to differentiate between
conformational changes and chain packing[19]. Contrary to
lytic TABs[17], cholesterol broadens the resonances of the
$-\overset{+}{N}Me_3$ site of DMPC sonicated bilayers (Figure 5.1) and,
besides observed deshieldings (Figure 5.2), also increases

the phospholipid acyl chain line widths (Figure 5.3).

Hydrophylic region. The conformation of the lecithin polar head group is similar in the monomeric, micellar and bilayer state and is independent of the fatty acyl chain length[7,20]. Bulky metabolic regulating additives such as cholesterol are unable to change the polar head group conformation[7,14,18,20—26]. Furthermore, ^{13}C NMR studies indicate that the presence of cholesterol in phospholipid bilayers has little or no influence on the internal motion of the choline methyls[14,16], nor does it effect the motion of the phosphate segment[14]. In other words, the factor governing our results will be a change of intermolecular head group distances of the lecithins (Figure 5.1).
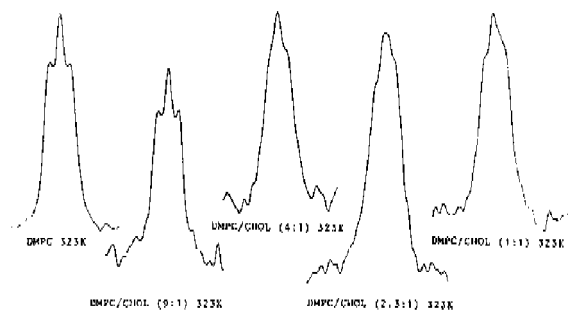

Figure 5.1 Cholesterol induced changes of the line shape of the $-\overset{+}{N}Me_3$ resonances of DMPC sonicated bilayers at 323K and DP = 8 Watts.

A change towards *larger* head group distances - and from our point of view subsequent *enhanced* mobilities for the $CH_2 \cdot \overset{+}{N}$ site - is frequently referred to[10,14]. This change is ascribed to the so-called "spacer"-effect cholesterol is supposed to induce for the head group region of the lecithin bilayer. However, from Figure 5.1 it is now clear that the $CH_2-\overset{+}{N}$ vector mobility of the lecithin around the CH_2-CH_2 head group axis actually *decreases* upon addition of the sterol.

Hydrophobic region. The resonances of cholesterol could

not be observed due to significant broadening. In agreement
with recently published data[8,16,27], we attribute this
broadening to strong dipolar interactions. The observed line
broadening of the resolved carbon resonances of the lecithin
acyl region of DMPC (Figure 5.3) is certainly - although
partially - caused by strong dipolar interactions too (lower
decoupling power enlarged the line widths of these carbon
resonances). However, non-motional aspects such as chemical
shift non-equivalences between the lecithin sn-1 and sn-2
chains and/or between the inside and outside monolayered
lecithins may be altered. The residual part of the line
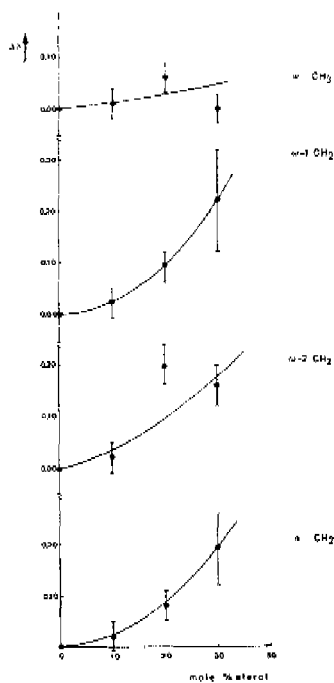broadening may depend on several motional restrictions[16,28-30].

*Figure 5.2 Cholesterol induced deshieldings of the lecithin
acyl chain region in DMPC sonicated bilayers at 323K and
DP = 8 Watts, versus the sterol concentration.*

The main factor which has to be taken into account is the
intramolecular process of chain reorientation. For the
very reason that its correlation time is typically 10^{-9} -
- 10^{-10} sec for small, non-sterol containing vesicles and
10^{-7} sec for large or sterol-rich particles[29,30], a change
in the rate of chain reorientation induces the largest line
broadening as compared to other processes[16,28-30]. For the
DMPC/cholesterol mixed bilayer systems, stability was
maintained for samples containing ca. 30 mole % sterol or
less. Up to this limit, it was possible, to estimate chemical
shift differences for the lecithin acyl chain region (Figure
5.2). For the carbon resonances investigated, deshieldings
increase with the effective sterol concentration. For the
hydrophobic interior it is possible to draw a plot of these
deshieldings versus the carbon atom position (Figure 5.4).
In agreement with recently published data[19], the pattern of
Figure 5.4 reveals a tendency towards more extension and/or
increased intermolecular packing. In connection with the
relatively small deshieldings of the ω-Me group, no large
conformational changes within the C-12/C-14 region as
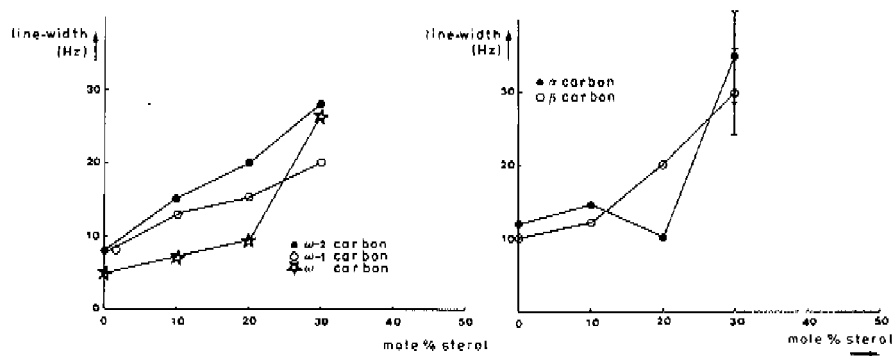compared with the pure lecithin vesicle are indicated.

*Figure 5.3   Cholesterol induced line widths of the lipid
acyl region upon incorporation in DMPC sonicated bilayers
at 323K and DP = 8 Watts, versus the concentration of the
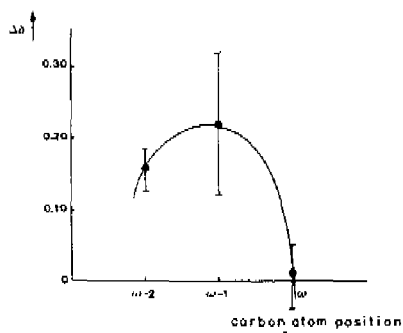sterol.*

Figure 5.4   Deshielding pattern for the hydrophobic acyl chain end of DMPC upon solubilization of 30 mole % cholesterol at 323K and DP = 8 Watts, versus the carbon atom position of DMPC.

Interpretations. From a strong increase in turbidity it is concluded that addition of cholesterol increases the vesicle size significantly. This is in agreement with the observations of *de Kruijff et al.*[21]. It is well-known that the sterols are located beyond the lecithin head group region of the vesicle[7,8] and thus no *direct* sterol-lipid interactions exist in the head group region. Thus the embedded sterol nuclei push the lecithin acyl chains aside and increase the average radius of curvature of the vesicle. The increase in particle size leads to higher aggregational densities between the lecithin head groups[18]. However, too close an approach of the repulsing lecithin head groups is avoided[18]. In order to minimize the free energy of the vesicle, a compensation occurs through an increase of the aggregational density of the hydrophobic interior. The implications for the ^{13}C NMR spectra are twofold. First, higher aggregational densities within the lecithin head group region decrease the lecithin head group mobility (see Chapter IV). Secondly, higher aggregational densities within the hydrophobic interior induce chain extension and/or reduced chain mobility (see Chapter IV). Indeed, cholesterol decreases the mobility of the lecithin $-\overset{+}{N}Me_3$

82

site around the CH_2-CH_2 head group bond (Figure 5.1). Due to the increase in the hydrophobic packing the resonances of cholesterol itself could not be observed, while also a decrease of the lecithin acyl chain motions was induced (Figure 5.3).

Besides this rather macroscopic view, a more detailed semi-quantitative interpretation of the data is possible, by means of a model of *Chan et al.*[31]. It suggests that incorporated cholesterol is complexed to one lecithin molecule and this complex in turn is associated with a second lecithin molecule via a *van der Waals*-type interaction. At low sterol concentrations (ca. 10 mole %), the remainder of the bilayer is built up by free lecithin and interfacial boundary lecithin. However, controversions exist about the binding sites within the complex[31]. At ca. 20 mole % sterol, free lecithin domains disappear, and only interfacial boundary lecithins remain between the 2:1 lecithin/cholesterol complexes[32]. Upon increasing the sterol concentration, the interfacial boundary lecithin disappears completely at 33.3 mole %, and only lecithin/cholesterol complexes remain.

From the observations presented in this Chapter, it is possible to add some additional quantitative data to the model of *Chan et al.*[31]: low concentrations of sterol (10 mole %) only influence the lecithin acyl region (Figure 5.3), while the lecithin head group mobilities remain unaltered (Figure 5.1). Broadening of the head group -$\overset{+}{N}Me_3$ resonance starts only at ca. 20 mole % of cholesterol. This indicates that the lecithin head group mobility around the CH_2-CH_2 head group linkage is only reduced, when free lecithin domains vanish. In other words, interfacial boundary lecithins are more rigid and more tightly packed than free lecithins. Enhancing the sterol concentration to levels where also interfacial boudary lecithins disappear - and thus lecithin/ cholesterol complexes remain - reduces the lecithin acyl and head group mobility even further. At this point, also stretching and/or packing of the acyl chains is very pronounced (Figure 5.2). Recapitulating, the fluidity increases along the series: sterol-complexed lecithin - boundary lecithin - free lecithin.

^{13}C NMR spectroscopy is applied to monitor the fluidity of DMPC sonicated bilayers upon incorporation of cholesterol. Cholesterol is pressed between lipid molecules, resulting in extremely broadened resonances which indicate low sterol mobilities. This is in line with observations by others[16]. Also, the results are similar to those of incorporated lytic compounds such as several TABs[17]. However, contrary to mixed bilayers of lecithins and TABs, the surrounding lecithins adjust to the bulk of the intercalated sterol nucleus. Cholesterol pushes the lecithin acyl chains aside and thus increases the average radius of curvature of the mixed vesicle. This in turn results in a decrease of the mobility of the $-\overset{+}{N}Me_3$ site of the lecithin around the CH_2-CH_2 head group bond. Furthermore, cholesterol broadens the ^{13}C NMR resonances of the lecithin acyl chains due to stronger dipolar interactions caused by retarded chain reorientation. Also, the sterol forces the lecithin chains towards more chain extension and/or larger chain packing.

At low sterol concentrations, it was observed that only the hydrophobic region of the membrane is rigidified while at higher (20 - 30 mole %) sterol contents, also the head group region is affected and rigidification of the entire membrane occurs. The results were interpreted semi-quantitatively in terms of a model concerning sterol-complexed lecithins, boundary lecithins and free lecithins.

V.4 Experimental

DMPC was purchased from Supelco, Inc. and Sigma. Cholesterol was obtained in 98% purity from Supelco, Inc. Pure DMPC vesicles were prepared as previously described[17]. Mixed sonicated bilayers of DMPC and cholesterol were prepared as follows. A chloroform solution of both constituents was evaporated to dryness under a stream of argon. Residual traces of organic storage solvent were removed overnight at $60^{\circ}C$ and 0.005 mm Hg. Deionized water was added and the sample was sonicated during one hour between $0^{\circ}C$ and $15^{\circ}C$ within a Branson Model 50-D ultrasonic water bath in NMR-tubes.

No degeneration or hydrolysis took place, as monitored with thin layer chromatography with $CHCl_3$: MeOH: H_2O = 65: 25: 4 (w/w) as eluens. Cholesterol-rich samples were always more turbid than the pure lecithin samples, indicating larger particle sizes. All samples maintained their stability during the experiments. Total concentration of lecithin and cholesterol was 50 mM for the pure and mixed samples.

The ^{13}C NMR spectra were run at 62.92 MHz on a Bruker WM 250 spectrometer under proton noise decoupling at 50^oC. The deuterium signal from C_6D_6 was employed as an external lock signal. Chemical shifts are related to Me_4Si (C_6D_6 at 128 ppm downfield from Me_4Si). 10,000 - 100,000 transients were accumulated in 4K data points zerofilled to 32K before Fourier Transformation. Spectral width was 2 kHz. No relaxation delay was employed. Pulse width was set to a 90° flip angle. The decoupling circuit was carefully tuned prior to the experiments in order to operate at levels exceeding 2 Watts.

References and notes

1. T.N. Estep, D.B. Mountcastle, Y. Barenholtz, R. Bittonen
   and T.E. Thompson, Biochemistry, 1978, *17*,1984;
   T.N. Estep, D.B. Mountcastle, Y. Barenholtz, R. Bittonen
   and T.E. Thompson, Biochemistry, 1979, *18*,2112;
   R. Jacobs and E. Oldfield, Biochemistry, 1979, *18*,3820.
2. M.C. Blok, L.L.M. van Deenen and J. de Gier, Biochim.
   Biophys. Acta, 1977, *464*,509;
   G. Gregoriadis and C. Davis, Biochem. Biophys. Res. Comm.,
   1979, *89*,1278;
   A. Sakanishi, S. Mitaku and A. Ikegami, Biochemistry,
   1979, *18*, 2636.
3. P.E. Godici and F.R. Landsbergen, Biochemistry, 1975, *14*,
   3927
4. E. Oldfield, M. Meadows, D. Rice and R. Jacobs,
   Biochemistry, 1978, *17*,2727.
5. A. Seelig and J. Seelig, Biochemistry, 1974, *13*,4839.
6. P.W. van Dijck, B. de Kruijff, L.L.M. van Deenen, J. de
   Gier and R.A. Demel, Biochim. Biophys. Acta, 1976, *455*,
   576, and references therein.
7. P.L. Yeagle, Acc. Chem. Res., 1978, *11*, 321, and references
   therein.
8. C.E. Dahl, Biochemistry, 1981, *20*,7158.
9. R.A. Demel and B. de Kruijff, Biochim. Biophys. Acta, 1976,
   488,36.
10. P.L. Yeagle, W. Hutton, C.H. Huang and R. Martin,
    Biochemistry, 1977, *16*,4344.
11. J.L. Browning, Biochemistry, 1981, *20*,7144, and references
    therein.
12. G. W. Stockton, C.F. Polnaszek, A.P. Tulloch, F. Hasan
    and I.C.P. Smith, Biochemistry, 1976, *15*,954.
13. H.U. Gally, A. Seelig and J. Seelig, Hoppe Seyler's Z.
    Physiol. Chem., 1976, *357*,1447.
14. M.F. Brown and J. Seelig, Biochemistry, 1978, *17*,381.
15. B. de Kruijff, R.A. Demel, A.J. Slotboom, L.L.M. van Deenen
    and A.F. Rosenthal, Biochim. Biophys. Acta, 1967, *1*,357;
    P. Joos and R.A. Demel, Biochim. Biophys. Acta, 1969, *183*,

447;

D. Marsh and I.C.P. Smith, Biochim. Biophys. Acta, 1973, *298*,133.

16. J.R. Brainard and E.H. Cordes, Biochemistry, 1981, *20*, 4607.

17. Chapter IV of this thesis.

18. C. Tanford, "The Hydrophobic Effect", Wiley, New York, 1980.

19. R.J.E.M. de Weerd, J.W. de Haan, L.J.M. van de Ven and H.M. Buck, J. Phys. Chem., 1982, *86*,2528 and references therein.

20. H. Hauser, W. Guyer, I. Pasher, P. Skrabal and S. Sundell, Biochemistry, 1980, *19*,366;
    H. Akutsu, Biochemistry, 1981, *20*,7359.

21. B. de Kruijff, P. Cullis and G.K. Radda, Biochim. Biophys. Acta, 1976, *436*,729.

22. J.M. Backer and E.A. Dawidowicz, Biochim. Biophys. Acta, 1979, *551*,260.

23. B. Bloj and D.B. Zilversmit, Biochemistry, 1977, *16*,3943.

24. L.R. McLean and M.C. Philips, Biochemistry, 1981, *20*,2893.

25. J.M. Backer and E.A. Dawidowicz, Biochemistry, 1981, *20*, 3805.

26. G. Govil and P.V. Hosur, "NMR Basic Princ. and Progress: Conformations of Biological Molecules", Springer Verlag, New York, 1982, *20*.

27. P.L. Yeagle, R.B. Martin, A.K. Lala, H.K. Lin and K. Block, Proc. Natl. Acad. Sci. USA, 1977, *74*,4924.

28. N.O. Petersen and S.I. Chan, Biochemistry, 1977, *16*,2657.

29. S.I. Chan, D.F. Bocian and N.O. Petersen, Mol. Biol. Biochem. and Biophys., 1981, *31*,1.

30. G.W. Feigenson and S.I. Chan, J. Amer. Chem. Soc.,1974, *96*,1312;
    P.K. Wolber and B.S. Hudson, Biochemistry, 1981, *20*,2800.

31. F.T. Presti and S.I. Chan, Biochemistry, 1982, *21*,3821;
    J.G. Parkes, H.R. Watson, A. Joyce, R.J. Phadke and I.C.P. Smith, Biochim. Biophys. Acta, 1982, *691*,24.

32. F.T. Presti, R.J. Pace and S.I. Chan, Biochemistry, 1982, *21*,3831.

CHAPTER VI

Chiral model membranes.
A CD and ^{13}C NMR study

VI.1 Introduction

Recently, a mechanism for the stereospecific hydride
uptake of the redox coenzyme NAD(P)$^+$ has been proposed[1,2].
It showed that this hydride uptake was mediated by the out
of plane orientation of the carboxamide group[3]. Experimental
evidence for this hydride transfer mechanism was offered by
the stereoselective reduction of (9R)-N-α-methylbenzyl-1-
propyl-2,4-dimethyl-3-carbamoylpyridinium cation by means of
sodium dithionite[2,4], resulting in one diastereoisomeric
pair (4S,9R)-(+)-N-α-methylbenzyl-1-propyl-2,4-dimethyl-
1,4-dihydronicotinamide and the corresponding (4R,9R)-(-)-
isomer, in which the carboxamide group is forced out of plane
by two adjacent methyl groups as was established by X-ray
molecular structure determinations and ^{1}H NMR lanthanide
induced shift experiments. The outcome of the reduction is
a *syn* orientation of the hydrogen at C-4 and the carbamoyl
moiety. Since it was demonstrated that the corresponding
2,4-dimethyl-3-carbamoylpyridinium cations can also be
optically active[5], the suggestion was put forward that the
absolute configuration of the carbamoylpyridinium moiety
controls the stereochemistry of the hydride uptake. This
behaviour is related to the well-known A or B specificity
of the coenzyme NAD(P)$^+$ under enzymatic conditions[6]. These
chiral nicotinamide compounds were used as detergents via
alkylation of the pyridine nitrogen with *n*-dodecyl bromide
and explored as chiral model compounds for the formation of
single micelles and as model substrates in vesicles of
chiral lecithins. Since previous studies suggest chiral
discrimination for several chiral surfactants[7], experiments

were carried out to search for enantiomeric differences using
highly purified enantiomerically pure nicotinamide detergents
under various conditions with CD and ^{13}C NMR.

VI.2 Synthesis of the optically active model substrates

The synthetic steps involved in the preparation of *8*
are outlined in Figure 6.1. Refluxing crotonaldehyde *1* and
ethyl-ß-aminocrotonate *2* in the presence of piperidine
according to Hantzsch[8] gave the dihydropyridine *3*. Oxidation
by means of *p*-chloranil yielded ethyl-2,4-dimethyl nicotinate *4*.
The 2,4-dimethylpyridinium carboxylic acid *5* was obtained after
hydrolysis and acidification of *4*. Deprotonation by triethyl
amine and chlorination resulted in 2,4-dimethylpyridinyl
carbochloride *6*, which was converted to *N,N*-dimethyl-2,4-
dimethyl-3-carbamoyl pyridine *7*. Alkylation with *n*-dodecyl
bromide afforded the racemic C$_{12}$CPB *8*[1]. The asymmetry of
compound *8* results from the steric interactions between both
ring methyls and the carbamoyl site, leading to an out of plane
orientation of the carbamoyl group[1,2,4]. The separation of
both enantiomers of *8* was accomplished by complexation with
optically pure silver-α-bromocamphor-Π-sulfonate monohydrate
and repeated crystallization of the diastereoisomeric mixture.
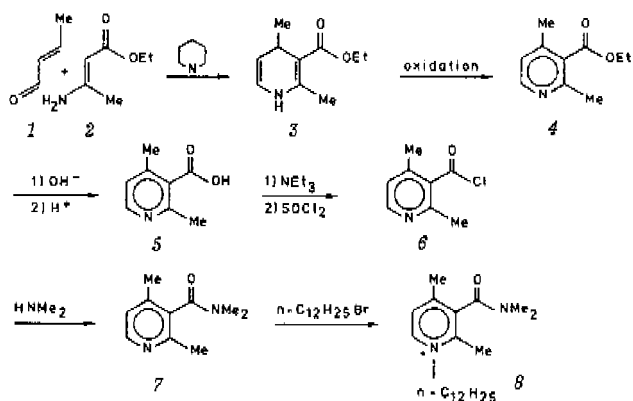Full details are presented in the Experimental Section VI.5.

Figure 6.1   The preparation of the racemic detergent 8.

VI.3.1. Single micelles of $C_{12}CPB$ as reference solutions for the mixed aggregates. Determination of the CMC by means of CD spectroscopy

When varying the concentration of 1-dodecylpyridinium iodide and the chloride, an abrupt change in the UV absorption around 280 nm was detected[9]. A similar procedure was applied to 1-dodecylnicotinamide chloride micelles[10]. The concentration at which this breakpoint occurred was interpreted as the CMC of the surfactant, since its value is in good agreement with the CMC obtained by other physico-chemical procedures[11]. The closely related compound *8*, however, showed no change in the UV spectral data for the same transition. Non micelle-forming compounds, such as the 1-methyl derivative *9*, act similar to *8*.
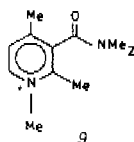
Characteristic differences between compounds *9* on the one hand and micellar *8* on the other hand are observed by means of CD (Figure 6.2a-b). The CD spectra of *8* and *9* show each two transitions at 240 nm and 270 nm. The extinction coefficients ($\Delta\varepsilon$) for compound *9* are constant upon dilution. This is valid for both wave lengths (Figure 6.2b). The $\Delta\varepsilon$ curve *versus* the concentration of *8* shows a remarkable discrepancy from *Lambert-Beer* around the CMC for the CD absorption at 240 nm (Figure 6.2a). One is able to notice (Figure 6.2a and Figure 6.3a) that an increase of the aggregational density - which is the result of an increase of the amphiphile concentration - alters the intensity of both CD bands. The change of the 240 nm band at concentrations above the CMC may be due to an increase of the very strong dichroic absorption at the short wave length side. However, the absolute intensity and position of this strong multiple band could not be detected properly
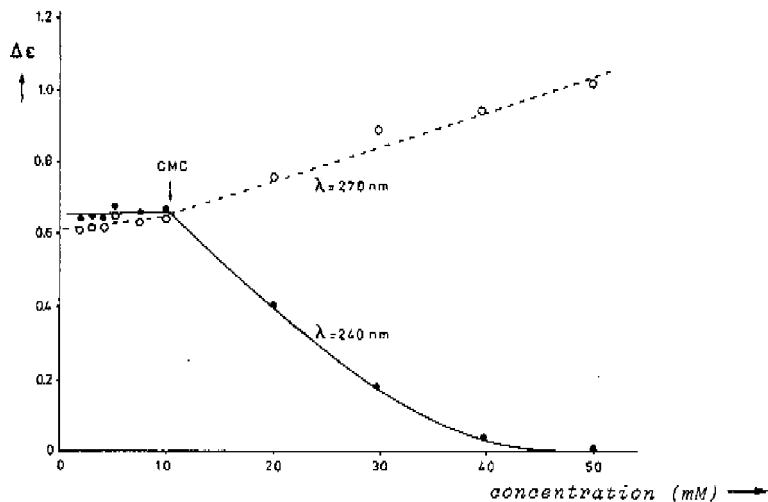
*Figure 6.2a Δε plot versus the concentration of (-)-$C_{12}CPB$.
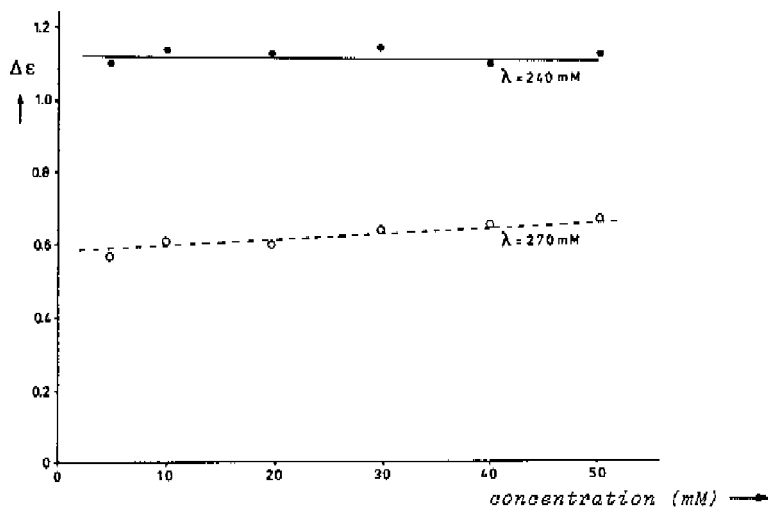A similar plot, although with negative Δε values, was obtained
for (+)-$C_{12}CPB$.*

Figure 6.2b Δε plot versus the concentration of (-)-9.
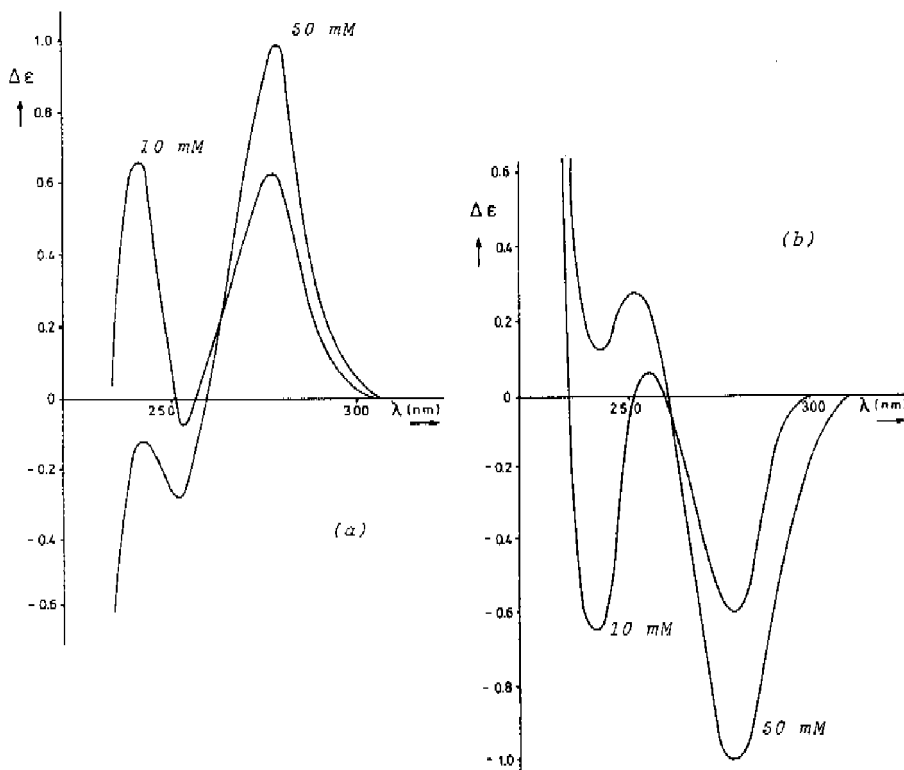
*Figure 6.3   Δε plot versus the wave length of (−)−C$_{12}$CPB
for different concentrations (a). Δε plot versus the wave
length of (+)−C$_{12}$CPB for different concentrations (b).*

due to an overload of the detection system. Explanation of
the concentration effects on the absorption band at 240 nm
in terms of other aspects, such as increasing particle sizes
and microscopic changes in solvent effects, are unlikely
because these would modulate all absorptions in a corresponding
manner[12,13]. Spectra similar to the 50 mM spectrum of Figure
6.3a and 6.3b are obtained for the 1-methyl analogue *9* in
acetonitrile[5]. This may indicate that (partial) dehydration
occurs upon aggregation which results in a less polar

environment for the carboxamide group of compound *8*. This
effectuates deviations from planarity within the carboxamide
group and/or deviations of the out of plane orientation of
the carboxamide group with respect to the pyridinium moiety[14].

*VI.3.2 The influence of chiral L-DMPC on the CD absorption
spectra of (-)- and (+)-C_{12}CPB*

Spontaneous formation of mixed micelles occurs when
DMPC molecules are mixed with a large excess of the chiral
C_{12}CPB amphiphile. The CD spectrum obtained for this mixed-
micellar dispersion is identical with the single-micelle
solution of *8* (compare Figure 6.3a (50 mM) with Figure 6.4a
(mixing ratio 1:4), and compare Figure 6.3b (50 mM) with Figure
6.4b (mixing ratio 1:4)). Low concentrations of L-DMPC do not
influence the rotational strengths of the absorptions of
(-)-*8* and (+)-*8* respectively. Changes in the chirality of
(-)-*8* and (+)-*8* respectively are seen upon a further increase
of the aggregational density (Figure 6.4a (mixing ratio 4:1)
and Figure 6.4b (mixing ratio 4:1) respectively).
Incorporation of low contents of (-)-*8* and (+)-*8* respectively
in L-DMPC *vesicles* shows unambiguously that a strong increase
of the aggregational density induces a complete disappearance
of the absorption band at 240 nm. However, one should keep
in mind that the λ-axis in Figure 6.3 and 6.4 is not identical
with the experimental base line. It is indicated by the decay
of the maximal value of the 240 nm absorption along the series:

monomeric *8* ⟶ micellar *8* ⟶ *8* in vesicles of DMPC
(Figure 6.3)   (Figure 6.3)   (Figure 6.4)

Furthermore, one should consider the effect of the particle
dimensions on the CD spectral data[12]. The probability of
absorption is proportional to the beam intensity. Since the
interior of a particle absorbs intensively, the effect of
a large particle is one of casting a shadow obscuring
chromophores behind it. This results in a decrease of the
CD band intensities[12], which is demonstrated by the decrease
of the Δε value of the absorption band at 280 nm by ca. 20%

going from the mixed-micellar state to the vesicular state (Figure 6.4a and 6.4b). Of course, this effect is proportional to the absolute band intensity. Since the CD band at 240 nm disappears *completely* going from the mixed-micellar to the vesicular state, the effect of increasing particle sizes is of minor importance for this particular absorption.
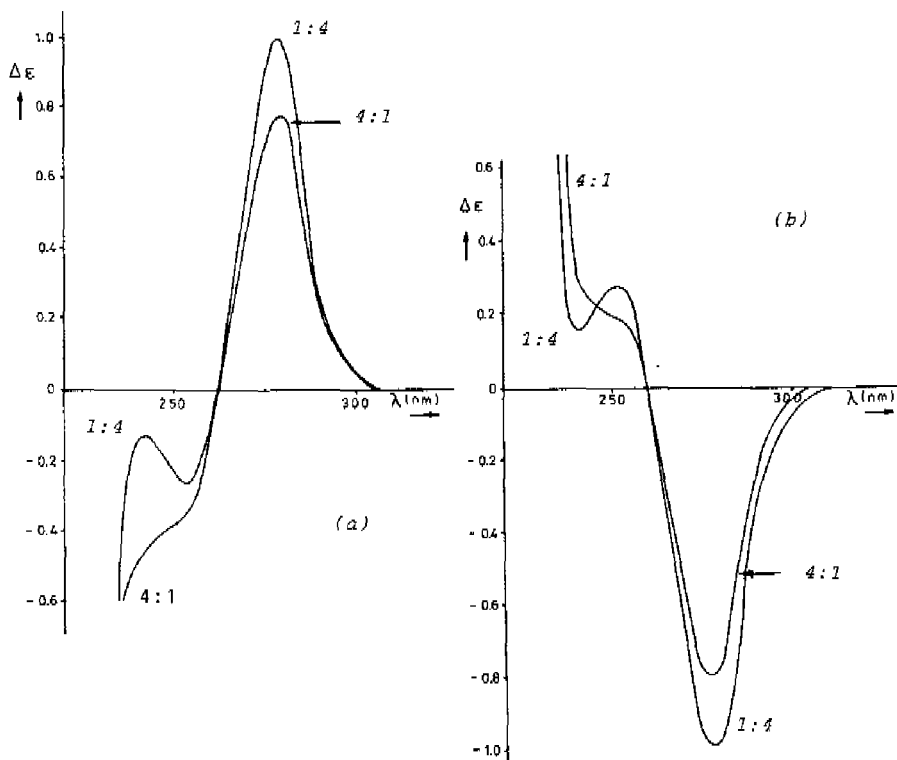

Figure 6.4   Δε plot versus the wave length of $(-)-C_{12}CPB$ incorporated in aggregates of L-DMPC (a). Δε plot versus the wave length of $(+)-C_{12}CPB$ incorporated in aggregates of L-DMPC L-DMPC (b). Molar lecithin/$C_{12}CPB$ mixing ratios are indicated. The 1:4 mixing ratio represents a mixed-micellar solution and the 4:1 mixing ratio represents a mixed-vesicular solution.

VI.3.3 ^{13}C NMR results of the mixed L-DMPC/C_{12}CPB dispersions

The results of Table VI.1 indicate that, comparable with the DMPC/TAB mixed aggregates of Chapter IV, squeezing occurs for the C_{12}CPB amphiphiles. Deshieldings are observed along the hydrophobic chain of the C_{12}CPB revealing chain extension, similar to the incorporated TABs[15]. When incorporated in the chiral L-DMPC vesicles, both C_{12}CPB enantiomers act similarly. No differences in the spectral parameters are observed when comparing the L-DMPC/(-)-C_{12}CPB mixed aggregates with the L-DMPC/(+)-C_{12}CPB mixed aggregates. In other words, there is no evidence that one of the C_{12}CPB enantiomers accommodates preferentially in the chiral-lecithin vesicle.

Table VI.1   Chemical shifts and deshieldings (in parentheses) of the C_{12}CPB amphiphiles upon mixing with L-DMPC^a

(-)-C_{12}CPB carbons	mixing ratios 4:1	mixing ratios 1:4
C-1	58.76 (+0.00)	58.76 (+0.00)
C-2	–	30.30 (+0.05)
C-3	26.47 (+0.15)	26.40 (+0.08)
C-10	32.58 (+0.47)	32.24 (+0.13)
C-11	23.17 (+0.33)	22.95 (+0.14)
C-12	14.25 (+0.06)	14.26 (+0.07)
(+)-C_{12}CPB carbons	mixing ratios 4:1	mixing ratios 1:4
C-1	58.76 (+0.00)	58.76 (+0.00)
C-2	–	30.29 (+0.05)
C-3	26.42 (+0.12)	26.37 (+0.07)
C-10	32.58 (+0.48)	32.22 (+0.12)
C-11	23.17 (+0.33)	22.93 (+0.14)
C-12	14.26 (+0.07)	14.24 (+0.05)

^{a}The total amphiphile concentration was 50 mM.

Table VI.2 offers the chemical shift of the carbonyl carbon
of the $C_{12}CPB$ as a function of the aggregational density.
In order to eliminate solvent effects, corresponding chemical
shifts of the non micelle-forming 1-methyl analogue 9
are also presented (Table VI.3).

Table VI.2 ^{13}C *NMR chemical shift of the carbonyl carbon
of the chiral $C_{12}CPB$ amphiphiles versus the aggregational
density*

	monomer (5 mM)	micelle (50 mM)	mixed micelle[a]	mixed vesicle[b]
		aggregational density		
$\delta_{C=O}$ (ppm)[a]	167.0±0.05	166.6±0.05	166.6±0.05	166.2±0.05

[a]The mixed micelle represents the L-DMPC/$C_{12}CPB$ 1:4 mixed
system.
[b]The mixed vesicle represents the L-DMPC/$C_{12}CPB$ 4:1 mixed
system.
[a]*Both* $C_{12}CPB$ enantiomers possess identical chemical shift
values.

It is well recognized that a large deshielding occurs
for the carbonyl carbon conjugated with an aromatic ring
when the carbonyl group has an out of plane orientation due to
the presence of an α-substituted t-Bu group. For instance,
a chemical shift difference of +8.6 ppm is observed between
the carbonyls of t-butyl-2,6-dimethylphenyl ketone and its
t-butyl analogue with no methyl substituents on the aromatic
ring: t-butylphenyl ketone[16]. The chemical shift changes which
were observed going from the mixed vesicular to the monomeric
solution (Table VI.2) may indicate a change of the average
carbonyl position with respect to the pyridinium ring. However,
one should realize that the effects are small, and that a partial
dehydration of the $C_{12}CPB$ carbonyl upon incorporation in

DMPC aggregates may already bring about such chemical shift changes as well[16].

Table VI.3 ^{13}C *NMR chemical shift of the carbonyl carbon of the chiral C_1CPB amphiphiles versus the concentration*

	5 mM	50 mM	with 10 mM DMPC[a]	with 40 mM DMPC[b]
$\delta_{C=O}$ (ppm)[c]	167.0±0.05	166.8±0.05	166.8±0.05	167.0±0.05

[a]Representation of the L-DMPC/C_1CPB 1:4 mixed systems.
[b]Representation of the L-DMPC/C_1CPB 4:1 mixed systems.
[c]*Both* C_1CPB enantiomers possess identical chemical shift values.

VI.4 Summary/conclusions

The CD spectral data of chiral C_{12}CPB are readily influenced by the aggregational density of the C_{12}CPB. A decay of the absorption band at 240 nm occurs when the intermolecular packing increases. The largest effect occurs for very dense DMPC vesicles in which the C_{12}CPB is incorporated. In order to interpret these observations in terms of a deviation of the planarity within the carboxamide group and/or deviations of the out of plane orientation of the carboxamide group with respect to the pyridinium moiety, ^{13}C NMR chemical shifts of the carbonyl carbon of the C_{12}CPB were measured. However, no definite conclusions could be reached. The hydrophobic alkyl chains of the C_{12}CPB were found to change their conformational equilibria towards more extension. As the (-)-C_{12}CPB and the (+)-C_{12}CPB enantiomer behave similarly, *no* intermolecular stereoselective interactions could be detected between the individual C_{12}CPB enantiomers in the L-DMPC vesicles.

In other words, although squeezing occurs for the C_{12}CPB amphiphiles in L-DMPC vesicles, the difference in the effective surface areas of the two diastereoisomeric C_{12}CPB/DMPC mixed-amphiphile aggregates is not large enough

to induce stereoselective interactions between both C_{12}CPB enantiomers in the L-DMPC vesicles.

Recently, *Tsai et al.*[7] showed spectral differences between several chiral phospholipids, which were ascribed to chiral recognition. These spectral differences are absent in the aggregates of L-DMPC with (-)-*8* and (+)-*8* respectively. Obviously, chiral recognition can easily be observed intramolecularly between diastereoisomers (*i.e.* diastereo-isomeric recognition).

VI.6 Experimental

— General remarks

The ^{1}H NMR spectra were recorded with a Varian EM-360 A NMR spectrometer using Me_4Si as internal standard (δ = 0.00). The ^{13}C NMR spectra were run at 75.476 MHz on a Bruker CXP 300 spectrometer under proton noise decoupling at 50°C. The deuterium signal from C_6D_6 was employed as an external lock signal. All chemical shifts are related to Me_4Si (C_6D_6 at 128 ppm downfield from Me_4Si). 10,000-100,000 transients were accumulated in 4K data points zerofilled to 32K points before Fourier Transformation. Spectral width was 17 KHz. No relaxation delay was employed. Pulse width was set to a 90° flip angle. The decoupling circuit was tuned prior to the various experiments in order to operate at levels of 8 Watts. The optical rotations were measured on an Optical Activity AA-10 polarimeter. The CD-spectra were recorded on a Jobin Yvon Dichrograph Mark III-S. The UV spectra were obtained from a Perkin-Elmer Double Beam Grating Spectrophotometer model 124. DMPC was purchased from Supelco, Inc. and Sigma. The preparation of (mixed) vesicles and (mixed) micelles was outlined already in Chapter IV. Ethyl-β-aminocrotonate *2* and crotonaldehyde *1* were purchased from Aldrich. Ethyl-2,4-dimethyl-1,4-dihydronicotinate *3*[8], ethyl-2,4-dimethyl-nicotinate *4*[8], 2,4-dimethyl-3-carboxylpyridine hydrochloride[2,5], *N,N*-dimethyl-2,4-dimethyl-3-carbamoylpyridine[5,17] and silver-(+)-α-bromocamphor-π-sulfonate monohydrate[18] were prepared using modified literature procedures. For all

measurements, the total amphiphile concentrations were 50 mM, unless indicated otherwise.

▸ (-)-*N,N*-dimethyl-1-dodecyl-2,4-dimethyl-3-carbamoylpyridinium bromide *8*

A stirred solution of dodecyl bromide (25 g; 100 mmol) and amide *7* were heated to 90°-100^oC during two days. The excess dodecyl bromide was decanted. The precipitate was washed with Et_2O and dried, which resulted in 6.6 g (69%) of bromide *8*: oil; ^{1}H NMR ($CDCl_3$) δ 0.90 (t,3,CH_2CH_3), 1.25 (m,20,10 CH_2), 2.50 (s,3,CH_3), 2.77 (s,3,CH_3), 3.00 (s,3,CH_3), 3.17 (s,3,CH_3), 4.73 (t,2,NCH_2), 7.80 (d,1,PyrH), 9.06 (d,1,PyrH).

A diastereomeric pair of *8* was obtained after complexation with silver-(-)-α-bromocamphor-II-sulfonate monohydrate. Repeated crystallization from acetone/hexane resulted in the pure (--) diastereoisomer. Treatment of the (--) complex with Amberlite IRA-400 (Br⁻-form) resulted in (-)-*8*: CD (H_2O) Δε +0.6 (278 nm), +0.65 (240 nm). $[\alpha]_D^{20}$= -12.4 (H_2O, c= 0.005 M).

▸ (+)-*N,N*-dimethyl-1-dodecyl-2,4-dimethyl-3-carbamoylpyridinium bromide *8*

Prepared analogously to (-)-*8* using silver-(+)-α-bromocamphor--II-sulfonate monohydrate: CD (H_2O) Δε -0.6 (278 nm), -0.65 (240 nm). $[\alpha]_D^{20}$= +12.3 (H_2O, c= 0.005 M).

References and notes

1. Abbreviations used: C_1CPB, N,N-dimethyl-1,2,4-trimethyl-
   -3-carbamoylpyridinium bromide; $C_{12}CPB$, N,N-dimethyl-
   -1-dodecyl-2,4-dimethyl-3-carbamoylpyridinium bromide;
   CD, Circular Dichroism; $NAD(P)^+$, nicotinamide adenine
   dinucleotide phosphate.
2. P.M. van Lier, M.C.A. Donkersloot, A.S. Koster, H.J.G.
   van Hooff and H.M. Buck, Recl. Trav. Chim. Pays-Bas,
   1982, *101*,119.
3. M.C.A. Donkersloot and H.M. Buck, J. Amer. Chem. Soc.,
   1981, *103*,6554.
4. G. Blankenhorn and E.G. Moore, J. Amer. Chem. Soc., 1980,
   102,1092.
5. H.J.G. van Hooff, P.M. van Lier, L.A.M. Bastiaansen and
   H.M. Buck, Recl. Trav. Chim. Pays-Bas, 1982, *101*,191.
6. R.M. Garavito, M.G. Rossmann, P. Argos and W. Eventoff,
   Biochemistry, 1977, *16*,5065.
7. K. Bruzik, S.M. das Gupta and M.D. Tsai, J. Amer. Chem.
   Soc., 1982, *104*,4682;
   M.D. Tsai, R-T. Jiang and K. Bruzik, J. Amer. Chem. Soc.,
   1983, *105*,2478.
8. A. Hantzsch, Ber., 1890, *23*,1474;
   K. Tsuda, Y. Satch, N. Itekawa and H. Mishima, J. Org.
   Chem., 1956, *21*,800.
9. W.D. Harkins, H. Krizek and M.L. Corrin, J. Colloid Int.
   Sci., 1951, *6*,576.
10. B.M. Anderson and C.D. Anderson, Biochim. Biophys. Acta,
    1970, *205*,161.
11. P. Mukerjee and K.J. Mysels, Natl. Bur. Stand. Ref. Data
    Ser. (U.S., Natl. Bur. Stand.) NSRDS-NBS, 1971, *36*.
12. M.M. Long and D.W. Urry, Mol. Biol. Biochem. and Biophys.,
    1981, *31*,143.
13. M. Legrand and M.J. Rougier, "Stereochemistry", Vol. 2
    (Ed. H.B. Kagan), G. Thieme Publ., Stuttgart, 1977, 33.
14. P.M. van Lier, G.H.W.M. Meulendijks and H.M. Buck,
    Recl. Trav. Chim. Pays-Bas, 1983, *102*,337.
15. Chapter IV of this thesis.

16. J.B. Stothers, "^{13}C NMR Spectroscopy" (Ed. A.T. Blomquist), Acad. Press, New York, 1972.

17. A. Ohno, M. Ikeguchi, T. Kimura and S.Oka, J. Amer. Chem. Soc., 1979, *101*,7036.

18. B.E. Douglas (Ed.), "Inorganic Synthesis, Vol. XVIII", Wiley & Sons, New York, 1978, 107.

CHAPTER VII

CPMAS NMR in non-hydrated and hydrated phospholipid aggregates and modelsubstrates

VII.1 Introduction

Nuclear magnetic resonance has been used extensively to gain insight into the structure and dynamics of model and biomembranes, in combination with many other techniques[1]. The often complex internal structures of many biomembranes, however, are not always accessible to spectroscopic methods. For example, rigid (parts of) membranes, having large internal viscosities, induce substantial line broadening of ^{13}C resonances monitored by common ^{13}C HR NMR. This type of NMR spectroscopy is mainly applicable to isotropic solutions. A way to overcome the detection of broad resonances is to eliminate the dipolar $^{13}C-^{1}H$ interactions contributing to the line width, through elevated power decoupling[2]. HR NMR in anisotropic systems became a routine method with the development of cross polarization magic angle spinning (CPMAS), which was first experimentally recognized by *Schaefer* and *Stejskal*[3]. It combines pulsed NMR excitation with high-speed sample rotation and high power decoupling. Rapid sample rotation around an angle of 54.7° with respect to the external magnetic field diminishes the chemical shift anisotropy contributions caused by non-averaged molecular orientations. In combination with strong dipolar decoupling "liquid-like" narrow lines are observed. The ^{13}C relaxation times in the solid state, however, are very long and large delay times are necessary to obtain reasonable signal to noise ratios. One way to prevent this is offered by cross polarization between the ^{13}C (rare spin) and ^{1}H nuclei[4], which is initiated by spin locking the protons[5]. In this manner, the magnetization of the ^{13}C and ^{1}H nuclei directed along the main axis of the external magnetic field,

possess the same time dependence, and thus energy transfer is possible *via* the spin-flip mechanism. As a result, the delay time is now controlled by the relaxation mechanism of the ^{1}H nuclei only, instead of the ^{13}C nuclei. Accordingly, the acquisition time becomes much shorter and relatively large signal to noise ratios are obtained readily.

Until now, ^{13}C-CPMAS has not been used extensively in the field of phospholipid research. However, the interest in applying this technique is increasing rapidly. ^{13}C-CPMAS spectra of phospholipids in the anisotropic bilayer state have been presented[6], revealing highly resolved resonances for unsonicated phospholipids in excess of water. In this Chapter, the ^{13}C-CPMAS experiment is used to gain insight into the molecular organization within phospholipid aggregates and model substrates at low water contents.

VII.2 The rotational speed dependence of the ^{13}C-CPMAS spectra

It should be stressed that, contrary to the HR measurements presented in the preceding Chapters, CPMAS experiments are in principle no longer non-destructive, due to the presence of strong ultracentrifugal forces in the sample at fast rotational sample speeds and a substantial heat transfer to the sample, especially when it absorbs radiofrequencies readily. Figure 7.1 indicates that sample rotation faster than ca. 2.6 KHz introduces additional resonances after a certain time interval (typically 30 hrs.). The clearest example is the *extra* low field resonance in the $-\overset{+}{N}Me_3$ region of the phospholipid at about 53 ppm. Not so very distinct, but also observable are the additional resonances in the acyl region between 24 and 29 ppm. These spectral changes are *not* observed when rotating the sample at 2.6 KHz. This indicates that the occurrence of the additional resonances is caused by an increase of the centrifugal force when increasing the rotor speed to 4 KHz. The latter frequency corresponds to a pressure at the rim of the rotor of ca. 20 atm. Obviously, at least one phase transfer is achieved at such large internal pressures.
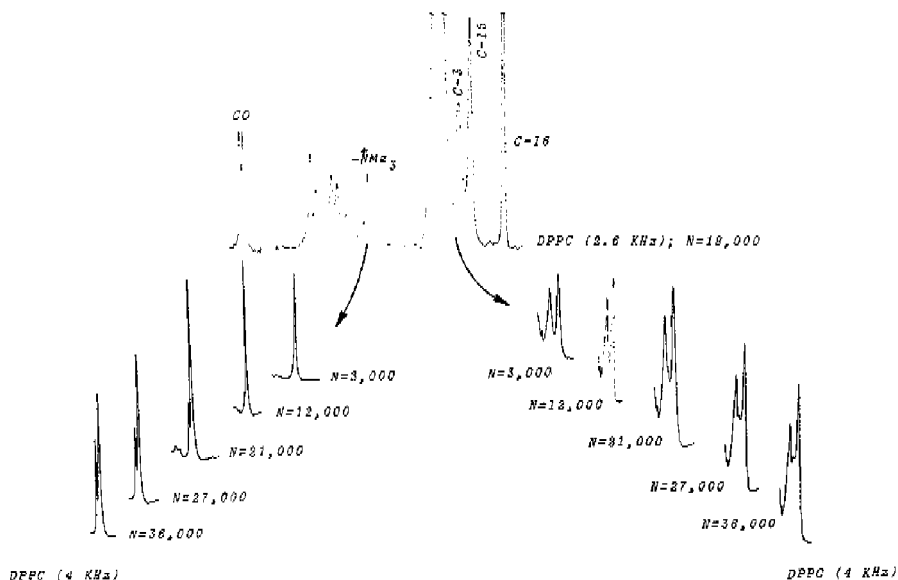
Figure 7.1   The rotational speed dependence of the ^{13}C-CPMAS spectrum of DPPC. The upper spectrum shows DPPC at 2.6 KHz sample spinning. The "53 ppm"-region (left) and the "24-29 ppm"-region (right) at 4 KHz spinning are shown below. The number of transients (N) is also indicated.

VII.3 Hydrated and non-hydrated DPPC

Amorphous samples of DPPC were prepared by dilution with a solvent and subsequent evaporation. Spectra like the one presented in Figure 7.1 were readily obtained. Upon hydration, the only change observed was the broadening of the carbonyl

Table VII.1   Chemical shifts of hydrated and non-hydrated DPPC, at 2.6 KHz sample spinning[a]

	non-hydrated DPPC[d]	hydrated DPPC[d]
CO	173.1	173.2
	172.2	
CHO[b]	70.8	71.2
CH$_2$N̄[c]	66.5	66.5
CH$_2$OP[b]	64.5	64.6
CH$_2$O[b]	62.7	63.3
CH$_2$OP[c]	60.4	60.1
N̄(CH$_3$)$_3$	54.0	54.5
C-2	35.3	35.3
	34.9	34.8
C-3	27.4	26.9
	27.0	
C-4 - C-13	32.7	33.0
C-14	33.9	34.3
	33.5	33.6
C-15	24.3	24.3
	23.7	23.9
C-16	14.2	14.4

[a]The chemical shifts (ppm) are related to adamantane (δ = 29.23 ppm).
[b]Backbone resonances.
[c]Head group resonances.
[d]The resolved resonances correspond to the *sn*-1 and *sn*-2 acyl chains of the DPPC. The reproducibility of the measurements was 0.5 ppm.

resonances of the *sn-1* and the *sn-2* chain: the two resonances
were no longer detected separately (Table VII.1). It indicates
that hydration occurs for this group in particular and not for
carbons located further inside the hydrophobic region. It was
impossible, unfortunately, to operate at higher water contents
due to a large heat uptake by the internal water amount, which
ultimately resulted in phase transitions and subsequent spinning
instability.

VII.4 Mixing TABs with DPPC in the hydrated phase

At the water contents investigated, DPPC possesses the
bilayer orientation[7]. Incorporation of $C_{14}TAB$ gave the
following implications (Table VII.2 and Figure 7.2). First,
the reproducibility of the chemical shifts (Table VII.2) was
estimated at 0.5 ppm. Thus, when chemical shift changes are
induced by interactions between $C_{14}TAB$ and DPPC, these do not
exceed 0.5 ppm. Such chemical shift changes are comparable
with the values obtained for lecithin dispersions with higher
water amounts[8]. In other words, when changes in conformation
or packing occur, these are not larger than those for the
micellar and vesicular phase[8]. Secondly, changes in DPPC and
$C_{14}TAB$ mobilities were studied. This was done by means of
the $T_{1\rho}^{H}$-values of the protons of both compounds (Figure 7.2,
only the readily detectable resonances of the methyl carbons
of the hydrophobic and hydrophilic region were observed). The
$T_{1\rho}^{H}$ relaxation time represents the time constant with which
the spin-locked magnetization in the rotating frame decays[4,9].
$T_{1\rho}^{H}$-values are usually much longer than the spin-spin
relaxation time T_2^{H} and shorter than the spin-lattice
relaxation time T_1^{H}. Typical values are $T_2^{H} \sim 10^{-5}$ s and
$T_{1\rho}^{H} \sim 10^{-4} - 10^{-2}$ s. Although $T_{1\rho}^{H}$ processes are influenced
by inter- and intramolecular spin diffusion[10,11] - and thus
their $T_{1\rho}^{H}$-values represent an *average* over all protons in the
amphiphiles - and, moreover in the case presented here,
internal methyl rotation[11] also contributes, some conclusions
can be reached from the plots of Figure 7.2. The $T_{1\rho}^{H}$ of DPPC
increases with raising concentrations of $C_{14}TAB$ (a fast decay
of the ^{13}C NMR signal intensity implies a short $T_{1\rho}^{H}$-value

Table VII.2 Chemical shifts of $C_{14}TAB$ and DPPC upon mixing

carbons[b]	mixing ratios[a]						
	9:1	4:1	2:1	1:1	1:2	1:4	pure
	C_{14}TAB						
$\overset{+}{N}(CH_3)_3$	53.5	53.6	53.6	53.6	53.6	53.6	53.6
C-1	66.4	66.5	66.4	66.5	66.4	66.4	66.4
C-2	-	-	-	-	-	-	24.6
C-3	-	-	-	-	-	-	29.6
C-12	34.4	34.5	34.5	34.4	34.2	34.7	34.7
C-13	-	-	23.7	23.6	23.7	23.7	23.8
C-14	-	16.8	16.8	16.7	16.7	16.8	16.8
	DPPC						
CHO[a]	71.0	70.1	71.2	71.3	71.5	70.9	
CH_2OP[a]	64.7	-	64.6	64.3	64.1	64.5	
CH_2O[a]	63.2	63.1	63.0	63.0	63.0	63.3	
CH_2OP[d]	60.1	60.3	60.0	60.0	60.0	-	
$CH_2\overset{+}{N}$[d]	66.4	66.5	66.5	66.5	66.4	66.4	
$\overset{+}{N}(CH_3)_3$	54.5	54.5	54.5	54.5	54.5	54.5	
CO	172.6	172.7	173.1	73.0	173.0	172.7	
	172.0	172.1	172.4	172.4	172.3	172.0	
C-2	-	35.8	35.1	35.1	35.1	35.2	
C-3	-	-	-	26.7	26.8	26.9	
	26.4	26.4	26.6	27.0	26.8	26.8	
C-4 - C-13	33.0	33.0	33.0	32.9	32.7	32.7	
C-14	34.0	34.5	34.0	33.9	34.2	33.9	
C-15	24.9	24.9	24.9	24.8	24.8	24.8	
	24.2	24.1	24.2	24.1	24.0	24.2	
C-16	14.5	14.7	14.4	14.4	14.4	14.4	

[a]Mixing ratios are defined as the quotient of the concentrations of the DPPC and the C_{14}TAB.
[b]Due to overlapping signals, spectral assignments of the carbons which are not mentioned were impossible, just as the carbons corresponding to the vacancies in the Table.
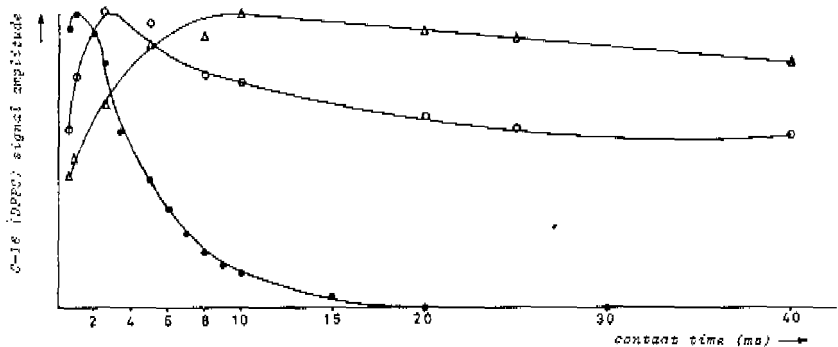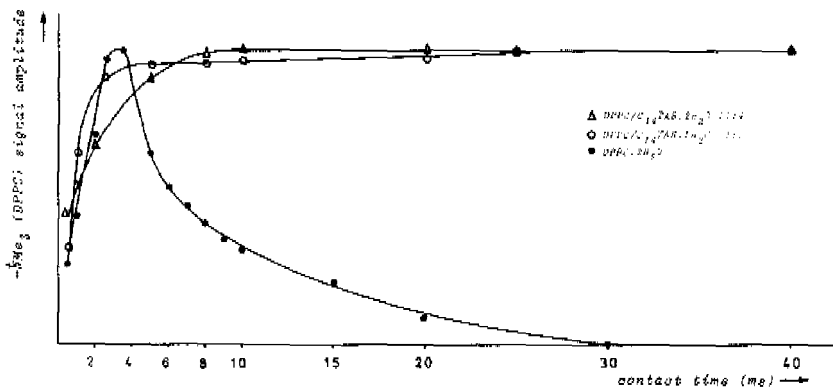[c]Backbone resonances.
[d]Head group resonances.

Figure 7.2   Cross polarization characteristics of the $-\overset{+}{N}Me_3$ and the hydrophobic methyls of the constituents of the $DPPC/C_{14}TAB.2H_2O$ aggregates. Mixing ratios are indicated. In each plot the arbitrary vertical scales are not comparable.
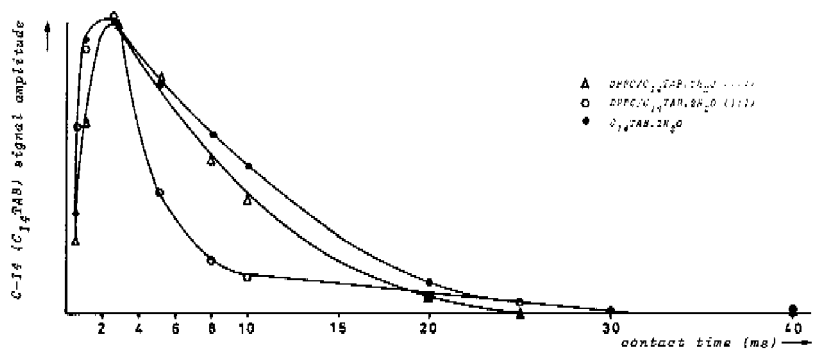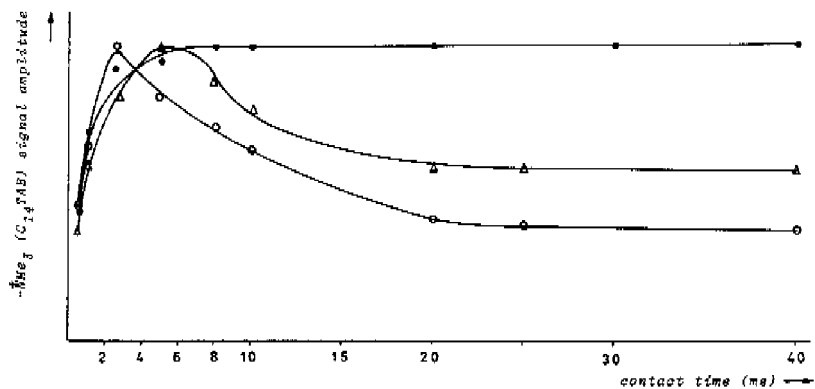
Figure 7.2   (continued)

and a slow decay corresponds with a long $T_{1\rho}^H$-value). These observations indicate that the lecithin mobility on the former mentioned time scale *increases*. The $T_{1\rho}^H$-value of $C_{14}TAB$ decreases when raising the concentration of DPPC. This indicates that $C_{14}TAB$ mobilities *decrease* when the DPPC concentration is raised.

VII.5 Summary/conclusions

The central questions in many studies of phospholipid bilayers are, as far as the hydrophobic parts are concerned, concentrated around the problem of occurrence of chain kinking and/or unpacking and the reasons for this. A number of studies have been performed using vibrational spectroscopy and NMR. A useful reference of the differences in vibrational spectroscopy was given by *Bush et al.*[12]. The measurements described in this Chapter concern only variations in water contents over a rather limited concentration range. The discussion is thus confined to this point. *Gaber et al.*[13] indicated that solid *n*-hexadecane and DPPC would have the same *anti/gauche* ratios. The chemical shifts of the pure DPPC phases indicate that DPPC, even in the absence of water, is less rigid and/or tightly packed than solid *n*-alkanes[14]. This is concluded from the fact that for DPPC shielding of about 1 ppm are found with respect to solid alkanes.

Hydration of the DPPC was found to influence the carbonyl carbons only. In the past, two moles of water per lipid molecule were claimed to induce conformational changes within head group and acyl tails, as detected by Raman spectroscopy[12,13]. In particular, *Bush et al.* came to the conclusion that addition of two moles of water effectuated a decrease of the crystallinity due to increased molecular motions in the head group region and the interfacial region. However, the conformational changes in the acyl chains are in the order of only 5%. These fall within the reproducibility of the CPMAS experiments presented here. Recently, the working procedure of *Gaber et al.*[13] was critically reviewed by *Snyder et al.*[15]. The latter indicated that care should be taken with the interpretations of *Gaber et al.*[13], using certain IR- or Raman absorption bands as

so-called *anti* or *gauche* markers. This, in *Snyder's* opinion,
could lead to erroneous results. This might also be the case
for the experiments of *Bush et al.*[12]. On the other hand,
however, the present CPMAS NMR results might verify the
outcome of *Bush et al.*[12] independently. It can be noted in
passing, that *Snyder's* suggestion that in the gel phase
of DPPC only interactions between all-*anti* chains occur,
fits in the present description of the NMR results[16].

$T_{1\rho}^H$ measurements indicate that sqeezing of the $C_{14}TAB$
substrate by lecithins takes place in the flat bilayer state,
analogously to the vesicular dispersions outlined in Chapter
IV. Obviously, small radii of curvature are not necessary to
obtain squeezing of the substrate. No evidence for large
conformational changes were found to occur simultaneously
with the squeezing of the $C_{14}TAB$ by DPPC. This is concluded
from the fact that the chemical shift changes to be expected
based on studies of more mobile systems, are of the same order
of magnitude as the reproducibility of the measurements
(see Chapters II and III).

VII.6 Experimental

Multibilayer dispersions of DPPC were prepared as follows.
A chloroform solution of the lecithin was evaporated to dryness
under a stream of argon. Residual traces of organic solvent
were removed overnight at 60^oC and at 0.005 mm Hg. The lecithin
was transferred to an Andrew-rotor and the appropriate amount
of deionized water was added (2 moles water on 1 mole lecithin).
Mixed multibilayer dispersions of DPPC and $C_{14}TAB$ were
prepared similarly, by drying a chloroform solution of both
constituents and subsequent adding the appropriate amounts
of water (2 moles water on 1 mole amphiphile, *i.e.* lecithin
plus TAB).

The ^{13}C-CPMAS NMR spectra were run at 75.476 MHz on a
Bruker CXP 300 spectrometer. The chemical shifts are related
to Me_4Si. 4,000-60,000 transients of 1K data points were
accumulated and zerofilled to 32K points prior to Fourier
Transformation. Spectral width was 17 KHz. The pulse delay
employed varied from 4 s for the non-hydrated samples to

15 s for the hydrated samples. The [1]H-pulse duration was 3 μs, corresponding to a [1]B-field of ca. 20 Gauss. The contact time employed was 2.5 ms and varied during the $T_{1\rho}^{H}$ experiments. The acquisition time was 29 ms and the rotor speed was 2.6 KHz, unless indicated otherwise.

References and notes

1. E. Grell (Ed.), "Molecular Biology, Biochemistry and Biophysics, Part 31: Membrane Spectroscopy", Springer Verlag, New York, 1981.
2. Chapter IV and V of this thesis.
3. J. Schaefer, E.O. Stejskal and R. Buchdahl, Macromolecules, 1975, *8*,291.
4. S.R. Hartmann and E.L. Hahn, Phys. Rev., 1962, *128*,2042.
5. A. Pines, M.G. Gibbey and J.S. Waugh, Chem. Phys. Lett., 1972, *15*,373.
6. R.A. Haberkorn, J. Herzfeld and R.G. Griffin, J. Amer. Chem. Soc., 1978, *100*,1296;
   J. Herzfeld, A. Roufosse, R.A. Haberkorn, R. Griffin and M.J. Glimscher, Phil. Trans. R. Soc. London B, 1980, *289*,459;
   R. Griffin, Meth. Enzym., 1981, *72*,108.
7. G. Büldt, H.U. Gally and J. Seelig, Nature, 1978, *271*,182.
8. Chapter III and IV of this thesis.
9. A.G. Redfield, Phys. Rev., 1955, *98*,1787.
10. D.W. McCall, Acc. Chem. Res., 1971, *4*,223.
11. A. Abragam, "The Principles of Nuclear Magnetism", Clarendon Press, London, 1961, 565.
12. S. Fowler Bush, R.G. Adams and I.W. Levin, Biochemistry, 1980, *19*,4429.
13. B.P. Gaber and W.L. Peticolas, Biochim. Biophys. Acta, 1977, *465*,260.
14. D.L. VanderHart, J. Magnetic Res., 1981, *44*,117.
15. R.G. Snyder and H.L. Strauss, J. Phys. Chem., 1982, *86*, 5145;
   R.G. Snyder, D.G. Cameron, H.L. Casal, D.A.C. Compton and H.H. Mantsch, C. R.-Conf. Int. Spectrosc. Raman, 7th, 1980, 622.
16. Future research in this area could concern a.o. the following subjects: inclusion of various model substrates in lecithin bilayers, and variable temperature CPMAS NMR. The first approach would allow comparisons with

interpretations obtained by vibrational spectroscopy and NMR. The second topic would bring valuable information regarding phase transitions. Sources are found in:

P.K. Wolber and B.S. Hudson, Biochemistry, 1981,*20*, 2800;

M.R. Paddy, F.W. Dahlquist, J.H. Davis and M. Bloom, Biochemistry, 1981, *20*,3152;

D.G. Cameron, E.F. Grudgin and H.H. Mantsch, Biochemistry, 1981, *20*,4496;

N. Yellin and J.W. Levin, Biochemistry, 1977, *16*,642 and Biochim. Biophys. Acta, 1977, *489*,177;

D.A. Pink, T.J. Green and D. Chapman, Biochemistry, 1981, *20*,6692.

Summary

Membrane mediated processes appear through the presence of incorporated substrates (proteins, cholesterol, single stranded amphiphiles). In general, the central part of the membrane is formed by a phospholipid bilayer. This bilayer is built up by a hydrophilic outside region (the phospholipid head groups) and a hydrophobic inside region (the phospholipid acyl chains), which shows fluid-like characteristics. A most convenient method in the study of the fluidity of the bilayer is ^{13}C NMR, capable of monitoring each individual carbon. However, this method has been hardly applied to (model systems for) biomembranes, because of the difficulties in interpreting the ^{13}C NMR spectral parameters.

This thesis describes a method which translates ^{13}C NMR spectral data into a number of aspects of the membrane fluidity. This method has been made suitable for measuring colloidal particles (micelles, vesicles and flat bilayers). The interpretations of the ^{13}C spectra were carried out in terms of membrane fluidity (*i.e.* changes in conformational equilibria, intermolecular hydrophobic interactions and intermolecularly correlated mobilities of the constituents of the colloidal particles). This procedure was first tested experimentally on well-defined single- and mixed-*micellar* structures of fatty acid salts with different *n*-acyl chain lengths. Then, the procedure was extended towards mixed micelles consisting of biological components and model compounds for biomembrane substrates, *i.e.* a short-chain lecithin and several single stranded trimethyl-ammonium bromides (TABs). It was shown, that the lecithin possesses the intrinsic property of making the incorporated TAB substrates rigid. A further extension towards large

anisotropic systems was made by the investigation of *vesicular* colloidal solutions of long-chain lecithins. It was shown, that at low concentrations of the TAB substrate also rigidity of the TABs was induced by the surrounding long-chain lecithins, without affecting the lecithins. Furthermore, it was demonstrated that upon disruption of the mixed-vesicular structure towards mixed-micellar structures through raised concentrations of substrate (ca. 1 equiv.), the rigidity of the TABs was reduced. Non-amphiphilic substrates such as cholesterol were reduced in their dynamics analogous to the amphiphilic TABs. In the case of intercalation of cholesterol, however, it was demonstrated that the sterol-surrounding lecithins were also made rigid. It was found to be related to the large dimension of the sterol.

Many of the metabolites traversing the biomembrane are optically active. The chiral single-stranded model substrate N,N-dimethyl-1-dodecyl-2,4-dimethyl-3-carbamoylpyridinium bromide (C_{12}CPB) was made rigid by the lecithins (analogous to the former mentioned substrates), which resulted in changes of the chirality of the substrate. In this case rigidification of the chiral C_{12}CPB was shown to affect CD spectral absorptions The possibility of a conformational change within the chiral polar head group of the C_{12}CPB was discussed.

Finally, the ^{13}C NMR operating procedure was applied to colloidal particles best resembling the biomembrane backbone, *i.e. bilayer* particles. Similar to micellar lecithins and vesicular lecithins, the lecithin molecules in the bilayer orientation were found to resist against disruption of the bilayer by substrates.

Biomembranes are much more complicated than the model systems described in this thesis. Nevertheless, a general membrane property was detected, *viz.* that membrane substrates are squeezed within the membrane, as induced by the surrounding lecithin molecules.

Samenvatting

Processen waarbij het membraan betrokken is, verlopen door de aanwezigheid van geinkorporeerde substraten (proteinen, cholesterol, n-alkylamfifielen). In het algemeen wordt het centrale deel van het membraan gevormd door een dubbellaag van fosfolipiden. Deze dubbellaag wordt opgebouwd door een hydrofiele buitenzijde (de kopgroepen van de fosfolipiden) en een hydrofobe binnenkant (de acyl ketens van de fosfolipiden), welke vloeistofeigenschappen vertoont. Een uiterst geschikte methode om de vloeibaarheid van de dubbellaag te bestuderen is ^{13}C NMR, welke in staat is om ieder koolstofatoom individueel te observeren. Echter, vanwege de moeilijkheden om de ^{13}C spektrale gegevens te interpreteren is deze techniek zelden toegepast op (modellen voor) biomembranen.

In dit proefschrift wordt een manier beschreven om de ^{13}C spektrale gegevens te interpreteren naar een aantal aspekten van het vloeistofkarakter van het membraan. Deze methode is toepasbaar gemaakt voor de studie van kolloidale deeltjes (micellen, vesicles en vlakke dubbellagen). De interpretaties van de ^{13}C spektra werden uitgevoerd in termen van de vloeibaarheid van het membraan (d.w.z. veranderingen van konformatie-evenwichten, intermolekulaire hydrofobe interakties en intermolekulair gekorreleerde mobiliteiten van de bestanddelen van de kolloidale deeltjes). In eerste instantie werd deze methodiek getest op goed gedefinieerde enkelvoudige en gemengde *micellen* van zouten van vetzuren met verschillende ketenlengtes. Vervolgens werd de interpretatiemethode uitgebreid naar gemengde micellen bestaande uit biologische verbindingen en modelsubstraten, d.w.z. een lecithine met een korte n-acylketenlengte en enkele n-alkyltrimethylammoniumbromides (TABs). Aangetoond

werd, dat de lecithinemolekulen de intrinsieke eigenschap bezitten om de geinkorporeerde TAB substraten te verstarren. Een verdere uitbreiding naar grote anisotrope systemen werd gemaakt door de bestudering van kolloidale oplossingen van *vesicles* van lecithines met een lange *n*-acylketenlengte. Het bleek, dat bij lage koncentraties van de TAB substraten eveneens verstarring optrad van de TAB molekulen. Dit werd veroorzaakt door de omringende lecithinemolekulen, zonder dat deze zelf werden beinvloed. Eveneens werd duidelijk dat, bij uiteenvallen van de vesiclestruktuur in micellaire strukturen onder invloed van ca. 1 equivalent substraat, de starheid van de TAB substraten afnam. Niet-amfifiele substraten zoals cholesterol verstarden eveneens, analoog aan de TABs. Echter bleek het dat, wat betreft het geinkorporeerde cholesterol, de omringende lecithinemolekulen ook verstarden. De oorzaak hiervan was de grote afmeting van het cholesterolmolekuul.

Een groot aantal metabolieten welke door het membraan getransporteerd worden, zijn optisch aktief. Het chirale modelsubstraat, N,N-dimethyl-1-dodecyl-2,4-dimethyl-3-carbamoyl-pyridiniumbromide (C_{12}CPB) verstarde onder invloed van de omringende lecithinemolekulen, analoog aan de TABs, hetgeen resulteerde in veranderingen in de chiraliteit van het substraat. In dit geval bleek, dat bij verstarring van het chirale C_{12}CPB CD-absorpties werden beinvloed. Een mogelijke konformatie-verandering in de chirale kopgroep van het C_{12}CPB werd besproken.

Tenslotte werd de ^{13}C NMR interpretatiemethode toegepast op kolloidale deeltjes welke de beste gelijkenis vertonen met de biologische lecithineaggregaten, namelijk de deeltjes met de *vlakke dubbellaag*orientatie. Analoog aan micellaire en vesiculaire lecithines werd gedemonstreerd dat ook in dit geval de lecithinemolekulen zich verzetten tegen het uiteenvallen van de dubbellaag o.i.v. *n*-alkylsubstraten.

Biomembranen zijn meer gekompliceerde systemen dan de in dit proefschrift beschreven modelsystemen. Niettemin werd een intrinsieke eigenschap van het membraan ontdekt, namelijk dat de membraansubstraten in het membraan worden samengedrukt door de omringende lecithinemolekulen.

Curriculum vitae

De auteur van dit proefschrift werd geboren op 18 mei 1955 te Tilburg. Na het behalen van het HBS-B diploma aan het Jacob Roelands College te Boxtel werd in september 1972 begonnen met de studie Scheikundige Technologie aan de Technische Hogeschool te Eindhoven. Het afstudeerwerk werd verricht bij de vakgroep Organische Chemie onder leiding van prof. dr. H.M. Buck en dr. ir. A.A. Macco. Het doctoraalexamen werd op 28 februari 1979 afgelegd. Tot 1 december 1979 was hij in dienst van de Technische Hogeschool te Eindhoven. Op 1 december 1979 trad hij in dienst van de Nederlandse Stichting voor Zuiver-Wetenschappelijk Onderzoek als wetenschappelijk assistent bij de vakgroep Organische Chemie. Het in dit proefschrift beschreven onderzoek stond onder leiding van prof. dr. H.M. Buck en dr. ir. J.W. de Haan. Thans is hij in dienst van International Flavors & Fragrances B.V. te Tilburg.

.

Dankwoord

Aan het totstandkomen van dit proefschrift hebben velen
een bijdrage geleverd, waarvoor ik ze zeer erkentelijk ben.
Enkelen wil ik met name noemen. Tegenover ing. M. Achten en
H.M.P.J. van Hal zou ik mijn hartelijke dank willen uitspreken
voor hun bijdragen op het experimentele gebied. Voor de
fysische metingen ben ik veel dank verschuldigd aan:
drs. L.A.M. Bastiaansen, G.J. Bezemer, P.L.M. van den Bosch,
H. Eding, dr. ir. J.W. de Haan en ing. L.J.M. van de Ven.
Dr. ir. J.W. de Haan en ing. L.J.M. van de Ven dank ik in
het bijzonder voor de vele opbouwende discussies die we
hebben gevoerd.

Mevrouw P. Meyer-Timan en H. Eding ben ik zeer erkentelijk
voor hun medewerking aan de uiteindelijke vormgeving van dit
proefschrift.

Stellingen

1. De konstatering dat fosfolipiden bij lage watergehaltes
   zijn georienteerd in de dubbellaagstruktuur, dient in
   overeenstemming te zijn met de binaire fasediagramgegevens.

   > V. Luzatti, "Biological Membranes, Physical Fact
   > and Function" (D. Chapman, Ed.), Acad. Press,
   > London, 1968, 71;
   > V. Luzatti, T. Gulik en A. Tardieu, Nature, 1968,
   > *218*,1031.

2. Het is opmerkelijk dat *Ebright* en *Wong* ervan uitgaan dat de
   adeninebase van cyclisch 3',5'-adenosinemonofosfaat (cAMP)
   direkt deelneemt aan de interaktie tussen DNA en het komplex
   van cAMP en het cAMP receptor proteine, terwijl uit röntgen-
   onderzoek door *McKay* en *Steitz* is gebleken dat het cAMP
   molekuul diep in het cAMP receptor proteine opgesloten ligt.

   > R.H. Ebright en J.R. Wong, Proc. Natl. Acad. Sci.
   > USA, 1981, *78*,4011;
   > D.B. McKay en T.A. Seitz, Nature, 1981, *210*,745.

3. Uit de resultaten van *van Haastert et al.* moet gekonkludeerd
   worden dat de vorming van een kovalente binding tussen het
   enzym en cyclisch 3',5'-adenosinemonofosfaat plaatsvindt
   door een aanval van een enzymligand op de *endo* positie van
   het fosfor atoom en niet, zoals door hen wordt verondersteld,
   op de *exo* positie.

   > P.J.M. van Haastert, P.A.M. Dijkgraaf, T.M. Konijn,

E.G. Abbad, G. Petridis en B. Jastorff, Eur.
J. Biochem., 1983, *131*,659.

4. Bij de bepaling van de stereochemie van de methylmalonyl
   coenzym A isomerisatie wordt geen rekening gehouden met
   het gegeven dat het gepostuleerde radikaalmechanisme voor
   de intramolekulaire koolstofmigraties kan leiden tot
   racemisatie van de chirale centra.

   J. Retey, Recent. Adv. Phytochem., 1979, *13*,1.

5. Het verdient aanbeveling om bij de bereiding van oestrogenen
   via asymmetrisch geinduceerde cyclisatiereakties,
   enantiomeer zuivere precursors te gebruiken.

   C.G.M. Janssen, proefschrift, T.H. Eindhoven, 1982;
   A.A. Macco en H.M. Buck, J. Org. Chem., 1981, *13*,
   2655.

6. De berekeningen van *Howell et al.*, welke aangeven dat er
   geen energiebarrière bestaat voor fragmentatie van PH_4
   naar PH_3 + H·, dienen kritisch te worden herbezien.

   J.H. Howell en J.F. Olsen, J. Amer. Chem. Soc.,
   1976, *98*,7119.

7. Het verdient aanbeveling om de rol van vijfgekoördineerde
   fosforintermediairen in fosfolipiden te onderzoeken.

8. De veronderstelling van *Roberts et al.* dat de koolstof-
   atomen van de *sn*-1 ketens van lecithines met korte acyl-
   ketenlengte langere ^{13}C spin-rooster relaxatietijden
   bezitten dan die van de *sn*-2 ketens, is aanvechtbaar.

   R.A. Burns en M.F. Roberts, Biochemistry, 1980,
   19, 3100.

9. Voor het juist interpreteren van spektrale gegevens van
   fosfolipide dubbellagen en vesicles met behulp van
   elektronen-spin-resonantie, moet men zich de verstorende
   effekten van de geinkorporeerde spinlabel duidelijk
   realiseren.

   > K. Madden, L. Kevan, P.D. Morse II en
   > R.N. Schwartz, J. Amer. Chem. Soc., 1982, *104*,10.

10. Analoog aan de preventieve werking van de bijsluitertekst
    van een medicinaal preparaat, zou een vergelijkbaar effekt
    verwacht kunnen worden indien op het etiket van alkoholika
    eveneens werd vermeld: ".... kan de rijvaardigheid
    beinvloeden".

R.J.E.M. de Weerd   Eindhoven, 4 oktober 1983.

Erratum

page 30, *Table II.3b*: C_{11}/C_7^c should read C_{11}/C_6^c, and C_{11}/C_6^c should read C_{11}/C_5^c. This is also valid for these abbreviations in the footnote of this Table.